NATIONAL LIBRARY
OTTAWA

CANADA

BIBLIOTHÈQUE NATIONALE
OTTAWA

NAME OF AUTHOR........David A.M. Switzer........

TITLE OF THESIS........N.M.R. Study of the Ruderman Kittel Interaction in White Tin Using Macroscopic Rotation...

UNIVERSITY..........University of Alberta........

DEGREE FOR WHICH THESIS WAS PRESENTED......M.Sc.........

YEAR THIS DEGREE GRANTED..........1973..................

Permission is hereby granted to THE NATIONAL LIBRARY OF CANADA to microfilm this thesis and to lend or sell copies of the film.

The author reserves other publication rights, and neither the thesis nor extensive extracts from it may be printed or otherwise reproduced without the author's written permission.

(Signed).... David Switzer ...

PERMANENT ADDRESS:

....774 Highland Ave

....Ottawa, Ontario

....

DATED... October 19 ...19 73

NL-91 (10-68)

THE UNIVERSITY OF ALBERTA

NMR STUDY OF THE RUDERMAN-KITTEL INTERACTION IN WHITE TIN USING MACROSCOPIC ROTATION

BY

© DAVID A. SWITZER

A THESIS

SUBMITTED TO THE FACULTY OF GRADUATE STUDIES AND RESEARCH

IN PARTIAL FULFILMENT OF THE REQUIREMENTS FOR THE DEGREE

OF MASTER OF SCIENCE

DEPARTMENT OF PHYSICS

EDMONTON, ALBERTA

FALL, 1973

THE UNIVERSITY OF ALBERTA

FACULTY OF GRADUATE STUDIES AND RESEARCH

The undersigned certify that they have read, and recommend to the Faculty of Graduate Studies and Research for acceptance, a thesis entitled NMR STUDY OF THE RUDERMAN-KITTEL INTERACTION IN WHITE TIN USING MACROSCOPIC ROTATION submitted by David A. M. Switzer in partial fulfilment of the requirements for the degree of Master of Science.

D. G. Hughes
Supervisor

....

....

....

Date October 18, 1973

ABSTRACT

This thesis describes a study of the rotationally invariant part of the electron-coupled nuclear spin-spin interaction, otherwise known as the Ruderman-Kittel interaction, in β (or white) tin. It is a continuation of the NMR study initiated in our laboratory by Smith (1972), in which the anisotropic nuclear spin interactions in β-tin are averaged by rotating a sample of tin powder at high speed using an air turbine. Provided the axis of rotation makes the so-called magic angle ($\cos^{-1} 1/\sqrt{3}$) with the external magnetic field, the broadening associated with the anisotropic interactions is completely removed and the NMR lineshape is governed by the Ruderman-Kittel interaction together with spin-lattice relaxation. The theoretical lineshape is synthesized and the strength of the Ruderman-Kittel interaction is obtained by fitting the theoretical lineshape to the experimental resonance.

Improvements made to the air turbine designed by Smith enabled us to record the Sn^{117} NMR signal with a greatly improved signal-to-noise ratio. The theoretical lineshape calculations made by Smith have been extensively revised and fewer approximations have been made. Also, a new fitting procedure has been developed which enables a theoretical lineshape which is computed numerically to be fitted to an experimental lineshape.

Agreement between experiment and a theoretical model, which as-assumes that only nearest neighbour spin-spin interactions are signi-

ficant, is very poor. Similarly, a model in which only second nearest neighbour interactions are non-zero, has been shown to be untenable. However, very good agreement has been obtained with the so-called Ruderman-Kittel model and we find that the strength of the interaction between nearest neighbour Sn^{117} and Sn^{119} nuclei is 3.04 ± 0.3 kHz. A comparison is made with other published values of this quantity.

Acknowledgements

I would like to express my sincere thanks to Dr. D. G. Hughes for suggesting this work. His interest and guidance during this project were much appreciated.

I would like to thank Dr. M. R. Smith, who did the original work on this subject, for his valuable discussions. Also I would like to thank Mr. P. Spencer for many helpful discussions and assistance.

I wish to acknowledge the assistance of members of the technical staff during this project.

I would like to thank the Unviersity of Alberta for the award of a GTA Scholarship and the National Research Council for the award of a Graduate Scholarship.

PAGE

LIST OF TABLES

LIST OF FIGURES

I INTRODUCTION

I(i) General

It has been known since the early work of Bloembergen and Rowland (1953) that the NMR linewidth of nuclei with $I=1/2$ cannot be wholly accounted for by direct nuclear magnetic dipole-dipole interactions and by a lifetime-limiting effect associated with spin-lattice relaxation. By measuring the Tl^{203} and Tl^{205} linewidths in various samples of thallium metal with different isotopic composition, Bloembergen and Rowland (1955) showed that an indirect interaction occurs between nuclear spins via the intermediary of the conduction electrons. In particular, they showed that the indirect interaction between two spins $\underline{I}_1$ and $\underline{I}_2$ consists of a scalar or rotationally invariant part of the form $J\underline{I}_1 \cdot \underline{I}_2$, sometimes given the name of pseudo-exchange interaction, together with a smaller anisotropic part, sometimes called the pseudo-dipolar interaction. A theory of the rotationally invariant part has been given by Ruderman and Kittel (1954), and indeed this interaction is also often called the Ruderman-Kittel interaction, a name which we shall adopt in this thesis.

The Ruderman-Kittel interaction between unlike neighbours contributes to the second moment of the NMR line (Ruderman and Kittel, 1954) and hence broadens it. On the other hand, the Ruderman-Kittel interaction between like neighbours leaves the second moment unaffected but increases the fourth and higher (even) moments. This implies a sharpening of the central part of the resonance, a phenomenon called exchange narrowing.

The study of the indirect nuclear spin-spin interaction is important on two counts:

1) It provides an understanding of the factors which contribute to the width and shape of NMR lines in general.

2) It provides information regarding the hyperfine interaction between the nuclear spins and conduction electrons in metals.

There is some uncertainty in the magnitude of the Ruderman-Kittel interaction in the case of white or β-tin, since all the methods used so far have required a knowledge of the second moment of the tin resonance. Values for the magnitude of the Ruderman-Kittel interaction between Sn^{117} and Sn^{119} nuclei which occupy nearest neighbour sites in β-tin range from 2.0 ± 0.5 kHz obtained by McLachlan (1968) to 4.1 ± .3 kHz obtained by Alloul and Deltour (1969). A method has recently been described by Smith (1972) and uses the so-called magic angle, high-speed rotation technique. This involves rotating the sample at high speed (in practice at several kHz) about an axis making an angle $\cos^{-1}(1/\sqrt{3})$ with the external magnetic field.

In this thesis we describe some additional work done on this problem. In particular, substantial refinements to the theory given by Smith (1972) are presented together with a description of improved rotors which enable a much better signal-to-noise ratio to be achieved. Also, a better procedure for fitting theoretical lineshapes to experimental resonances is described.

In sections I(ii) and I(iii) of this thesis, a simple picture of NMR and a discussion of the magic angle, high-speed rotation technique are given. Section II contains the theoretical background for this thesis. In section III a discussion of the equipment and experimental method are given. In section IV the fitting procedure is described and the results are presented and discussed.

I(ii) A Simple Picture of NMR

Purcell, Torrey and Pound, (1946) and Bloch, Hansen and Packard (1946) carried out the first spin resonance experiments on nuclei in liquids and solids. When a nucleus with spin quantum number I is subjected to a steady magnetic field $\underline{H}_o$, there are 2I+1 equally spaced magnetic energy levels, with a separation

$$\Delta E = \mu H_o/I = \gamma\hbar H_o \tag{1}$$

between adjacent energy levels. Here $\mu = \gamma\hbar I$ is the maximum z component of the nuclear magnetic moment (z is taken to be in the same direction as $\underline{H}_o$) and γ is the gyromagnetic ratio of the nucleus. If a group of nuclei which interact negligibly with each other are allowed to come to equilibrium with a heat reservoir at temperature T, a net magnetization, M_z, in the z direction is established which obeys the well known Curie law $M_z \propto 1/T$. When an rf magnetic field of frequency

$$\omega_o = \gamma H_o \tag{2}$$

is applied perpendicular to $\underline{H}_o$, there is a net absorption of energy from the rf field with a new equilibrium value of M_z. Because of the finite lifetime of the magnetic energy levels due to the interaction with the heat reservoir, there is also absorption of energy from the rf field for frequencies close to ω_o. For a group of spin 1/2 nuclei which interact only with a heat reservoir, the shape of the absorption spectrum is Lorentzian, the half-width of the spectrum being equal to $2W/\pi$, where $W = 1/2T_1$ is the transition rate and T_1 is the spin-lattice relaxation time.

For solids, the direct magnetic dipole-dipole interaction between nuclei is important (Van Vleck, 1948). Classically, the dipole-dipole interaction can be considered in the following way. Each nuclear magnet finds itself not only in the applied steady magnetic field $\underline{H}_o$, but also in a small local field $\underline{H}_{loc}$ produced by neighbouring nuclear moments. The magnitude and direction of $\underline{H}_{loc}$ differs from nuclear site to nuclear site, depending on the relative disposition of their magnetic quantum number m (where m can take on values -I, -I+1,...,I). The distribution of H_{loc} has a mean value of zero and a width of the order μ/r^3 where r is the nearest neighbour distance. As the resonance frequency of each nucleus takes on different values due to the variation in $\underline{H}_{loc}$, the resonance will be further broadened (in addition to lifetime broadening).

In a metal, another important interaction is that between nuclear spins and the electronic spins. A simple way to examine this is to consider the magnetic field produced by electronic spins. This rapidly fluctuating field can be divided into its time-average and the difference between the time-average and the value of the field at a given time. The time-averaged field, which to a good approximation is parallel to $\underline{H}_o$, causes a shift ΔH of the resonance which is proportional to H_o (and usually down field). This shift was first observed by Knight (1949) and the so-called Knight Shift K is defined as $\Delta H/H_o$. When the time-averaged distribution of the electrons about a nuclear site has lower than cubic (or tetrahedral) symmetry, the Knight Shift is anisotropic, that is it depends on the orientation of the metal with respect to $\underline{H}_o$. It can be shown that the Knight Shift is a second rank tensor. This is a further source of broadening when the sample is in the form of a powder since the various grains of the powder will have different orientations with respect to $\underline{H}_o$. The time-dependent magnetic field caused by the electronic spins gives rise to a spin-lattice relaxation.

A second effect of the time-averaged magnetic field is the indirect interaction which was previously mentioned in section I(i). The existence of such an interaction can be visualized by the following picture (Slichter, 1963). Consider two magnetic nuclei amongst non-magnetic nuclei. The effect of the spin of one of the nuclei is, in general, to make the nuclear site more favourable for an electron with a spin parallel to the magnetic moment of the nucleus. The zero states of the electrons are Bloch states and in order to increase the probability of an electron with a negative spin orientation being in the vicinity of a nuclear site of negative magnetic moment, it is necessary to mix Bloch states of negative spin orientation and with wavevector k greater than the Fermi wavevector k_f (because of the exclusion principle). These Bloch states are in phase at the [illegible]e but become progressively more out of phase with increasi[illegible] distance from the magnetic nucleus. This implies that the conduction electron density oscillates about the average value. The magnitude of the oscillations decreases with increasing distance. Consequently, the second magnetic nucleus experiences a different time-averaged magnetic field, thereby giving rise to an interaction.

There is also a nuclear quadrupole interaction but this interaction does not occur in tin as the magnetic isotopes of tin have a spin of 1/2. As a result we will not describe this interaction.

I(iii) Macroscopic Rotation

The first studies using the sample rotation technique were made by Andrew et al (1958) to confirm the theoretical predictions of Anderson (1954) and Pake (1956) that hindered rotation in a solid should not cause a reduction in the second moment of the NMR spectrum. When they rotated the sample as a whole, Andrew et al found that the central part of the spectrum was narrowed but sidebands appeared in such a way that the second moment remained invariant. Narrowing by macroscopic rotation at the magic angle has been studied in more detail by Andrew and Newing (1958), Andrew and Jenks (1962) and Schwind (1967). It has been shown by Kessemeier (1967) that if the rate of rotation is much greater than the NMR linewidth of the stationary sample, the central part of the resonance is resolved from the sidebands, and only the time-averaged interactions need be included in the Hamiltonian to study the central part. A comprehensive study has been undertaken by Andrew and Farnell (1968) in connection with the averaging of anisotropic interactions by rotation.

II THEORY

II(i) General

The Hamiltonian of a group of nuclear spins interacting with a 'thermal bath' of conduction electrons in a metal can be written as

$$\mathcal{H} = \hbar E + \hbar F + \hbar Q \tag{1}$$

where $\hbar E$ involves only the nuclei, $\hbar F$ involves only the thermal bath and $\hbar Q$ is the interaction between the nuclei and thermal bath. Q can be written as

$$Q_{\alpha f u \alpha' f' u'} = \sum_q K^q_{\alpha\alpha'} H^q_{fuf'u'} \tag{2}$$

where α, α' are eigenvalues of E, and f, f' are eigenvalues of F of degeneracy u and u' respectively; K^q is an observable of the nuclei and H^q is an observable of the thermal bath. For a metal we have

$$\hbar Q = \sum_i a_i \underline{I}_i \cdot \sum_\ell \underline{S}_\ell \delta(\underline{r}_{i\ell} - \underline{R}_i) + \sum_i b_i \underline{I}_i \cdot \sum_\ell \underline{\underline{D}}_{\ell i} \cdot \underline{S}_\ell + \sum_i c_i \underline{I}_i \cdot \sum_\ell \underline{L}(\underline{r}_{i\ell})/r_{i\ell}^3 \tag{3}$$

where $a_i = 8\pi\gamma_e\gamma_i\hbar^2/3$, $b_i = \gamma_e\gamma_i\hbar^2$, $c_i = 2\gamma_e\gamma_i$, $\underline{\underline{D}}_{\ell i} = {}_{\ell}1\{|\underline{r}_{i\ell}-\underline{R}_i|^3 - (\underline{r}_{i\ell}-\underline{R}_i)\cdot(\underline{r}_{i\ell}-\underline{R}_i)/|\underline{r}_{i\ell}-\underline{R}_i|^5\}$ and γ_i and γ_e are the gyromagnetic ratios of the ith nucleus and an electron respectively. $\underline{L}(\underline{r}_{i\ell})$ is the angular momentum operator for the ℓth electron with respect to the ith nucleus as center and $\underline{r}_{i\ell}$ is the position vector for the ℓth electron with respect to the ith nucleus (Das and Mahanti, 1968). The first term in (3) is the so-called Fermi contact interaction and the second term describes the dipolar interaction between the nuclear spins and the electron spins.

The density matrix operator (Davydov, 1966 p. 42) for the nuclei and the bath is ρ and is assumed to be of the form (Redfield, 1957)

$$\rho_{\alpha f u \alpha' f' u'}(t) = \sigma_{\alpha\alpha'}(t) P(f) \delta_{ff'} \delta_{uu'} \tag{4}$$

with

$$P(f) = \exp(-\hbar f/kT)/\Sigma_{f'u'} \exp(-\hbar f'/kt). \tag{5}$$

Redfield found that

$$d\sigma/dt \cong (\sigma(t+\Delta t)-\sigma(t))/\Delta t = i\,[\sigma, E+M+N] + R \tag{6}$$

if $\Delta t >> \tau_c$, and $M,N,R << 1/\tau_c < kT/\hbar$, where τ_c can be thought of as the classical correlation time for the random magnetic fields produced at the nuclear sites by the electrons. Redfield showed that the matrix elements of the operators M and N are

$$M_{\alpha\alpha'} = \Sigma_q K^q_{\alpha\alpha'} \Sigma_{fu} H^q_{fufu} P(f) \tag{7}$$

$$N_{\alpha\alpha'} = \Sigma_\gamma \Sigma_{qq'} K^{q'}_{\gamma\alpha'} K^q_{\alpha\gamma} \pi^{-1} \int_{-\infty}^{\infty} d\omega\; j_{qq'}(-\omega)/(\tfrac{1}{2}\alpha+\tfrac{1}{2}\alpha'-\gamma-\omega) \tag{8}$$

Also he found that

$$(R\sigma)_{\alpha\alpha'} = \Sigma_{\beta\beta'} R'_{\alpha\alpha'\beta\beta'} \sigma_{\beta\beta'} \tag{9}$$

and

$$R'_{\alpha\alpha'\beta\beta'} = \Sigma_{qq'}\{K^q_{\alpha\beta} K^{q'}_{\beta'\alpha'}(j_{qq'}(\alpha-\beta)+j_{qq'}(\alpha'-\beta')) - \delta_{\alpha\beta}\Sigma_\gamma K^q_{\beta'\gamma} K^{q'}_{\gamma\alpha'} j_{qq'}(\beta'-\gamma) e^{\hbar(\beta'-\gamma)/kT} - \delta_{\alpha'\beta'} \Sigma_\gamma K^q_{\alpha\gamma} K^{q'}_{\gamma\beta} j_{qq'}(\beta-\gamma) e^{\hbar(\beta-\gamma)/kT} \tag{10}$$

where

$$j_{qq'}(\omega) = \pi \int_{-\infty}^{\infty} df\; \{\Sigma_{uu'} P(f) H^q_{(f-\omega)ufu'} H^{q'}_{fu'(f-\omega)u}\, \eta_u(f-\omega)\eta_{u'}(f)\}$$

and $\eta_u(f)$ is the density of states for eigenvalue f and degeneracy u. In writing (10), Redfield assumed that only secular terms contributed to $R'_{\alpha\alpha'\beta\beta'}$, that is only terms where $\alpha-\alpha'-\beta+\beta' = 0$. However, for non-secular terms, Redfield showed that one must multiply the right hand side of (10) by a term of the form

$$A_{\alpha\alpha'\beta\beta'} = \{e^{i(\alpha-\alpha'-\beta+\beta')\Delta t}-1\}/(\alpha-\alpha'-\beta+\beta')\Delta t\,. \qquad (11)$$

M can be identified with the Knight Shift operator (K^q in (2) is taken to be one of the components of the spin operator for one of the nuclei because of (3)) and N is the indirect spin-spin interaction operator (ignoring terms in (8) where q and q' refer to the same nuclear spin). The R' operator is the relaxation operator.

The operator $\hbar(E+M+N)$ can therefore be expressed as

$$-\hbar\sum_i \gamma_i \underline{I}_i\cdot(\underline{\underline{1}}+\underline{\underline{K}})\cdot\underline{H}_o + h\sum_{i<j}\underline{I}_i\cdot(\underline{\underline{J}}_{ij}+\underline{\underline{D}}_{ij})\cdot\underline{I}_j \qquad (12)$$

where $\underline{\underline{K}}$ is the Knight Shift tensor, and $\underline{\underline{J}}_{ij}$ and $\underline{\underline{D}}_{ij}$ are respectively the indirect tensor and the dipolar interaction tensor between nuclei i and j. It follows that (6) can be written in the form

$$d\sigma/dt = i\left[\sigma,(-\sum_i\gamma_i\underline{I}_i\cdot(\underline{\underline{1}}+\underline{\underline{K}})\cdot\underline{H}_o + 2\pi\sum_{i<j}\underline{I}_i\cdot(\underline{\underline{J}}_{ij}+\underline{\underline{D}}_{ij})\cdot\underline{I}_j)\right] + R'\sigma\,. \qquad (13)$$

II(ii) Effect of Macroscopic Rotation on $\underline{\underline{K}}$, $\underline{\underline{J}}$, and $\underline{\underline{D}}$

Because of the short correlation time of the conduction electrons ($\tau_c \simeq 10^{-11}$ seconds) and the fact that the period of the macroscopic rotation is typically 10^{-4} seconds, we can allow $\underline{\underline{K}}$, $\underline{\underline{J}}$ and $\underline{\underline{D}}$ in (13) to be time dependent. However, as pointed out in I(iii), the shape of the central part of the resonance is governed by the time-average of $\underline{\underline{K}}$, $\underline{\underline{D}}$ and $\underline{\underline{J}}$. The R operator in (13) is assumed to be unaffected by macroscopic rotation, since McLachlan (1968) found that the T_1 of Sn^{119} in β-tin was essentially independent of crystal orientation (the connection between T_1 and R is established in section II(iv)).

To find the time-averaged operators, it is noted that the interactions involving $\underline{\underline{K}}$, $\underline{\underline{J}}$ and $\underline{\underline{D}}$ are of the form $\underline{A}\cdot\underline{\underline{T}}\cdot\underline{B}$ where $\underline{A}$ and $\underline{B}$ are time independent vectors. Because of the symmetry of the crystal structure of β-tin, $\underline{\underline{T}}$ must be symmetric matrix (Smith, 1972, p. 94). Following Andrew and Farnell (1968), we can decompose the tensor into two parts, $\underline{\underline{T}}'$ and $\underline{\underline{T}}^*$, where $\underline{\underline{T}}'$ is equal to $(1/3)\mathrm{Tr}(\underline{\underline{T}})\underline{\underline{1}}$ and $\underline{\underline{T}}^*$ is a traceless tensor equal to $\underline{\underline{T}} - \underline{\underline{T}}'$. Because $\underline{\underline{T}}^*$ is symmetric

$$\underline{A}\cdot\underline{\underline{T}}^*\cdot\underline{B} = \sum_{\alpha\beta} T^*_{\alpha\beta} A_\alpha B_\beta = \sum_{\alpha\beta n} C_{\alpha n} C_{\beta n} T^*_n A_\alpha B_\beta \tag{14}$$

where $C_{\alpha n}$ and $C_{\beta n}$ are the direction cosines between the axes x, y and z fixed with respect to the laboratory (represented in (14) by the indices α and β) and the principal axes of the tensor. The T_n's are the principal values of the tensor $\underline{\underline{T}}^*$. Using the relations $A_+ = A_x + iA_y$ and $A_- = A_x - iA_y$ plus similar relations for B_+ and B_-, we obtain

$$\underline{A}\cdot\underline{\underline{T}}^{*}\cdot\underline{B} = \sum_n T_n(D_n+E_n+F_n+H_n+I_n) \qquad (15)$$

where

$$D_n = C_{3n}^2 A_z B_z$$

$$E_n = (1/4)(A_+B_- + A_-B_+)(C_{1n}^2 + C_{2n}^2)$$

$$F_n = (1/2)(C_{1n}C_{3n} - iC_{2n}C_{3n})(A_+B_z + A_zB_+)$$

$$G_n = (1/2)(C_{1n}C_{3n} + iC_{2n}C_{3n})(A_-B_z + A_zB_-)$$

$$H_n = (1/4)(C_{1n}^2 - 2iC_{1n}C_{2n} - C_{2n}^2)A_+B_+$$

$$I_n = (1/4)(C_{1n}^2 + 2iC_{1n}C_{2n} - C_{2n}^2)A_-B_- .$$

We now consider the truncated part of (15), that is, we consider the terms D_n and E_n. We can ignore the remaining terms when $\underline{A}$ and $\underline{B}$ represent spin vectors since these terms give rise to weak resonances at frequencies 0, $2\omega_o$, and $3\omega_o$, resonances which we are not interested in. We have

$$\left(\sum_{\alpha\beta} T_n C_{\alpha n} C_{\beta n} A_\alpha B_\beta\right)^{trunc} = \sum_n T_n\{C_{3n}^2 A_z B_z + (1/4)(A_+B_- + A_-B_+)(C_{1n}^2 + C_{2n}^2)\}$$

$$= \sum_n T_n\{C_{3n}^2 A_z B_z + (1/2)(A_xB_x + A_yB_y)(1 - C_{3n}^2)\}$$

$$= \sum_n T_n(-1/2)C_{3n}^2(A_xB_x + A_yB_y - 2A_zB_z). \qquad (16)$$

In appendix I we show that the time-averaged value of C_{3n}^2 is 1/3 if the magic angle condition is satisfied. Since $\underline{\underline{T}}^{*}$ is traceless and $\overline{C_{3n}^2}$ is 1/3, the right hand side of (16) reduces to zero. Thus we have

$$\overline{(\underline{A}\cdot\underline{\underline{T}}^{*}\cdot\underline{B})^{trunc}} = 0. \qquad (17)$$

If truncation is justified, then the time-averaged interaction (when the magic angle condition is satisfied) reduces to

$$\overline{\underline{A}\cdot\underline{\underline{T}}\cdot\underline{B}} = (\underline{A}\cdot\underline{B})(1/3)\mathrm{Tr}(\underline{\underline{T}}). \qquad (18)$$

For the dipolar interaction, $\underline{A}$ and $\underline{B}$ are spin vectors, and truncation is justified. Moreover, the dipolar interaction tensor is traceless. As a result, the time-averaged interaction is equal to zero.

The indirect interaction between nuclei can also be written in the form $\underline{A}\cdot\underline{\underline{T}}\cdot\underline{B}$, where $\underline{A}$ and $\underline{B}$ are spin operators. As a result the time-averaged indirect interaction becomes

$$\overline{\sum_{i<j} \underline{I}_i\cdot \underline{\underline{J}}_{ij}\cdot \underline{I}_j} = \sum_{i<j} J_{ij}\underline{I}_i\cdot \underline{I}_j \qquad (19)$$

where $J_{ij} = (1/3)\mathrm{Tr}(\underline{\underline{J}}_{ij})$.

Finally, the Zeeman interaction can be written in the form $\underline{A}\cdot\underline{\underline{T}}\cdot\underline{B}$. However $\underline{A}$ is a nuclear spin vector and $\underline{B}$ is the steady magnetic field $\underline{H}_o$ in this case. The sum of $\underline{H}_o$ and the magnetic field caused by the electronic spins is, to a good approximation, in the z direction (Abragam, 1961) and the interaction can be written as

$$-\sum_i \hbar\gamma_i(1+K_{zz})I_{iz}H_o \qquad (20)$$

It follows that terms E_n through I_n in (15) are zero in this case, and equation (17) obtained for the truncated interaction can therefore be applied. Thus the time-averaged Zeeman interaction is

$$-\sum_i \hbar\gamma_i(1+K)I_{iz}H_o \qquad (21)$$

where $K \equiv (1/3)\mathrm{Tr}(\underline{\underline{K}}) = (1/3)(K_1+K_2+K_3)$. For β-tin $K_3 \equiv K_\parallel$ and $K_1 = K_2 \equiv K_\perp$ because of the $\overline{4}$ axis of symmetry.

In summary, the time-averaged value of $\hbar(E+M+N)$ is

$$\hbar(E+M+N) = \sum_i \hbar\gamma_i(1+K)I_{iz}H_o + \hbar\sum_{i<j} J_{ij}\underline{I}_i\cdot \underline{I}_j \qquad (22)$$

when the magic angle condition is satisfied.

II(iii) The Ruderman-Kittel Interaction

The usual method of finding a theoretical expression for the Ruderman-Kittel interaction is to consider $\hbar Q$ as a perturbation of $\hbar(E+F)$ in (1) and to find the second-order correction to the energy levels. The first order correction is responsible for the Knight Shift and will not be discussed here. The second order correction is

$$\Delta E_{0\alpha} = \sum_{n\alpha'} |(0\alpha|\hbar Q|n\alpha')|^2/(E_0+E_\alpha-E_n-E_{\alpha'}) \tag{23}$$

where $|n\alpha')$ is a product of a many-electron state $|n)$ of energy E_n, and a many-nucleus state $|\alpha')$ of energy $E_{\alpha'}$. The unperturbed state of the electrons and nuclei is $|0\alpha)$. Examination of equation (3) shows that $\hbar Q$ is of the form $\sum_i (H_{en})_i$, that is, it can be written as a sum of terms, each one involving only one nucleus. By expanding $\hbar Q$ in terms of $(H_{en})_i$ one obtains terms of the form

$$|(n\alpha|(H_{en})_i|0\alpha)|^2/(E_0+E_\alpha-E_n-E_{\alpha'}) \tag{24}$$

which involve only one nucleus. Since we are only interested in interactions involving pairs of nuclei such terms as (24) are omitted and we retain only the cross terms of (23), and thus

$$\Delta E_{0\alpha} = \sum_{i<j} \sum_{n\alpha'} (0\alpha|(H_{en})_i|n\alpha')(n\alpha'|(H_{en})_j|0\alpha)/(E_0+E_\alpha-E_n-E_{\alpha'}). \tag{25}$$

Because the electronic energy states are essentially continuous and the energy difference between the unperturbed and perturbed electronic states is usually greater than $|E_\alpha-E_{\alpha'}|$, the denominator of (25) is approximated as E_0-E_n. Also, the interaction $(H_{en})_i$ takes the form $\underline{I}_i\cdot\underline{G}_i$, where $\underline{G}_i$ does not involve the nuclear spin operator. Thus

$$\Delta E_{0\alpha} = \sum_{\beta\beta'} \sum_{\alpha'} \sum_{i<j} \{(\alpha|I_{i\beta}|\alpha')(\alpha'|I_{j\beta'}|\alpha)\sum_n (0|G_{i\beta}|n)(n|G_{j\beta'}|0) + c.c.\}/(E_0-E_n). \tag{26}$$

We could have obtained $\Delta E_{o\alpha}$ as a first order perturbation contribution if the term $\mathcal{H}_{eff}$ had been added to (1) where

$$\mathcal{H}_{eff} = \sum_{i<j} \sum_{\beta\beta'} I_{i\beta} (J_{ij})_{\beta\beta'} I_{j\beta'} \tag{27}$$

and

$$(J_{ij})_{\beta\beta'} = \sum_n \{(0|G_{i\beta}|n)(n|G_{j\beta'}|0) + c.c.\}/(E_o - E_n). \tag{28}$$

$\mathcal{H}_{eff}$ is equivalent to operator N of (6) if the terms of N which involve only one nucleus are excluded. We shall henceforth assume that the indirect interaction is given by (27).

The right hand side of (28) can be written as (Mahanti and Das, 1968)

$$(J_{ij})_{\beta\beta'} = (J_{ij})^{(1)}_{\beta\beta'} + (J_{ij})^{(2)}_{\beta\beta'} + (J_{ij})^{(3)}_{\beta\beta'} + (J_{ij})^{(4)}_{\beta\beta'} \tag{29}$$

where

$$(J_{ij})^{(1)}_{\beta\beta'} = \sum_n B_n \{(0|G^{cont}_{i\beta}|n)(n|G^{cont}_{j\beta'}|0) + c.c.\}$$

$$(J_{ij})^{(2)}_{\beta\beta'} = \sum_n B_n \{(0|G^{cont}_{i\beta}|n)(n|G^{dip}_{j\beta'}|0) + (0|G^{dip}_{i\beta}|n)(n|G^{cont}_{j\beta'}|0)\}$$

$$(J_{ij})^{(3)}_{\beta\beta'} = \sum_n B_n \{(0|G^{orb}_{i\beta}|n)(n|G^{orb}_{j\beta'}|0) + c.c.\}$$

$$(J_{ij})^{(4)}_{\beta\beta'} = \sum_n B_n \{(0|G^{dip}_{i\beta}|n)(n|G^{dip}_{j\beta'}|0) + c.c.\}$$

and

$$G^{cont}_{i\beta} = a_i \sum_\ell S_{\ell\beta} \delta(\underline{r}_{i\ell} - \underline{R}_i)$$

$$G^{dip}_{i\beta} = b_i \sum_{\ell\beta'} (D_{\ell i})_{\beta\beta'} S_{\ell\beta'}$$

$$G^{orb}_{i\beta} = c_i \sum_\ell L_\beta(\underline{r}_{i\ell})/r^3_{i\ell}$$

$$B_n = (E_o - E_n)^{-1}.$$

Some of the cross terms involving the contact, dipolar and orbital contributions have been excluded from the right hand side of (29) since they are equal to zero when the orbital momentum is quenched (Mahanti and Das, 1968).

If the electron energy surfaces are spherical, the term $(J_{ij})^{(2)}_{\beta\beta'}$ is dipolar in form and contains no diagonal components (Mahanti and Das, 1968). The term $(J_{ij})^{(3)}_{\beta\beta'}$, again assuming spherical energy surfaces, has only diagonal components, while the term $(J_{ij})^{(4)}_{\beta\beta'}$ is composed of two parts, a dipolar part and a diagonal part (Mahanti and Das, 1968). These authors showed that for Rb and Cs, the contributions of $(J_{ij})^{(3)}_{\beta\beta'}$ and $(J_{ij})^{(4)}_{\beta\beta'}$ to the diagonal terms of $\underline{\underline{J}}_{ij}$ are small compared to the contributions of $(J_{ij})^{(1)}_{\beta\beta'}$.

For $(J_{ij})^{(1)}_{\beta\beta'}$ we have

$$(J_{ij})^{(1)}_{\beta\beta'} = a_i a_j \sum_{\underline{nks}} \sum_{n'\underline{k}'s'} B\{(n\underline{k}s|S_\beta \delta(\underline{r}-\underline{R}_i)|n'\underline{k}'s')(n'\underline{k}'s'|S_{\beta'}\delta(\underline{r}-\underline{R}_i)|n\underline{k}s) + \text{c.c.}\} \quad (30)$$

where the sum $\sum_{\underline{\underline{nks}}}$ in (30) is over occupied Bloch electron states. Also, n represents the band of the Bloch state in the first Brillouin zone, k is the wavevector and s is the electron spin of the electron state. The sum $\sum_{n'\underline{k}'s'}$ is over the unoccupied electron states and B is equal to $(E_{n\underline{k}s}-E_{n'\underline{k}'s'})^{-1}$. This expression has been rewritten as

$$(J_{ij})^{(1)}_{\beta\beta'} = \sum_{ss'nn'\underline{k}\underline{k}'} (n\underline{k}|\delta(\underline{r})|n'\underline{k}')(n'\underline{k}'|\delta(\underline{r})|n\underline{k})e^{-i(\underline{k}-\underline{k}')\cdot\underline{R}_{ij}}(s|S_\beta|s')B(s'|S_{\beta'}|s)$$

by various authors (see for example Slichter, 1963). Here $\underline{R}_{ij} = \underline{R}_i - \underline{R}_j$ and $|n\underline{k}s) = |s)|n\underline{k})$. The probability of a state $|n\underline{k}s)$ being occupied is $f(n\underline{k}s)$ and of a state $|n\underline{k}s)$ being unoccupied is $1-f(n\underline{k}'s)$, where f is the Fermi-Dirac distribution function. It follows that

$$(J_{ij})^{(1)}_{\beta\beta'} = \sum_{n\underline{k}} \sum_{n'\underline{k}'} \sum_{ss'} (n\underline{k}|\delta(\underline{r})|n''\underline{k}'')(n''\underline{k}''|\delta(\underline{r})|n\underline{k})e^{-i(\underline{k}-\underline{k}).\underline{R}_{ij}} \times$$

$$(s|S_\beta|s')(s'|S_{\beta'}|s)B\{1-f(n'\underline{k}'s')\}f(n\underline{k}s) \qquad (31)$$

where the sums $\Sigma_{n\underline{k}s}$ and $\Sigma_{n'\underline{k}'s'}$ are now over all states. Because $f(n\underline{k}s)$ is approximately the same for spin up or spin down states, and matrix elements vary slowly with energy, we can replace $f(n\underline{k}s)$ by $f(n\underline{k})$ and B by $(E_{n\underline{k}}-E_{n'\underline{k}'})^{-1}$ (Slichter, 1963). As a result of this approximation, and since

$$\sum_{ss'}(s|S_\beta|s')(s'|S_{\beta'}|s) = \sum_s (s|S_\beta S_{\beta'}|s) = \mathrm{Tr}(S_\beta S_{\beta'}) = \delta_{\beta\beta'}/2, \qquad (32)$$

we have

$$(J_{ij})^{(1)}_{\beta\beta} I_{i\beta} I_{j\beta} = (J_{ij})^{(1)} \underline{I}_i \cdot \underline{I}_j$$

$$= -(1/V)^2 \sum_{n\underline{k}} \sum_{n'\underline{k}'} I_{nn'}(\underline{k},\underline{k}') f(n\underline{k})\{1-f(n'\underline{k}')\} e^{i(\underline{k}-\underline{k}')\cdot\underline{R}_{ij}}/(E_{n\underline{k}}-E_{n'\underline{k}'}) \qquad (33)$$

where $I_{nn'}(\underline{k},\underline{k}') = -a_i a_j \frac{V^2}{2} |\psi_{n\underline{k}}(0)|^2 |\psi_{n'\underline{k}'}(0)|^2$ and $\psi_{n\underline{k}}(\underline{r})$ is the wavefunction of $|n\underline{k})$ in the coordinate representation. Different authors have made various approximations in applying (33). In particular Ruderman and Kittel (1954) assumed that the electron energy surfaces are spherical, and that $I_{nn'}(\underline{k},\underline{k}')$ can be approximated by its value at the Fermi surface. Ruderman and Kittel found that

$$J_{ij} = (2/9\pi)\gamma_e^2 \gamma_i \gamma_j \hbar^2 m^* |\psi_{k_f}(0)|^4 F(2k_f|\underline{R}_{ij}|) \qquad (34)$$

where $F(x) = \{x\cos(x) - \sin(x)\}/x^4$ and m^* is the effective electron mass. The form of F(x) is shown in figure 1. A more general expression was obtained by Mahanti and Das (1968), who lifted the restriction that $I_{nn'}(\underline{k},\underline{k}')$ be evaluated at the Fermi surface and that

Figure 1 .Graphical Representation of F(x)

The number n shows the position of $x = 2k_f R_{ij}$, where R_{ij} is the distance between nth nearest neighbours.

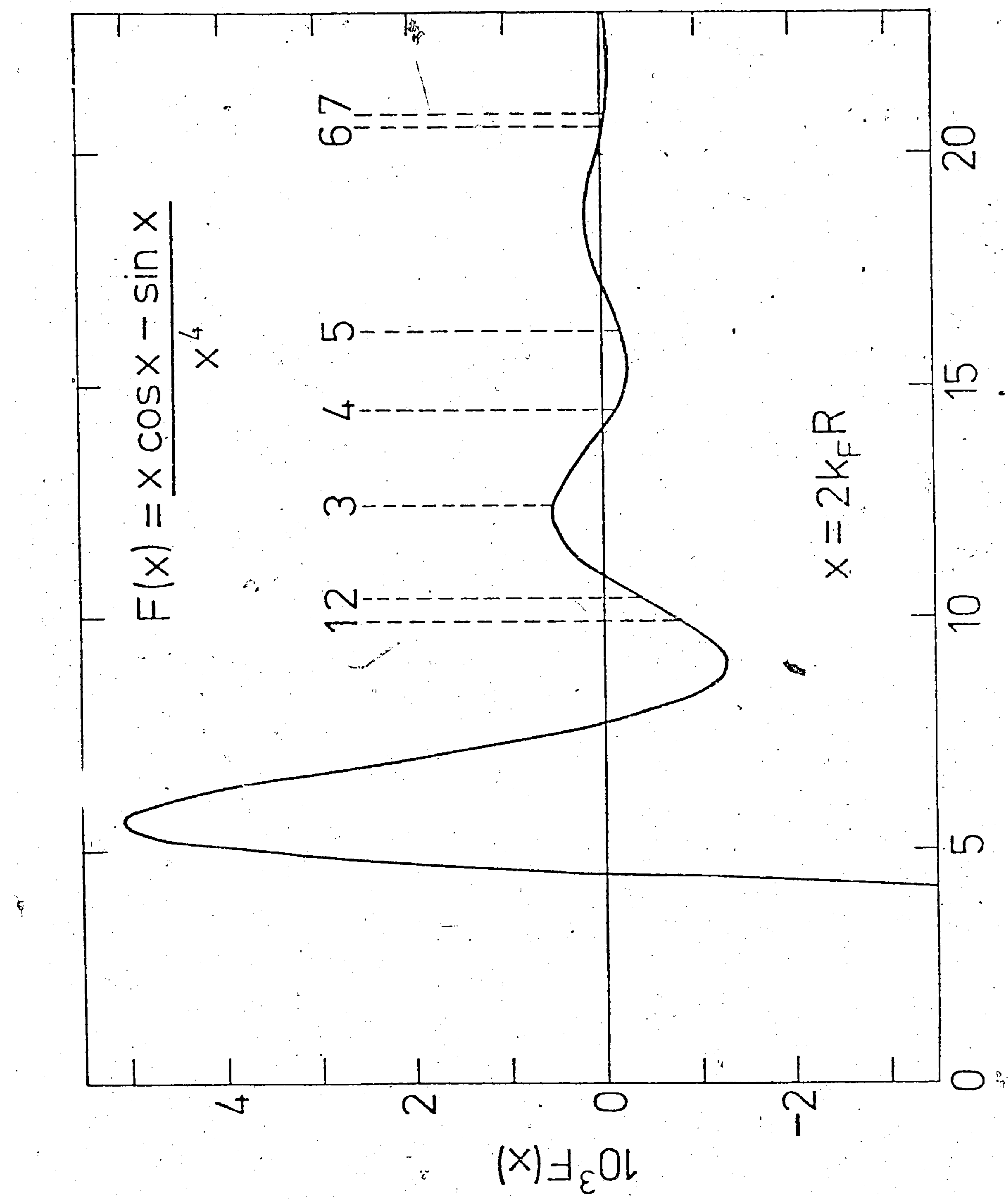
F(x) = (x cos x − sin x) / x^4
10^3 F(x)
x = 2k_F R
4
2
0
−2
0
5
10
15
20
1 2
3
4
5
6 7

the bands be parabolic. They obtained

$$J_{ij}^{(1)} = \{c/2(2\pi)^3 R_{ij}^2\}\int_0^{k_f} dk\ m^*(k)k\Phi(n\underline{k},n'\underline{k}')\sin(2kR_{ij}) \qquad (35)$$

where $c = -(16/3)^2\pi^2\gamma_i\gamma_j\gamma_e^2\hbar^4$ and $\Phi(n\underline{k},n'\underline{k}') = |\psi_{nk}(0)|^2|\psi_{n'k'}(0)|^2$.

Finally Roth, Zeiger and Kaplan (1966) lifted the restriction of spherical energy surfaces and derived more general expressions for $J_{ij}^{(1)}$. In particular, they found that $J_{ij}^{(1)}$ was proportional to R_{ij}^{-1} for directions perpendicular to two flat regions of the Fermi surface and $J_{ij}^{(1)}$ was proportional to R_{ij}^{-2} for directions perpendicular to the axis of a cylindrical region of the Fermi surface.

II(iv) Theoretical Lineshapes of Configurations of One, Two and Three Magnetic Nuclei

In this thesis we shall be comparing the experimental Sn^{117} resonance in a sample of β-tin which is rapidly rotated at the magic angle, with a theoretical lineshape in which only spin-lattice and Ruderman-Kittel interactions affect the lineshape. Because of the small abundance of magnetic isotopes in natural tin (0.35%, 7.67% and 8.68% for Sn^{115}, Sn^{117} and Sn^{119} respectively (NMR Tables, Varian Associates, 5th edition, 1965)), we synthesize the theoretical lineshape by combining, in appropriate proportions, the lineshapes of nuclei which are interacting with zero, one or two other magnetic nuclei. The probability of finding three or more magnetic nuclei in the vicinity of a particular nucleus is small.

Before proceeding, we shall discuss the application of equation (6) to the particular problem of calculating lineshapes in β-tin. This equation was obtained by assuming that the terms M, N and R' are much less than $1/\tau_c$. For β-tin the Knight Shift is approximately .73% (Smith, 1972) with a result that, for a field of approximately 5 kG, the order of magnitude of M for β-tin is 50 kHz. The magnitude of the Ruderman-Kittel interaction for nearest neighbours is a few kHz. Finally, the magnitude of R' is of the order of 6 kHz since T_1 is approximately 170 microseconds for Sn^{117} (it will be shown in this section that R' is of the order of $1/T_1$). Since $1/\tau_c$ is approximately 10^{11} seconds^{-1}, M, N and R' are much less than $1/\tau_c$.

When non-secular terms are included in equation (6), the effect of the terms $R'_{\alpha\alpha'\beta\beta'}$ for which $(\alpha-\alpha'+\beta-\beta')\Delta t \gtrsim 1$ can be ignored compared to the effect of terms $R'_{\alpha\alpha'\beta\beta'}$ for which

$$(\alpha-\alpha'+\beta-\beta')\Delta t \ll 1 \qquad (36)$$

because of the terms $A_{\alpha\alpha'\beta\beta'}$ (see equation (11)). As we neglect terms $R'_{\alpha\alpha'\beta\beta'}$ which do not satisfy (36) when calculating the lineshapes, we can replace $A_{\alpha\alpha'\beta\beta'}$ by the value 1 (the magnitude of $A_{\alpha\alpha'\beta\beta'}$ approaches 1 as $(\alpha-\alpha'+\beta-\beta')\Delta t$ approaches zero) and regain (6).

The equation can be simplified by considering the high temperature limit and short correlation time approximation, that is when $|E_\alpha - E_{\alpha'}|/\hbar \ll \tau_c^{-1} < kT/\hbar$, where E_α and $E_{\alpha'}$ represent eigenvalues of $\hbar(E+M+N)$. We can then replace $R'\sigma = R'(\sigma-\sigma^T)$ by $R(\sigma-\sigma^T)$ where R is derived from R' by using $k_{qq'}(\omega) \equiv j_{qq'}(\omega)e^{h\omega/2kT}$ in place of $j_{qq'}(\omega)$, the result being that $R_{\alpha\alpha'\beta\beta'} = R_{\beta\beta'\alpha\alpha'}$. Also we can set $k_{qq'}(\omega) = k_{qq'}(0)$ (Redfield, 1957). These approximations can be made since at room temperature (the temperature of the β-tin sample), $kT/\hbar \simeq 4\times10^{13}$ seconds^{-1}, $\tau_c \simeq 10^{-11}$ seconds and $|E_\alpha - E_{\alpha'}|/\hbar \simeq 10^8$ seconds^{-1}. We make two assumptions about $k_{qq'}$ which simplify the calculations. The first is that $k_{qq'}(0) = 0$ unless $q = q'$. Classically this means that there is no correlation between the random magnetic fields at different nuclear sites and between the various components of the random field at a given nuclear site. This turns out to be a good approximation for β-tin (Winter, 1972). The second assumption is that $k_{qq}(0) = k'$ where k is independent of q. This is a good approximation since McLachlan (1968) found that T_1 for Sn^{119} was essentially orientation independent.

Next we show that the resonance lineshape is unaffected by the operator N which appears in equation (6) provided N commutes with M_x , the x-component of the magnetization operator. The expectation value of M_x, is given by

$$\langle M_x\rangle = \sum_\alpha (\alpha|\sigma M_x|\alpha) \qquad (37)$$

and thus

$$\langle \dot{M}_x\rangle = \frac{d\langle M_x\rangle}{dt} = \sum_\alpha (\alpha|\dot{\sigma} M_x|\alpha) \qquad (38)$$

Substituting (6) into (38) we find that

$$\langle \dot{M}_x\rangle = \sum_\alpha (\alpha|[\sigma, E+M+N] M_x|\alpha) \qquad (39)$$

As a result, the value of $\langle M_x\rangle$ is not affected by N if $\sum_\alpha (\alpha|[\sigma,N]M_x|\alpha)$ is zero. This is easily shown to be the case if $[M_x,N] = 0$. We have

$$\sum_\alpha (\alpha|\sigma N M_x - N\sigma M_x|\alpha) = \sum_\alpha (\alpha|\sigma M_x N - N\sigma M_x|\alpha) = Tr(\sigma M_x N) - Tr(N\sigma M_x) = 0$$

since the trace is invariant under cyclic permutation of σ, M_x and N.

Finally we include the rf field (linearly polarized in the x direction). If H_{rf} is the rf field interaction, we have for equation (6)

$$\dot{\sigma}_{\alpha\alpha'} = i(E_{\alpha'}-E_\alpha)\sigma_{\alpha\alpha'} + \sum_{\beta\beta'} R_{\alpha\alpha'\beta\beta'}(\sigma_{\beta\beta'}-\sigma^{T}_{\beta\beta'}) + i\{\sum_{\alpha''}\sigma_{\alpha\alpha''}(\alpha''|H_{rf}|\alpha') - (\alpha|H_{rf}|\alpha'')\sigma_{\alpha''\alpha'}\}. \qquad (40)$$

Here E_α is an eigenvalue of the eigenstate $|\alpha)$ for the operator $\hbar(E+M+N)$, and the subscripts refer to the different eigenstates of this operator. From (10) we find

$$R_{\alpha\alpha'\beta\beta'} = (1/2\hbar^2)(2J_{\alpha\beta\alpha'\beta'} - \delta_{\alpha\beta}\Sigma J_{\gamma\alpha'\gamma\beta'} - \delta_{\alpha'\beta'}\Sigma J_{\gamma\beta\gamma\alpha}) \qquad (41)$$

where

$$J'_{\alpha\beta\alpha'\beta'} = \sum_{jq} 2\hbar^2\gamma_j^2 k'(\alpha|I_{jq}|\beta)(\beta'|I_{jq}|\alpha') . \qquad (42)$$

The index j is summed over the nuclei and q takes the values x, y and z. In obtaining (42), we have made use of the approximations involving $k_{qq'}$ ($k_{qq'} = \delta_{qq'}k'$).

In the following subsections A), B), C) and D) we consider the spectrum of nuclei which interact with no unlike nuclei, one unlike and no like nuclei, two unlike and no like nuclei, and one like and one unlike nuclei respectively. For these cases we have $\omega_X=\gamma_X(1+K)H_0$, and W_X is the relaxation rate of the [illegible] nucleus.

A) No Unlike Nuclei Affecting the Resonance

The lineshape function in this case has been shown previously (Smith, 1972) to be given by

$$\chi(\omega) = 4iZ_X\{i(\omega_X-\omega)-2W_X\}^{-1} \qquad (43)$$

where $Z_X = \gamma_X^2\hbar^2\omega_X/32kT$. We note that equation (43) applies whatever the number of like nuclei which are interacting since $J_{ij}\underline{I}_i\cdot\underline{I}_j$, where i and j are any two nuclei of a group of like nuclei, commutes with $M_X = \sum_\ell \gamma_\ell\hbar I_{\ell x}$, the x-component of the magnetization operator for the group.

B) One Unlike Nucleus (and No Like Nuclei) Affecting the Resonance

For this so-called XA case we generalize the calculation previously made by Smith (1972); we allow for different spin-lattice relaxation rates W_X and W_A for the X and A nuclei.

The four eigenstates are $|++)$, $|+-)$, $|-+)$ and $|--)$ which we number as $|1)$, $|2)$, $|3)$ and $|4)$ respectively. The symbol $|-+)$ represents the state where I_z of the nucleus X (whose spectrum we are determining) is -1/2 and I_z of the unlike nucleus A is +1/2. Using equation (40) we have

$$\dot{\sigma}_{12} = i\omega_{12}\sigma_{12} + i(\sigma_{11}^{T}-\sigma_{22}^{T})H_{21}/\hbar + R_{1212}\sigma_{12} + R_{1234}\sigma_{34} \quad (44)$$

$$\dot{\sigma}_{34} = i\omega_{34}\sigma_{34} + i(\sigma_{33}^{T}-\sigma_{44}^{T})H_{43}/\hbar + R_{3434}\sigma_{34} + R_{3412}\sigma_{12}.$$

Here H_{ij} is $(i|H_{rf}|j)$, while $\omega_{12} = \omega_X - J_{AX}\pi$ and $\omega_{34} = \omega_X + J_{AX}\pi$. Also $\omega_{ij} = (E_j-E_i)/\hbar$ and $H_{ij} = 0$ for $i>j$ except H_{21} or H_{43}. We used $R_{\alpha\beta\alpha\beta}\sigma_{\alpha\beta}$ since $\sigma_{\alpha\beta}^{T}=0$ if $\alpha=\beta$. We have only considered the time derivatives of σ_{12} and σ_{34} since σ_{ij}^{*} is equal to σ_{ji}. Also $\dot{\sigma}_{11}$ and $\dot{\sigma}_{22}$, which are respectively proportional to H_{12}^2 and H_{34}^2, can be ignored for low amplitudes of the rf field. Finally, we do not need to consider σ_{14} and σ_{23} since the rf field does not cause transitions between states $|1)$ and $|4)$ and between $|2)$ and $|3)$. The differences between equations (44) and those of Smith's for this case occur in the relaxation terms, the R's. We recalculate these terms and then alter Smith's results for the lineshape function by taking into account these differences.

It follows from equation (41) that

$$R_{\alpha\beta\alpha\beta} = -\sum_j \gamma_j^2 k'\{(\beta|\underline{I}_j^2|\beta)+(\alpha|\underline{I}_j^2|\alpha)\} + 2\sum_j \sum_q \gamma_j^2 (\alpha|I_{jq}|\alpha)(\beta|I_{jq}|\beta)k'. \quad (45)$$

The first part of the right hand side of (45) is equal to $-(3/2)k'(\gamma_X^2 + \gamma_A^2)$ which equals $-(3/2)(W_X+W_A)$ where $k'\gamma_X^2$ is defined as W_X, the spin-lattice relaxation rate for the X nucleus and $k'\gamma_A^2$ is defined as W_A, the spin-lattice relaxation rate of the A nucleus. The second part of (45) is equal to $(W_A - W_X)/2$ with the result that

$$R_{1212} = R_{3434} = -W_A - 2W_X . \tag{46}$$

By rearranging (41) for the case where α, α', β and β' are all unequal we find

$$R_{\alpha\beta\alpha'\beta'} = \sum_j \gamma_j^2 k'\{(\alpha|I_{j+}|\alpha')(\beta'|I_{j-}|\beta) + (\alpha|I_{j-}|\alpha')(\beta'|I_{j+}|\beta)\} \tag{47}$$

where $I_{j+} = I_{jx} + iI_{jy}$ and $I_{j-} = I_{jx} - iI_{jy}$. It follows that

$$R_{1234} = R_{3412} = \gamma_A^2 k' + \gamma_A^2 k' = 2W_A , \tag{48}$$

the lineshape function is given by

$$\chi(\omega) = 2iZ_X(\lambda_{34} + \lambda_{12} - 2W_A)/(\lambda_{12}\lambda_{34} - W_A^2) \tag{49}$$

where $\lambda_{ij} = i(\omega_{ij} - \omega) - W_A - 2W_X$.

C) Two Unlike Nuclei (and No Like Nuclei) Affecting the Resonance

For this case there are three nuclei: the nucleus X (whose spectrum we are calculating), and the two unlike nuclei, A and A'. The prime indicates that the two A type nuclei are differently coupled to the X nucleus and the spectrum is called the XAA' spectrum. In his calculations of the XAA' spectrum, Smith (1972) assumed that $W_X = W_A$ and that the A and A' nuclei are not coupled. Since we wish to remove these restrictions it is necessary to recalculate the XAA' spectrum ab initio.

The eigenstates for this case (and case D in which we consider the AA' resonance) are given in table 1(a). In table 1(b) a transition $\alpha \leftrightarrow \alpha'$ is considered to belong to the XAA' spectrum if

Table 1 The Eigenstates and Transition Energies for the $\underline{X}AA'$ and $\underline{AA'}X$ Spectra

Table 1(a) gives the eigenstates and Table 1(b) gives the transition energies in units of h. The symbols D and 2α are defined as $(J_{AA'}^2 + (J_{AX}-J_{A'X})^2/4)^{\frac{1}{2}}/2$ and $\sin^{-1}(J_{AA'}/2D)$ respectively (Pople et al, 1959). Here we have $\nu_{ij} = \omega_{ij}/2\pi$.

$|1\rangle = |+++\rangle$

$|2\rangle = |++-\rangle$

$|3\rangle = \cos\alpha\,|+-+\rangle + \sin\alpha\,|-++\rangle$

$|4\rangle = -\sin\alpha\,|+-+\rangle + \cos\alpha\,|-++\rangle$

$|5\rangle = \sin\alpha\,|+--\rangle + \cos\alpha\,|-+-\rangle$

$|6\rangle = -\cos\alpha\,|+--\rangle + \sin\alpha\,|-+-\rangle$

$|7\rangle = |--+\rangle$

$|8\rangle = |---\rangle$

(a)

LEVELS BETWEEN WHICH THERE IS A TRANSITION	TRANSITION TYPE	TRANSITION ENERGY (IN UNITS OF h)
8 ⟷ 6	AA′	$\nu_{68} = \nu_{AA'} + 1/4\,(-2J_{AA'} - J_{AX} - J_{A'X}) - D$
7 ⟷ 4	AA′	$\nu_{47} = \nu_{AA'} + 1/4\,(-2J_{AA'} + J_{AX} + J_{A'X}) - D$
5 ⟷ 2	AA′	$\nu_{25} = \nu_{AA'} + 1/4\,(2J_{AA'} - J_{AX} - J_{A'X}) - D$
3 ⟷ 1	AA′	$\nu_{13} = \nu_{AA'} + 1/4\,(2J_{AA'} + J_{AX} + J_{A'X}) - D$
8 ⟷ 5	AA′	$\nu_{58} = \nu_{AA'} + 1/4(-2J_{AA'} - J_{AX} - J_{A'X}) + D$
7 ⟷ 3	AA′	$\nu_{37} = \nu_{AA'} + 1/4\,(-2J_{AA'} + J_{AX} + J_{A'X}) + D$
6 ⟷ 2	AA′	$\nu_{26} = \nu_{AA'} + 1/4\,(2J_{AA'} - J_{AX} - J_{A'X}) + D$
4 ⟷ 1	AA′	$\nu_{14} = \nu_{AA'} + 1/4\,(2J_{AA'} + J_{AX} + J_{A'X}) + D$
8 ⟷ 7	X	$\nu_{78} = \nu_{X} - 1/2\,(J_{AX} + J_{A'X})$
5 ⟷ 3	X	$\nu_{35} = \nu_{X}$
6 ⟷ 4	X	$\nu_{46} = \nu_{X}$
2 ⟷ 1	X	$\nu_{12} = \nu_{X} + 1/2\,(J_{AX} + J_{A'X})$
5 ⟷ 4	X	$\nu_{45} = \nu_{X} - 2D$
6 ⟷ 3	X	$\nu_{36} = \nu_{X} + 2D$

(b)

$\left|\frac{E_\alpha - E_{\alpha'}}{\hbar}\right|$ is nearer ω_X than ω_A (otherwise the transition belongs to the $A\acute{A}X$ spectrum). The frequencies ω_X and ω_A are assumed to be far enough apart that the probability of the rf field flipping an A nucleus is negnegligible near For the XAA' spectrum we need only consider the time derivatives of σ_{12}, σ_{35}, σ_{36}, σ_{45}, σ_{46} and σ_{78}. The time derivatives of the other values of σ_{ij} are not considered because the transitions $i \leftrightarrow j$ are part of the $AA'X$ spectrum or for reasons similar to those given in part B. For the XAA' spectrum we have

$$\sigma_{\alpha\alpha'} = i\omega_{\alpha\alpha'}\sigma_{\alpha\alpha'} + iU_{\alpha\alpha'} + \Sigma R_{\alpha\alpha'\beta\beta'}\sigma_{\beta\beta'} \tag{50}$$

where α,α' and β,β' take on values 1,2; 3,5; 3,6; 4,5; 4,6; and 7,8. Also

$$U_{ij} = \hbar^{-1}(\sigma_{ii} - \sigma^T_{jj})H_{ji} = (2\hbar)^{-1}(\sigma_{ii} - \sigma^T_{jj})H_{xo}M_{ji}e^{i\omega t}. \tag{51}$$

Here $M_{ji} = (j|M_x|i)$, where $M_x = -\Sigma_\ell \gamma_\ell \hbar I_{\ell x}$, and H_{xo} is the amplitude of the linearly-polarized rf field of frequency ω. We can approximate U_{ij} as

$$U_{ij} \simeq \omega_X H_{xo} e^{i\omega t}(j|-\Sigma_\ell \gamma_\ell \hbar I_{\ell x}|i)/16kT \tag{52}$$

since $\sigma^T_{ii} - \sigma^T_{jj} = (e^{-E_i/kT} - e^{-E_j/kT})/(\Sigma_\ell e^{-E_\ell/kT})$

$$\simeq \{(E_j - E_i)/kT\}/(\Sigma_\ell e^{-E_\ell/kT}) \simeq \hbar\omega_X/8kT.$$

It should be noted that $R_{\alpha\alpha'\beta\beta'} = R_{\beta\beta'\alpha\alpha'}$, and that $R_{1278} = 0$ since $R_{1278} = (1/2\hbar^2)2J_{1728} = (1/\hbar^2)\Sigma_j \Sigma_q 2\hbar^2\gamma_j^2(1|I_{jq}|7)(8|I_{jq}|2)k'$ and $(8|I_{jq}|2) = 0$. For R_{nmnr} where m is not equal to r, we have

$$R_{nmnr} = (2J_{nnmr} - \Sigma_q J_{qmqr})/2\hbar^2 \tag{53}$$

and

$$\sum_q J_{\ell m \ell r} = \sum_j \sum_q \sum_\ell 2\hbar^2\gamma_j^2 k'(\ell|I_{jq}|m)(r|I_{jq}|\ell)$$
$$= \sum_j \sum_q 2\hbar^2\gamma_j^2 k'(r|I_{jq}^2|m) = \sum_j 2\hbar^2\gamma_j^2 3k'(r|m)/4 = 0 \qquad (54)$$

since the eigenstates are orthogonal. Finally

$$\hbar^{-2}J_{nnmr} = \sum_j \sum_q 2\gamma_j^2(r|I_{jq}|n)(r|I_{jq}|m)k'$$
$$= 2k'\{\gamma_A^2(n|I_{Az}|n)(r|I_{Az}|m)+\gamma_A^2(n|I_{Az}|n)(r|I_{Az}|m)\}. \qquad (55)$$

Using (54) and (55), we obtain

$$R_{3536} = -R_{3545} = -R_{3646} = -W_A\cos(2\alpha)\sin(2\alpha) \qquad (56)$$

where α is defined in table 1.

For R_{mnmn} we have

$$2\hbar^2 R_{mnmn} = 2J_{mmnn} - \sum_q (J_{qmqm}+J_{qnqn}) \qquad (57)$$

and

$$\sum_q (J_{qmqm}+J_{qnqn}) = \sum_j \sum_q \sum_\ell \{2\hbar^2\gamma_j^2(q|I_{j\ell}|m)(m|I_{j\ell}|q)k' + 2\hbar^2\gamma_j^2(q|I_{j\ell}|n)(n|I_{j\ell}|q)k'\}$$
$$= 2\hbar^2\sum_j \gamma_j^2 k'\{(n|\underline{I}_j^2|n)+(m|\underline{I}_j^2|m)\} = 3\hbar^2(2W_A+W_X). \qquad (58)$$

After determining J_{mmnn} for each R_{mnmn}, we have

$$R_{1212} = R_{7878} = -2W_A-2W_X$$
$$R_{3535} = R_{4646} = -3W_A-W_A\cos(2\alpha)-2W_X \qquad (59)$$
$$R_{3636} = R_{4545} = -3W_A+W_A\cos(2\alpha)-2W_X.$$

For R_{mnqr} such that all subscripts are different and at least one of the subscripts is not 3, 4, 5 or 6 we have

$$\hbar^2 R_{mnqr} = J_{mqnr} = \sum_j \sum_\ell 2\gamma_j^2 k'(m|I_{j\ell}|q)(r|I_{j\ell}|n)$$
$$= \sum_j \gamma_j^2 k'\{(m|I_{j+}|q)(r|I_{j-}|n) + (m|I_{j-}|q)(r|I_{j+}|n)\}. \qquad (60)$$

Using (60) we have

$$R_{1235} = R_{1246} = R_{3578} = R_{4678} = W_A \sin(2\alpha)$$
$$R_{1245} = R_{4578} = -R_{1236} = -R_{3678} = W_A \cos(2\alpha). \qquad (61)$$

Finally we need to determine R_{3546} and R_{3645}. In this case

$$\hbar^2 R_{mnqr} = J_{mqnr} = 2k'\gamma_A'^2\{(m|I_{Az}|q)(r|I_{Az}|n)+(m|I_{A'z}|n)(r|I_{A'z}|n)\}. \qquad (62)$$

Using (62) we find that $R_{3546} = R_{3645} = W_A \sin^2(2\alpha)$.

Letting $\sigma_{ij} = r_{ij}\exp(i\omega t)$ be the solution, we obtain a set of linear equations, which in matrix form is

$$\underline{\underline{A}}\cdot\underline{r} = iH_{xo}Z_X\underline{P}/\gamma_X\hbar \qquad (63)$$

where $\underline{A}$, $\underline{r}$ and $\underline{P}$ are given in table 2(a). To calculate the spectrum we note that

$$\langle M_X\rangle = \sum_{ij}\sigma_{ij}(i|M_X|j) = \text{Real}\{-\gamma_X\hbar\underline{r}\;\underline{P}e^{i\omega t}\} \qquad (64)$$

since $-\gamma_X\hbar P_{ij}/2 = (i|M_X|j)$. Since $\langle M_X\rangle$ is equal, by definition, to the real part of $\chi(\omega)H_{xo}e^{i\omega t}$, we have

$$\chi(\omega)H_{xo} = -\gamma_X\hbar\underline{r}\cdot\underline{P}\;. \qquad (65)$$

D) One Unlike Nucleus and One Like Nucleus Affecting the Resonance

The eigenstates for this case are identical with the eigenstates for the $\underline{X}AA'$ spectrum and are given in table 1(a). The transitions and the corresponding frequencies are given in table 1(b). We shall merely quote the result in matrix form since the method is similar to that used to find the $\underline{X}AA'$ spectrum. We find

Table 2 Matrices and Vectors for the $\underline{AA'}X$ and $X\underline{AA'}$ Spectra

The symbols S and C are defined as sin2α and cos2α respectively. Table 2(a) gives $\underline{A}$, $\underline{P}$ and $\underline{r}$ for the $X\underline{AA'}$ spectrum. Here $\mu_{ij} = i(\omega_{ij}-\omega) - 2W_X - V_{ij}$, where $V_{12} = V_{78} = 2W_A$, $V_{35} = V_{46} = W_A(3+C^2)$ and $V_{36} = V_{45} = W_A(3-C^2)$. Table 1(b) gives $\underline{\underline{A}}$, $\underline{P}$ and $\underline{r}$ for the $\underline{AA'}X$ spectrum. Here $\mu_{ij} = i(\omega_{ij}-\omega) - 3W_A - W_X$; and $p_1 = \sin\alpha - \cos\alpha$ and $p_3 = \sin\alpha + \cos\alpha$.

$$
\underline{\underline{A}} = \begin{bmatrix}
\mu_{12} & W_A S & -W_A C & W_A C & W_A S & 0 \\
W_A S & \mu_{35} & -W_A CS & W_A CS & W_A S^2 & W_A S \\
-W_A C & -W_A CS & \mu_{36} & W_A S^2 & W_A CS & -W_A C \\
W_A C & W_A C & W_A S^2 & \mu_{45} & W_A CS & W_A C \\
W_A S & W_A S^2 & W_A CS & W_A CS & \mu_{46} & W_A S \\
0 & W_A S & -W_A C & W_A C & W_A S & \mu_{78}
\end{bmatrix}
$$

$$\underline{p}^T = \left[1, S, -C, C, -S, 1\right]$$

$$\underline{r}^T = \left[r_{12}, r_{35}, r_{36}, r_{45}, r_{46}, r_{78}\right]$$

(a)

$$
\underline{\underline{A}} = \begin{bmatrix}
\mu_{68} & W_X S & -W_A C & 0 & 0 & -W_X C & -W_A S & 0 \\
W_X S & \mu_{47} & 0 & W_A C & W_X C & 0 & 0 & -W_A S \\
-W_A C & 0 & \mu_{25} & W_X S & W_A S & 0 & 0 & W_X C \\
0 & W_A C & W_X S & \mu_{13} & 0 & W_A S & -W_X C & 0 \\
0 & W_X C & W_A S & 0 & \mu_{58} & W_X S & -W_A C & 0 \\
-W_X C & 0 & 0 & W_A S & W_X S & \mu_{37} & 0 & W_A C \\
-W_A S & 0 & 0 & -W_X C & -W_A C & 0 & \mu_{26} & W_X S \\
0 & -W_A S & W_X C & 0 & 0 & W_A C & W_X S & \mu_{14}
\end{bmatrix}
$$

$$\underline{r}^T = \left[r_{68}, r_{47}, r_{25}, r_{13}, r_{58}, r_{37}, r_{26}, r_{14}\right]$$

$$\underline{p}^T = \left[p_1, -p_1, p_3, p_3, p_3, p_3, p_1, -p_1\right]$$

(b)

that

$$\chi(\omega)H_{xo} = -\gamma_A \hbar \underline{r}\cdot\underline{P} \tag{66}$$

where $\underline{r}$ is the solution of the mátrix equation

$$\underline{\underline{A}}\cdot\underline{r} = iH_{xo}Z_A\underline{P}/\gamma_A\hbar. \tag{67}$$

Here $\underline{\underline{A}}$ and $\underline{P}$ are given in table 2(b) and $Z_A = \gamma_A^2\hbar^2\omega_A/32kT$.

It should be noted that (66) gives the spectrum for both the A and A$'$ nuclei. As we require the spectrum for the A nucleus, it is necessary to substitute the vector $\underline{P} = (-a,b,a,b,b,a,b,-a)^T$, where $a = \sin\alpha$ and $b = \cos\alpha$, in ..ace of $\underline{P}$ in (66).

II(v) Theoretical Models of the Ruderman-Kittel Interaction in β-tin

In this section we show how the theoretical Sn^{117} NMR line-shape in β-tin is synthesized. We first consider the spectrum of each Sn^{117} nucleus, taking into account, insofar as possible, the interactions with other magnetic nuclei located in the first, second and third nearest-neighbour shells (since the Ruderman-Kittel interaction is believed to be of moderately short range, it is possible to neglect more distant magnetic nuclei or to treat their effect in a more approximate fashion). We therefore need only consider the more common configurations or small groups in which we find a Sn^{117} nucleus. Because of the complexity of the calculation, we have so far been able to derive expressions only for groups of one, two and three nuclei (apart from the trivial case where there are four or more nuclei which are all identical). This is not a severe limitation since the isotopic abundance of the magnetic nuclei Sn^{115}, Sn^{117} and Sn^{119} is so small (see section II(iv)) that the probability of finding more than two magnetic nuclei in the inner three shells is small (according to Smith (1972), the probability is 19.7%).

We consider three theoretical models for the Ruderman-Kittel interaction in β-tin. For each model we take different relative values of the strength of the first, second and third nearest neighbour interactions. However, before discussing each model individually, we shall describe a slight modification to the notation. By X<u>X</u>A we mean that both the X' and A nuclei interact with the X nucleus but not with each other. This contrasts with the notation $\underline{X}X'A$ in which there is in general an interaction between all three nuclei. We similarly dis-tinguish between the $A\underline{X}A'$ and the $\underline{X}AA'$ cases.

The first model that we shall consider is the nearest neigh-bour model. Here, we only consider interactions between nearest neigh-bour magnetic nuclei (each site has four nearest neighbours). We con-sider the following basic configurations: $\underline{X}$, $\underline{X}A$, $\underline{X}AA'$, $A\underline{X}A'$, $\underline{X}X'A$ and $X'\underline{X}A$. For this model and the second nearest neighbour model (to be described) there is an interaction between the X' and A nuclei, but not between the X and A nuclei for the $\underline{X}X'A$ configuration. Similar-ly there is an interaction between the A and A' nuclei but not between the X and A' nuclei for the $\underline{X}AA'$ configuration. Some of the other con-figurations have resonances which are equivalent to one of the basic configurations (for example, the $\underline{X}X'$ configuration has a resonance which is identical to the $\underline{X}$ configuration, and the $\underline{X}AX'$ configuration has the same spectrum as the $\underline{X}A$ configuration if there is no interac-tion between the X and X' nuclei). The probabilities of nuclei having a resonance equivalent to one of the basic configurations' resonances are given in table 3 under the heading 'exact'. For this model, 86.67% of the Sn^{117} nuclei have a resonance equivalent to the reso-nance of one of the basic configurations. For the remaining 13.33% of the Sn^{117} nuclei, we have approximated their resonance by the reso-nance of the basic configuration which it most resembles. The prob-abilities of these approximate resonances are given under the heading 'approx.' and the sum of the exact and approximate probabilities are

SYNTHESIS OF Sn^{117} SPECTRUM (β-TIN)

SPECTRUM	NEAREST-NEIGHBOURS (4) ONLY			SECOND NEAREST-NEIGHBOURS (2) ONLY		
	EXACT	APPROX.	TOTAL	EXACT	APPROX.	TOTAL
$\underline{X}$	0·6173	0·0298	0·6471	0·8139	0·0021	0·8160
$\underline{X}A$	0·1572	0·0040	0·1612	0·1369	0·0000	0·1369
$X'\underline{X}A$	0·0251	0·0386	0·0637	0·0105	0·0033	0·0138
$\underline{X}X'A$	0·0251	0·0153	0·0404	0·0105	0·0010	0·0115
$A\underline{X}A$	0·0193	0·0207	0·0400	0·0068	0·0014	0·0082
$\underline{X}AA'$	0·0227	0·0249	0·0476	0·0113	0·0023	0·0136
TOTALS	0·8667	0·1333	1·0000	0·9899	0·0101	1·0000

Table 3 The Probabilities for the First and Second Nearest Models

given under the heading 'total' in table 3.

The second nearest neighbour model is similar to the nearest neighbour model except that only second nearest neighbour interactions are considered. All other Ruderman-Kittel interactions are assumed to be negligible. As there are only two second nearest neighbour sites for each nuclear site, the probabilities for the configurations listed in table 3 differ from those for the nearest neighbour model.

The third model is the Ruderman-Kittel model. Here we use equation (34) to obtain the relative values of J_{ij} for each nucleus i and j. Using the information given in the caption of figure 2, we obtain relative values of 1.0, 0.478, -0.603 and 0.145 for J_{ij} for first, second, third and fourth nearest neighbour nuclei. We see that the fourth nearest neighbour interaction is relatively small, thereby justifying our decision to treat explicitly only those magnetic nuclei in the inner three shells, which consist of four nearest neighbour, two second nearest neighbour and four third nearest neighbour sites.

The probabilities of occurence of $\underline{X}$, $\underline{X}A$, $\underline{X}AA'$ and $\underline{X}X'A$ configurations are given in table V of Smith's thesis and will not be repeated here (in arriving at these probabilities, Smith ignored the Sn^{115} isotope because of its relatively small abundance). However, it should be noted that in 26.7% of the configurations involving three magnetic nuclei, the two magnetic neighbours are either first, second or third nearest neighbours of each other. We have taken such 'cross' interactions into account though they were ignored by Smith.

Finally, we take into account in an approximate fashion the effect of magnetic neighbours outside the inner three shells. The most

Figure 2 Structure of β-tin

The point group symmetry for β-tin is $\bar{4}$ 2 m, with a = 5.831 Å and c = 3.181 Å at room temperature (Pearson, 1967). The numbered nuclei are examples of the nearest neighbours to nucleus A, the number n indicating the nth nearest neighbour. The number of first, second, third and fourth nearest neighbour nuclei are four, two, four and four respectively. Using this structure and the free electron model, we obtain a value of $2k_f$ = 3.272×10^8 cm^{-1}.

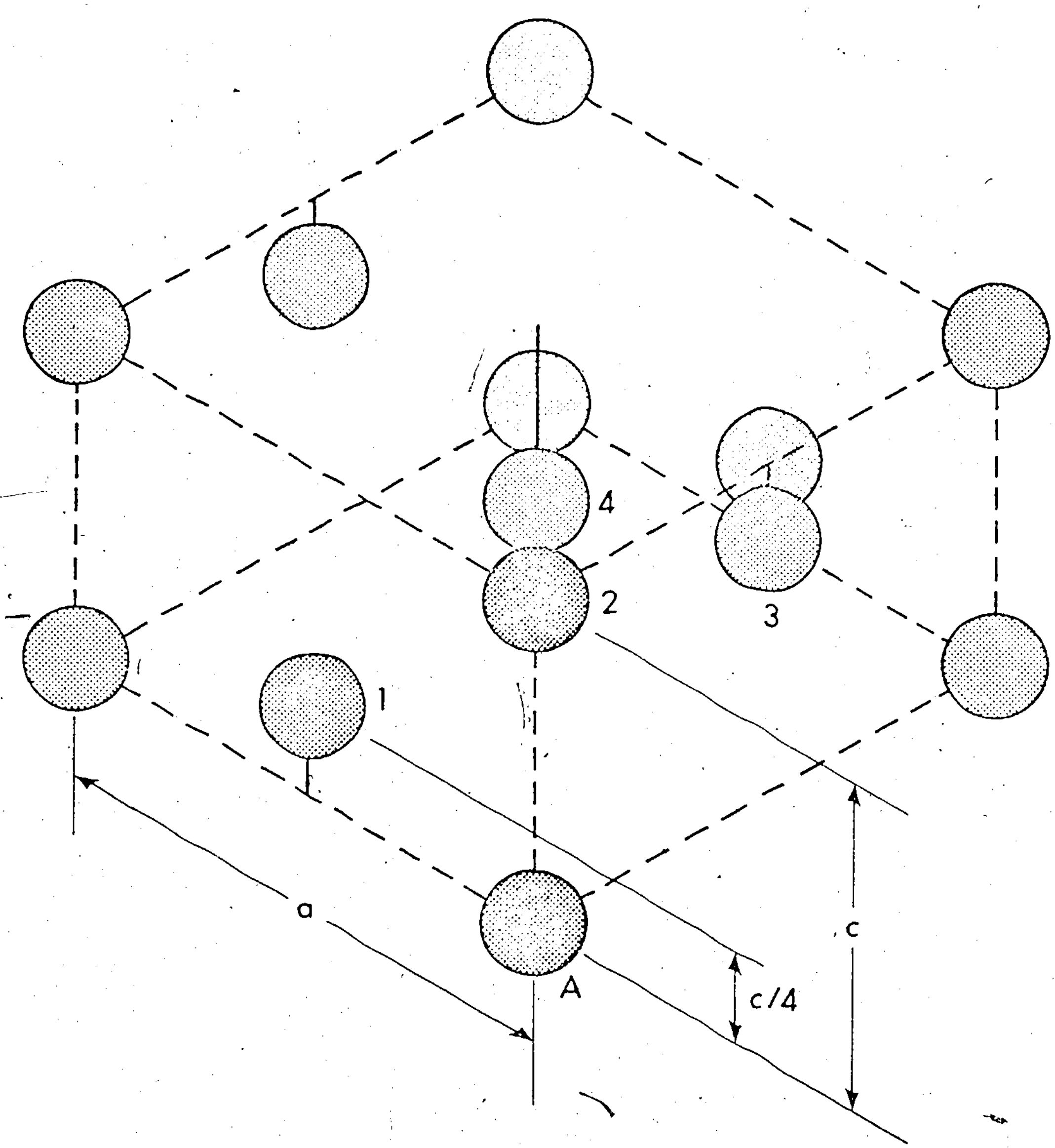
4
2
3
1
a
A
c/4
c

important effect of such nuclei is the broadening produced by the unlike nuclei. However their effect is approximately equivalent to an apparent increase in the relaxation rate of the X nucleus. This point is discussed in appendix IV.

It will be seen that we have ignored interactions between the more distant magnetic nuclei and those located in the inner three shells. It can be shown that this is quite a good approximation (D. G. Hughes, private communication). The effect of mutual interactions between nuclei outside the inner three shells are expected to be equivalent to a small reduction in the average spin-lattice relaxation rate of such nuclei. Such effects are taken into account by the introduction of a fitting parameter ξ as described in appendix IV.

The theoretical spectra which are required to synthesize the Sn^{117} lineshape are found using the results of section II(iv). To find the X and XA lineshapes, we use equations (43) and (49) respectively. The XAA′ lineshape is given by equation (65) in conjunction with equation (63). The XX′A lineshape is given by quation (66) together with (67). The solution of equation(65) is given in appendix II while the solution of (66) is given in appendix III.

III APPARATUS AND EXPERIMENTAL PROCEDURE

In order to study the Ruderman-Kittel interaction, samples of tin were rapidly rotated about an axis inclined at the magic angle to $\underline{H}_o$. While this could be done by spinning the sample about a vertical axis and tilting the magnet until the magic angle condition is satisfied, we chose to spin the sample about an axis inclined to the vertical so that the magnet could be kept horizontal.

The high speed rotation was achieved using an air turbine similar to that pioneered by Beams (1937). In this system air under pressure passes through fine holes or jets drilled at a suitable angle in a conical stator and impinges upon flutings machined into a conical rotor. These jets of air lift the rotor off the stator and start it spinning. The rotor does not fly out of the stator but rides upon a thin cushion of air just above the stator surface, as can be understood by the application of Bernoulli's principle. According to this principle the pressure on the underside of the rotor is related to atmospheric pressure by the relation

$$P_{lower} + \rho v^2/2 = P_{atmos} \tag{1}$$

where ρ is the density of air and v is the velocity of the air in contact with the underside of the rotor. Since P_{lower} is smaller than P_{atmos}, there is a downward force on the rotor which tends to keep the rotor in the stator. Indeed, this force even enables the rotor to spin upside down.

Since the turbine had to be operated within the rf coils of the Varian NMR probe, the stator and rotor were made of nylon. Most of the rotors were made out of Delrin (Ertacetyl H) which has better mechanical properties than ordinary nylon (much larger moduli of elasticity and about 20% greater tensile strength). The stator was constructed so that the axis of rotation of the rotor made an angle of 40 degrees to the cylindrical stator support which just fitted within the Varian probe. Because the stator support was perpendicular to $\underline{H}_o$, the axis could make any angle between 50 and 90 degrees with $\underline{H}_o$, merely by rotating the whole stator assembly. The magic angle ($54^o44'$) could therefore be obtained by suitably orientating the stator.

The stator previously described by Smith (1972) was used for the present measurements. However, our rotors differed substantially from those used by Smith, and the design is shown in figure 3. They were hollowed out so as to achieve a maximum sample volume consistent with stable rotation within the Varian probe (inner diameter 1.7 cm). The sample volume of the rotors ranged between 0.23 and 0.25 cm^3 and was 2 or 3 times as large as those used by Smith. Another point should should be made about our design. The center of the plane through x'-x and perpendicular to the axis of symmetry of the rotor, a, is approximately in the same position during rotation. The center of gravity, g, obviously lies along the axis of rotation. As a result, the axis of rotation goes through points g and a to a good approximation. Thus, large perturbations result if the angle between the line g-a and the line a-b is large. This can occur for slight asymmetry of the rotor if g is very close to a. In our design, g was located as far above the x-x' plane as possible. We attribute the improved stability of

Figure 3 The Rotor and Stator

Here a, b, x, x' and g are defined in the main body of the thesis; jets of air pass through a from d; e is the stabilizing (relief) jet (Smith, 1972); f gives the position of the walls of the interior of the Varian probe; g' gives the position of the receiver coils; h and i represent the two parts of the stator which are glued together (Smith, 1972).

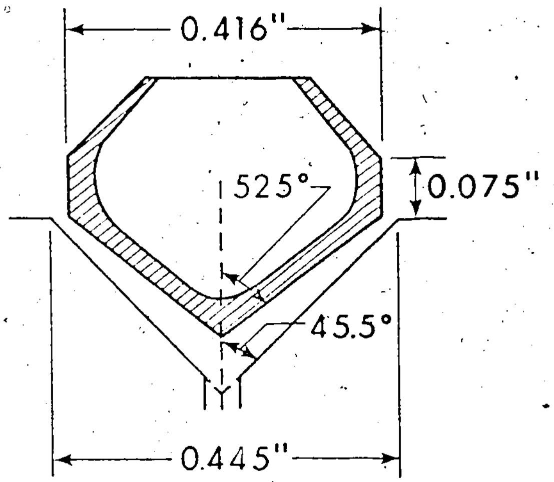
0.416"
525°
0.075"
45.5°
0.445"

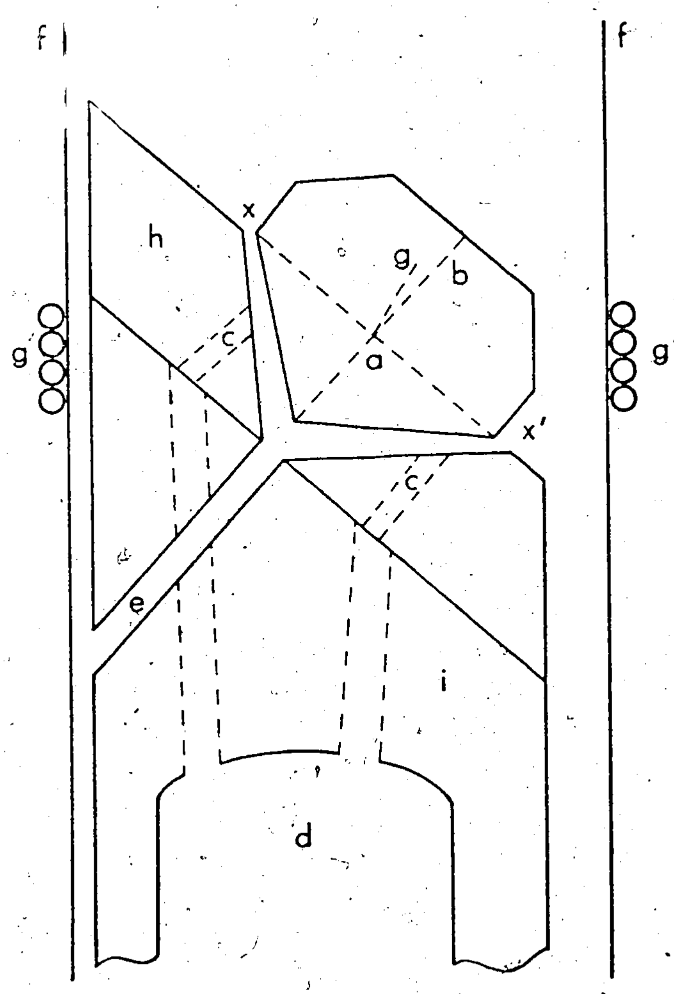
f
f
x
h
g
b
c
a
g
g'
x'
c
e
i
d

our rotors largely to this modification. We also found that a more stable rotation of the rotors was achieved when the maximum diameter of the rotor was less than the diameter of the top of the conical section of the stator. Both eight and twelve flute rotors were used. However, little consistent difference between the two types was observed.

In order to achieve full penetration of the rf field into the metal, the samples consisted of powder set in epoxy glue. The tin was purchased from Fisher Scientific Company. The purity is believed to be in the range 99.9 to 99.99%. However attempts to confirm this with Fisher Scientific have so far failed. In order to accurately determine the magic angle setting, a small amount of aluminum powder (roughly 10% by volume) was added to the tin powder and the magic angle was obtained using the Al^{27} resonance.

The advantages in using the Al^{27} resonance to find the magic axis are:

(a) The spin-lattice relaxation time, T_1, for Al^{27} is approximately 6.3 milliseconds at room temperature so that the linewidth (defined as the interval between points of maximum and minimum slope of the absorption line) associated with the T_1 broadening is 30 Hz (compared with more than 1 kHz for Sn^{117} and Sn^{119}).

(b) The natural abundance of Al^{27} is 100% which means that the Ruderman-Kittel interaction should not broaden the Al^{27} resonance in pure aluminum (at least in principle).

(c) The peak to peak derivative linewidth in a stationary sample of aluminum is 9.4 kHz (Gutowsky and McGarvey, 1952), whereas the corresponding linewidth for Sn^{117} and Sn^{119} in pure tin is 3 kHz or more (the precise value depends on the field strength because of the anisotropic Knight Shift).

(d) For equal numbers of nuclei, the NMR signal strength for Al^{27} at constant frequency is more than 8 times as strong as that of Sn^{117}. Moreover only 7.67% of natural tin nuclei are Sn^{117} whereas 100% of aluminum nuclei are Al^{27} (NMR Tables, Varian Associates, 5th edition, 1965).

It should be noted that there is a possibility of a nuclear quadrupole interaction in aluminum on account of the spin number 5/2 of Al^{27}. Lattice defects or strains may give rise to non-zero electric field gradients at the nuclear sites. However, this quadrupole broadening should average out provided the sample is spun sufficiently rapidly.

In making the samples, sufficient epoxy was used to avoid air bubbles in the mixture, since these would seriously unbalance the rotors.

The equipment used to supply the air to the turbine has been described by Smith (1972) and will not be described here. Standard techniques were used to measure the speed of the rotors (Henriot and Huguenard, 1925).

The NMR signals were observed in the absorption mode using a commercial Varian wide-line spectrometer, model VF16B. It was found that the noise output of the spectrometer increased when the rotor was spinning. The excess noise was found to extend over a wide frequency range so that it could not easily be filtered out. Its magnitude was found to be proportional to the rf voltage across the transmitter coil, indicating that the source of the problem was a microphonic vibration of the NMR coil system which modulated the coupling between the transmitter and receiver coils. It was found that placing cotton wool near the top of the Varian probe (where the sample was introduced into the probe) reduced the microphonic effect, presumably by damping out the acoustic vibrations. Also, masking tape was placed along the inner walls of the Varian probe (except over the receiver coil) to further reduce microphonics. As a precaution, we reduced the audio bandwidth of the spectrometer immediately following the detector from about 10 kHz to about 500 Hz to prevent overloading due to the large signal present at the frequency of rotation (approximately 5 kHz).

The NMR signals were recorded as the first derivative of the absorption by using a sinusoidal field modulation at 37 Hz in conjunction with lock-in detection. The output of the lock-in detector was fed to a 1024-channel digital signal averager, Fabritek model 1062. A block diagram of the equipment is shown in figure 4.

Synchronization of the magnetic field sweep and the internal sweep of the Fabritek signal averager was achieved by triggering the signal averager with a signal from a photodiode which was turned on by light reflected from a piece of aluminum foil attached to the rotating field-sweep potentiometer of the Varian Fieldial regulator. Repeated sweeps through the resonance made during a 12 hour period were stored in one half of the memory of the signal averager. This procedure enabled us to cancel any slight asymmetry in the signal caused by the

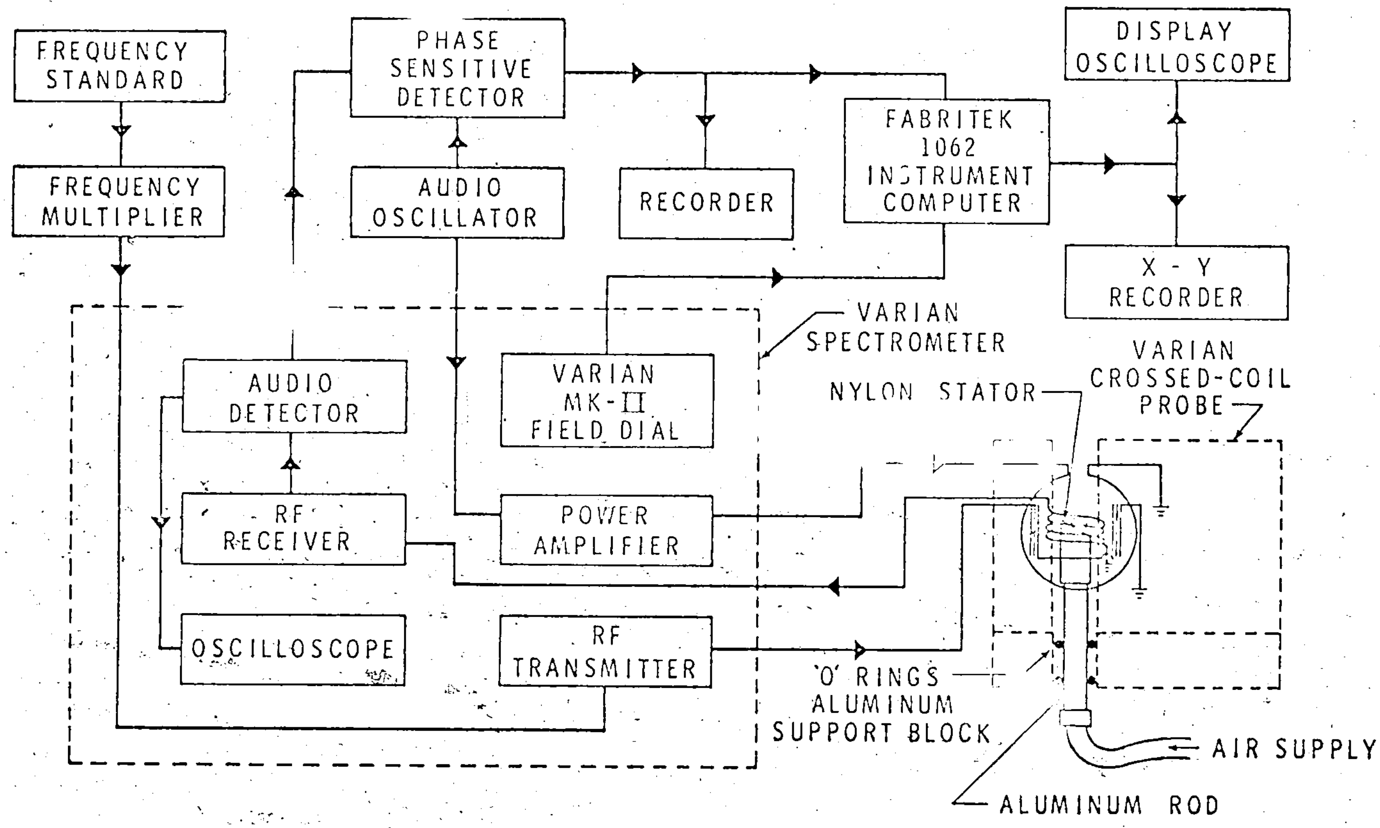

Figure 4 Block Diagram of Apparatus

lock-in detector, by switching the polarity of the signal fed into the signal averager from the lock-in detector after each twelve hour run. The results of each 12 hour run were then transferred (with appropriate polarity) into the other half of the signal averager's memory. After the the entire series of runs was completed, the resonance curve was read out onto an x-y recorder and a theoretical lineshape was fitted to it in the manner described in the next section.

IV RESULTS AND DISCUSSION

IV(i) Experimental Sn^{117} Resonance in β-tin

The derivative of the Sn^{117} NMR absorption signal in a stationary sample of β-tin at room temperature (22°C) is shown in figure 5. In obtaining this resonance, H_0 was 7000 gauss and the magnitude of the magnetic field modulation was 2.32 gauss. The asymmetry of the resonance is characteristic of the anisotropic Knight Shift in a polycrystalline sample in which the nuclei are located at axially symmetric sites. The rf transmitter voltage was adjusted so that saturation effects (Bloembergen, Purcell and Pound, 1948) were negligible.

The effect of rotating the sample at the magic angle with an angular speed of 5.4 kHz is shown in figure 6. The resonance is the result of summing 25 twelve-hour runs. The resonance is quite symmetric showing that the anisotropic Knight Shift has been averaged out. Rotational sidebands, separated from the main resonance by 5.4 kHz, are clearly visible. In order to obtain a reasonably faithful reproduction of the absorption derivative, the modulation amplitude was reduced to 0.32 gauss in obtaining this resonance. Also, the rf transmitter voltage was reduced to such a level that the loss of peak-to-peak intensity due to saturation amounted to less than 3%. Both these adjustments reduced the signal intensity.

Since we wish to compare the lineshape of the experimental resonance with theory, it is necessary to correct for the residual

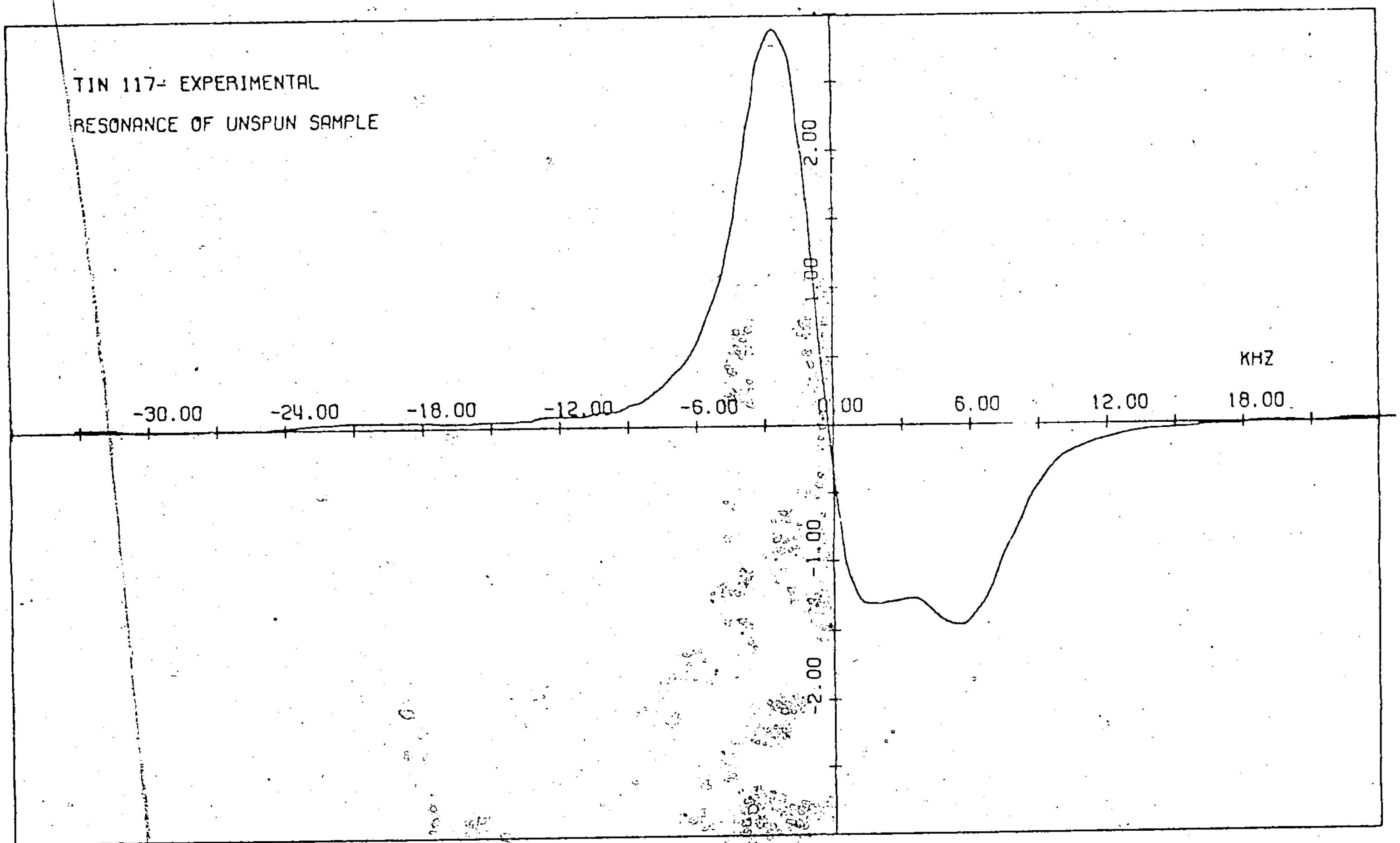

Figure 5-Experimental Resonance (unspun)

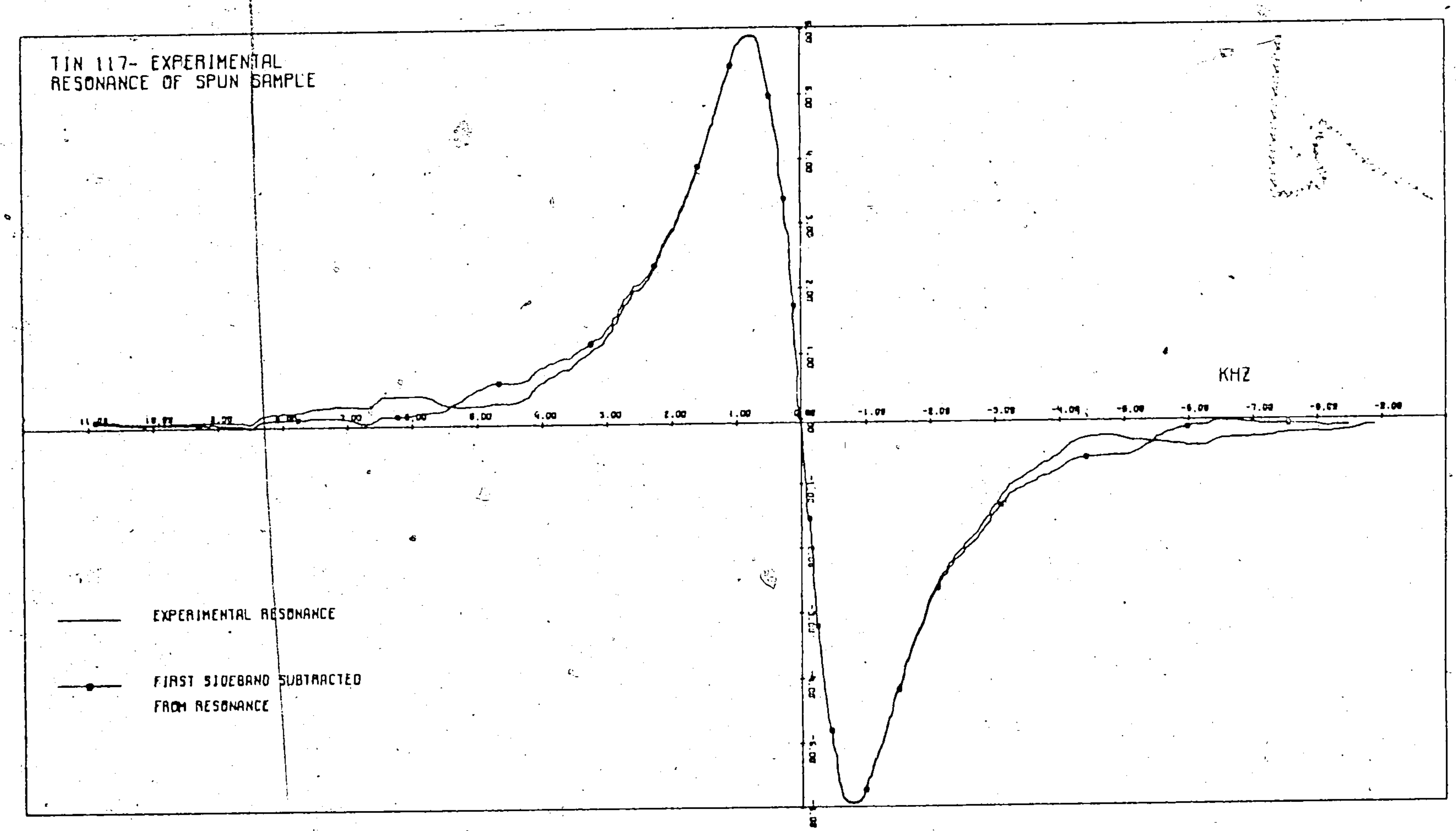

Figure 6 Experimental Resonance (spun at 5.4 kHz)

instrumental distortion caused by the finite modulation amplitude and the rf transmitter voltage. The corrections which are applied to the theoretical rather than the experimental lineshape have been described by Smith (1972). The value of the "saturation" parameter ρ, defined in Appendix IV of Smith's thesis, was .025 for the resonance shown in figure 6.

Finally, the experimental resonance was corrected by subtracting the rotational sidebands. These were assumed to be of the same shape as the main resonance, and their amplitude was estimated by visual examination of the resonance in figure 6. The experimental resonance, corrected by removal of the sidebands, is also shown in this figure. This is the resonance which will be compared with theory.

IV(ii) Procedure for Fitting the Theoretical Lineshape to the Experimental Resonance

The "cross-over" or central frequency, and the baseline of the experimental resonance were first determined. The "cross-over" point can be found quite accurately on account of the steep slope of the absorption derivative near the center, and it was assumed that this point coincides with the center of the theoretical lineshape. Next, the experimental resonance was digitized by measuring the intensity f_i (relative to the previously chosen baseline) at a series of equally spaced frequencies ν_i on either side of the cross-over point. A total of 61 points were taken consisting of the origin (cross-over) and 30 points on each side. Since the interval between points $\nu_{i+1}-\nu_i$ was 141 Hz, the fitting region extended over 8.46 kHz.

To take account of the different intensity of the theoretical and experimental lineshapes, and to allow for possible error in the baseline determination, the theoretical lineshape intensity at frequencies ν_i was expressed in terms of the normalized theoretical lineshape function $g(\nu)$ in the form

$$h(\nu_i) = \alpha_1 + \alpha_2 g(\nu_i). \qquad (1)$$

The quantities α_1 and α_2 are therefore the baseline correction and normalizing factor respectively.

The fitting was done using the least squares criterion that

$$\chi^2 = \Sigma(f_i - h(\nu_i))^2/\sigma_i^2 \qquad (2)$$

is a minimum with respect to the fitting parameters. The quantity σ_i is the standard deviation of the ith data point as estimated from the signal-to-noise ratio of the experimental resonance.

The normalized theoretical lineshape function $g(\nu)$ is a function of the fitting parameters α_3, α_4, ... α_N, for a total of N-2, while the lineshape function $h(\nu)$ is a function of N parameters. For example, in the nearest and second nearest neighbour models, N is 3 and α_3 is the value of the J coupling between nearest and second nearest neighbours respectively. In the Ruderman-Kittel model, N is 4 since there is an extra fitting parameter α_4 which takes account of interactions with distant nuclei. In this case, α_4 is equivalent to the parameter ξ defined in section II(iv).

For the fitting procedure, we require the values of $\partial g(\nu_i)/\partial\alpha_j$. However, since the calculations of $g(\nu_i)$ in general involve the inversion of an 8×8 matrix (the matrix $\underline{\underline{A}}$ in table 2(b)), this has to be done numerically for each value of i and for each value of α_j, and it is not possible to express $g(\nu)$ as a simple function of the α_j's. We therefore approximate $g(\nu_i)$ in the form of the Taylor expansion

$$g(\nu_i) = A_i + \sum_{j=3}^{N} B_{ij}\delta\alpha_j + \sum_{jk=3}^{N} C_{ijk}\delta\alpha_j\delta\alpha_k \qquad (3)$$

where

$$\alpha_j = \alpha_{jo} + \delta\alpha_j \qquad (4)$$

and α_{jo} is a suitably chosen value of α_j. The coefficients A_i, B_{ij} and C_{ijk} were found for each value of i for the nearest neighbour model (where N = [illegible]) by fitting nine different explicitly calculated theoretical curves to equation (3). The nine theoretical curves corresponded to values of $\alpha_3 = |J_2| = 2.0, 2.25, 2.50, \ldots 4.0$ kHz, α_{jo} being equal to 3.0 kHz. Since the coefficients are overdetermined, their 'best' value was found using a least squares fit. As a check on the validity of (3) over such an extended range of α_3, the nine theoretical curves were reconstructed using the expansion. They were found to be in excellent agreement with the original explicitly calculated curves. The above procedure was then repeated for the second nearest neighbour model. For the Ruderman-Kittel model where N=4, a total of 18 theoretical curves were used to calculate the coefficients A_i, B_{ij}, and C_{ijk}.

IV(iii) Results

The fits of the experimental resonance of Sn^{117} for the nearest neighbour model, the second nearest neighbour model and the Ruderman-Kittel model are shown in figures 7, 8 and 9 respectively. For these fits we used a value of T_1 = 169.5 microseconds. This was obtained using the measured value of 155 ± 3 microseconds for Sn^{119} in β-tin at room temperature (295°K) (Dickson, 1969), and using the fact that T_1 is inversely proportional to the square of the gyromagnetic ratio and that $\gamma_{Sn^{119}}/\gamma_{Sn^{117}}$ = 1.046535 ± .000003 (Smith, 1972). The value of σ_i is taken to be .04 intensity units of figure 6 except for the cross-over frequency and the three frequency values on either side of it. For these seven frequency values, σ_i is taken to be .32 intensity units. The fits for the nearest and second nearest neighbour models are poor with χ^2 being equal to 5860 and 12,750 respectively. However, for the Ruderman-Kittel model the fit was good, the value of χ^2 being equal to 127. For this model the value of J, where J is the value of $|J_{i\ell}|$, i and ℓ being a pair of nearest neighbouring Sn^{117} and Sn^{119} nuclei, is 3.04 ± .06 kHz (this implies that J is equal to 2.9[illegible] .06 kHz for two Sn^{117} nuclei and 3.18 ± .06 kHz for two Sn^{119} nuclei). The error is determined from the fit (Guest, 1961). The value of ξ is .49 ± .05, the error again determined from the fit. We have not taken into account other sources of error; this is done in section IV(iv).

IV(iv) Discuss[illegible]

It is clear from figures 7 and 8 that the first and second nearest neighbour models are in very poor agreement with experiment.

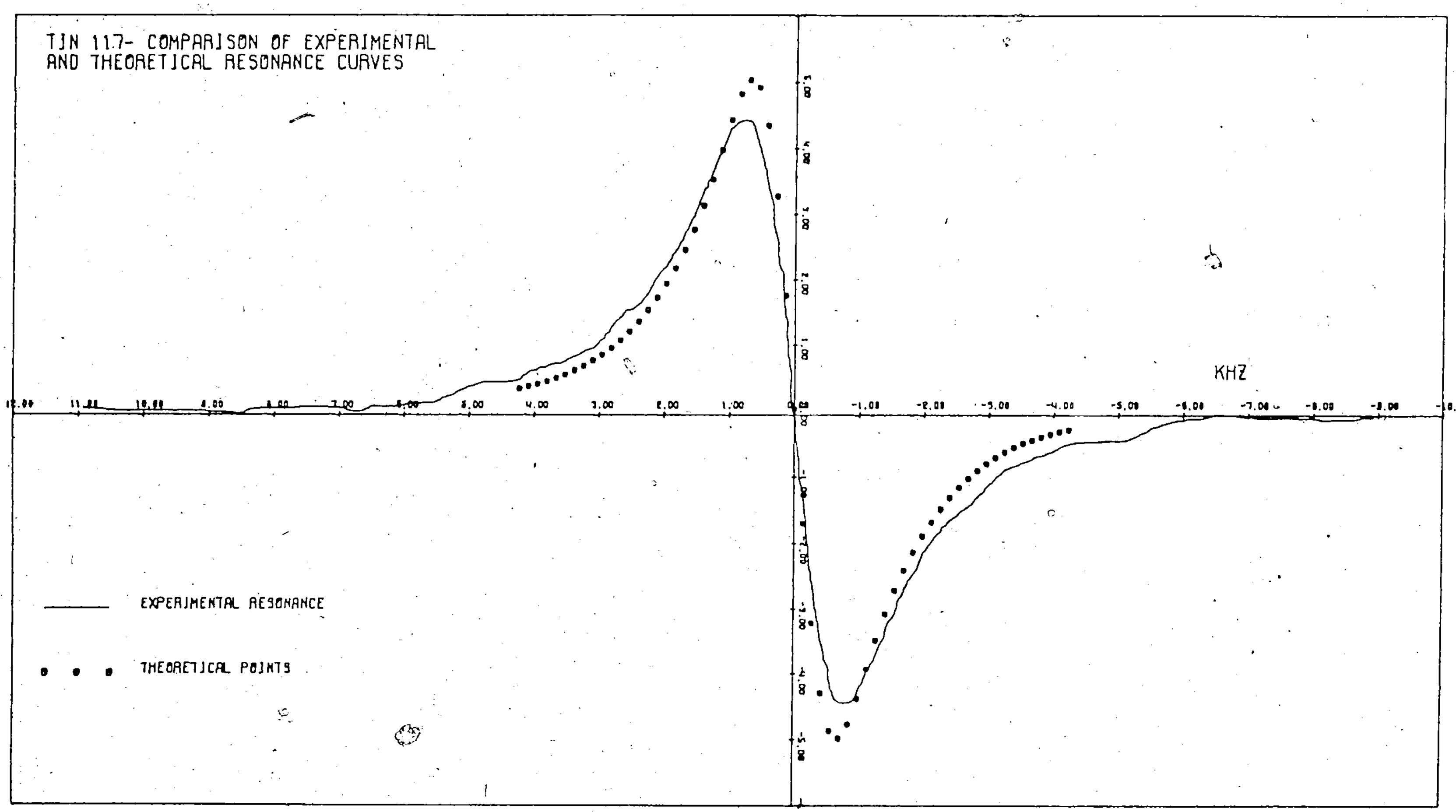

Figure 7 The First Nearest Neighbour Model Fit

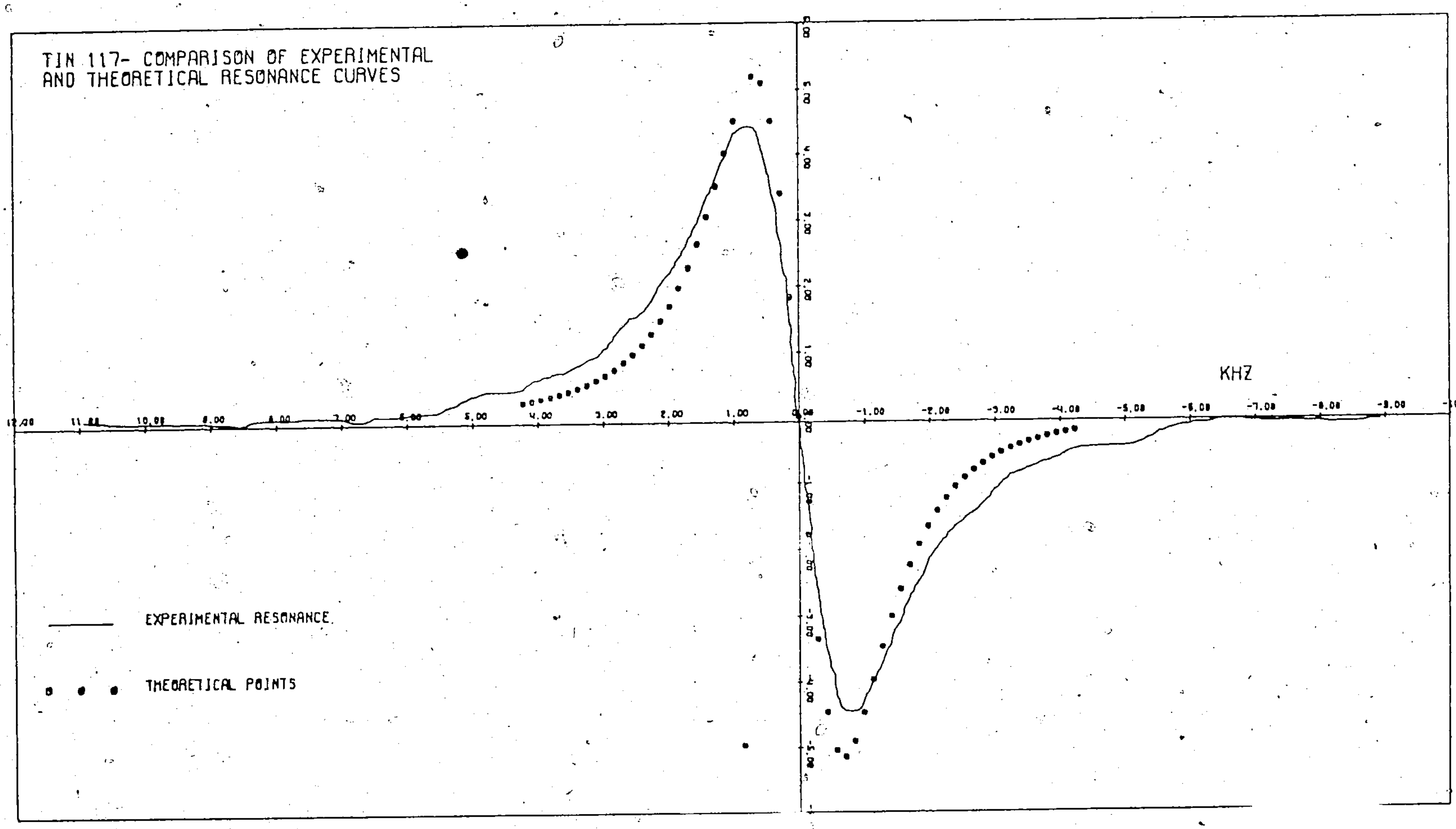

Figure 8 The Second Nearest Neighbour Model Fit

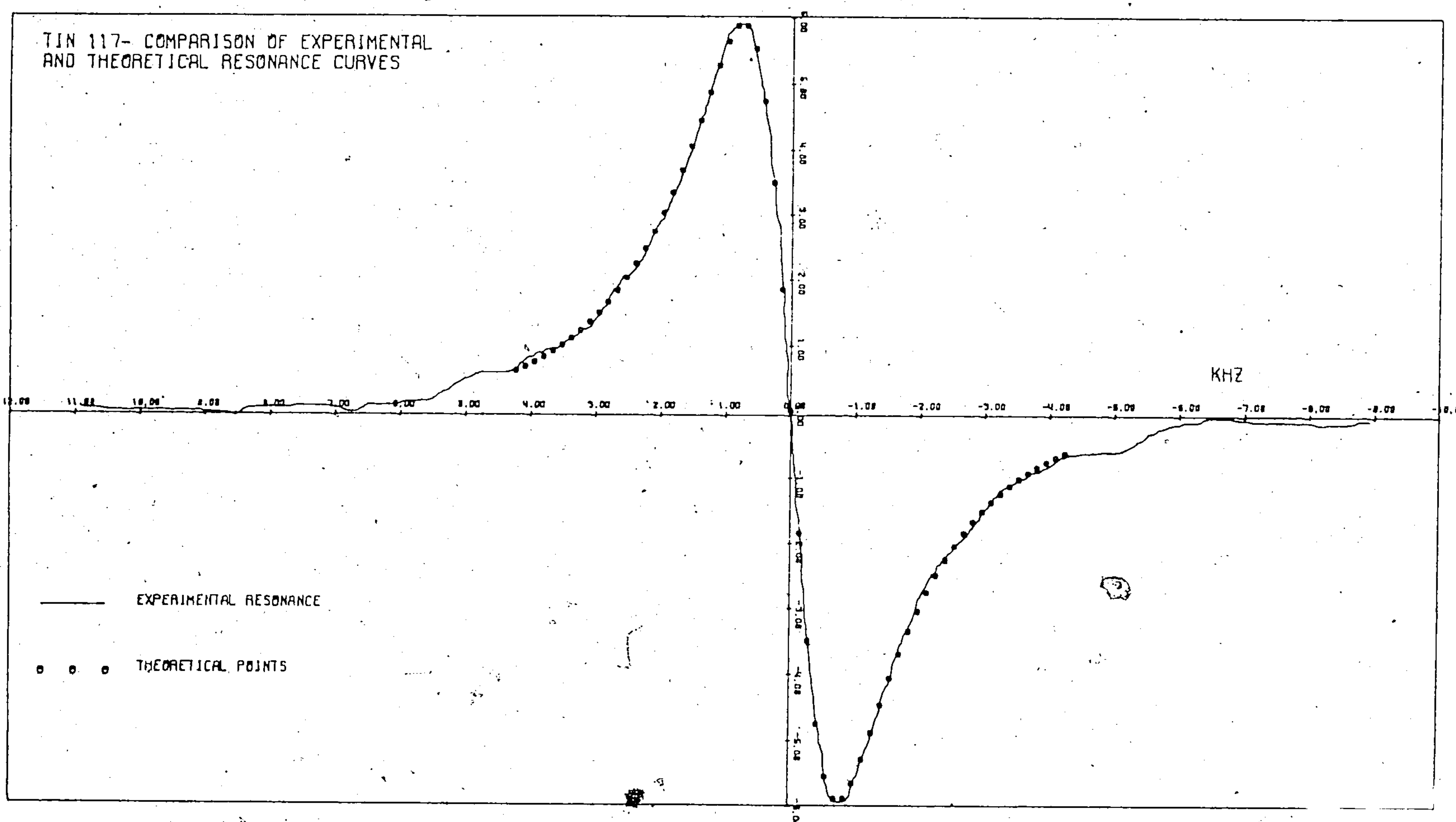

Figure 9 The Ruderman-Kittel Model Fit

It follows that neither the first nearest neighbour nor the second nearest neighbour interaction is dominant in β-tin. It has been suggested (Sharma et al, 1969) that the second nearest neighbour interaction could well be dominant, on account of a hole surface in the fourth zone of the Fermi surface with fairly flat faces perpendicular to the [001] direction. According to the results of Roth et al (1966) this should give a strong interaction in the [001] direction, that is, in the direction of the second nearest neighbours. Our results show quite definitely that this is not the case.

It can be seen in figure 9 that the agreement between experiment and the Ruderman-Kittel theoretical model is very good. The 'goodness of fit' parameter χ^2 was found to be 127 as opposed to the 'expected' value of 56. However, such a discrepancy is by no means unreasonable since we estimated the magnitude of the noise by a visual examination of figure 6, an unreliable procedure. On the basis of the results presented in this thesis there is no reason to doubt the validity of the Ruderman-Kittel model as applied to β-tin.

It will be noted that our value of J depends upon the values of T_1 which we have assumed for Sn^{117} and Sn^{119} in β-tin. In order to check this point, we repeated the fitting procedure by assuming a 2% error in the T_1 value as given by Dickson (1969). However, the value of J was found to be changed by only 0.03 kHz, so it is clear that uncertainty in T_1 is not of major importance in our determination of J.

Another possible source of systematic error in our J value arises from the difficulty of estimating the amplitude of the rotational sidebands. Any error in the sideband amplitude will obviously affect the corrected lineshape within the fitting region which extends 4.2 kHz on either side of the cross-over point. We estimate that the error in J arising from this uncertainty is about 0.15 kHz.

Another source of systematic error in our value of J arises from the various approximations made in synthesizing the theoretical lineshape. We estimate this to be about ±.25 kHz. By combining the various errors we estimate our value of J for the interaction between Sn^{117} and Sn^{119} nuclei which are nearest neighbours to be

$$J = 3.04 \pm 0.3 \text{ kHz} .$$

We note that the Ruderman-Kittel fit was really a two-parameter fit, since the parameter ξ representing the effect of distant nuclei was allowed to differ from the value of unity. The fact that ξ was found to be 0.49 ±.05 indicates that the broadening caused by unlike magnetic nuclei outside the inner three shells is significant. We attribute the fact that ξ is less than unity to a combination of the following reasons:

(a) In the derivation of equation (3) in appendix IV, it was assumed that the linewidth contributions due to each distant magnetic nucleus add linearly. However, this is only true if the lineshapes associated with these interactions are Lorentzian (Hughes and MacDonald, 1961) and if they are independent. In actual fact, the lineshapes converge slightly faster than a Lorentzian function (D.G. Hughes, private communication), and one might therefore expect the resulting linewidth to be somewhat smaller than the sum of the individual linewidths, that is, one would expect ξ to be less than unity.

b) Mutual interactions among the distant magnetic nuclei outside the inner three shells have been neglected. However, mutual spin flips associated with the $J\underline{I}_1 . \underline{I}_2$ interaction will, if the nuclei are of like species, tend to reduce the broadening cause by these nuclei, by a 'motional narrowing' effect. This again would tend to reduce ξ.

(c) No account has been taken of the experimental error in the T_1 value given by Dickson (1969). However, it is intuitively obvious that a 2% error in Dickson's value would have a large effect on ξ.

Apart from the value of 1.89 ± 0.09 kHz found by Smith (1972) for the strength of the Ruderman-Kittel interaction between nearest neaghbours in β-tin, the following values appear in the literature:

2.0 ± 0.5 kHz (McLachlan, 1968)

2.5 kHz (Karimov and Schegolev, 1961)

4.1 ± 0.3 kHz (Alloul and Deltour, 1969).

Also Sharma et al (1969) concluded that the 'exchange narrowing' they observed with a crystal of isotopically pure Sn^{119} was consistent with Alloul and Deltour's value.

A major drawback of the various methods used by McLachlan, Karimov and Schegolev, Alloul and Deltour, and Sharma et al, is their reliance on the measured value of the second moment of the Sn^{119} resonance in natural tin at low temperatures. The difficulty in measuring this second moment is illustrated by the fact that Karimov and Schegolev found that the second moment is 1.2 ± 0.3 $(kHz)^2$ whereas Alloul and Deltour obtained a value of 2.5 ± 0.3 $(kHz)^2$.

In addition, we feel that McLachlan's value of J is unreliable since he assumed that the crystal structure of β-tin is hexagonal close packed and that only the nearest neighbour Ruderman-Kittel interaction was significant.

Karimov and Schegolev, on the other hand, ignored the pseudo-dipolar interaction entirely. This appears to be an important omission since McLachlan found that the pseudo-dipolar interaction was of the same order of magnitude as the dipolar interaction.

Alloul and Deltour's data, obtained using a spin-echo method, is unfortunately by no means easy to interpret. We therefore feel that any discrepancy between their value and ours may well be due to a combination of the approximations made in their theory, and any error in the measured value of the second moment of the Sn^{119} resonance.

Finally, we ask why the value of J obtained by Smith should be so much smaller than our value. We believe that the main cause was the poor signal-to-noise ratio of the resonances obtained by Smith, together with the restricted field sweep used by him (10 gauss compared with 25 gauss in our case). The rotational sidebands are barely visible in Smith's resonances because of the poor signal-to-noise ratio, and they were not corrected for. The 'wings' of the resonance therefore converge more rapidly in the fitting region because of the sidebands, thereby giving the small value of J. Moreover, Smith did not do a two parameter fit as we did. Rather, he had to assume a value for the parameter ξ (proportional to BJ in his notation). The value he assumed turned out to be larger than the one we found. This again would tend to give too small a value of J. Also, in synthesizing the theoretical lineshape Smith made several approximations which we have avoided, though it is difficult to tell whether these would be likely to give too high or too low a value of J.

In order to confirm our value of the strength of the nearest neighbour Ruderman-Kittel interaction, we suggest examining the Sn^{119} resonance in the same way as was done for the Sn^{117} resonance in this thesis. Finally, it should be possible to computationally broaden the Sn^{117} resonance we obtained with the spinning sample, by the anisotropic Knight Shift and direct dipolar broadening, both of which are known. A comparison with the Sn^{117} resonance of the stationary sample would then reveal whether the pseudo-dipolar interaction produces significant broadening in β-tin.

REFERENCES

Abragam A., 1961, The Principles of Nuclear Magnetism, (Oxford: The University Press).

Alloul H. and Deltour R., 1969, Phys. Rev. 183, 414.

Anderson P.W., 1954, J. Phys. Soc. Japan 9, 316.

Andrew E.R., Bradbury A. and Eades R.G., 1958, Nature 182, 1659.

Andrew E.R. and Farnell L.F., 1968, Molec. Phys. 15, 157.

Andrew E.R. and Jenks G.J., 1962, Proc. Phys. Soc. 80, 663.

Andrew E.R. and Newing R.A., 1958, Proc. Phys. Soc. 72, 959.

Beams J.W., 1937, J. Appl. Phys. 8, 795.

Bloch F., Hansen W.W. and Packard M.E.,1946, Phys. Rev. 70, 474.

Bloembergen N., Purcell E.M. and Pound R.V., 1948, Phys. Rev. 73, 679.

Bloembergen N. and Rowland T.J., 1953, Acta Met. 1, 731.

Bloembergen N. and Rowland T.J., 1955, Phys. Rev. 97, 1679.

Davydov A.S., 1966, Quantum Mechanics, (Ann Arbor, Michigan: NEO Press).

Dickson E.M., 1969, Phys. Rev. 184, 294.

Guest P., 1961, Numerical Methods of Curve Fitting, (Cambridge: University Press).

Gutowsky H.S. and McGarvey B.R., 1952, J. Chem. Phys. 20, 1472.

Henriot H. and Huguenard E., 1925, Comptes Rendus 180, 1389.

Hughes D.G. and MacDonald D.K.C., 1961, Proc. Phys. Soc. 78, 75.

Karimov Y.S. and Schegolev I.F., 1961, JETP (English Translation) 13, 908.

Kessemeier H. and Norberg E.R., 1967, Phys. Rev. 155, 321.

Knight W.D., 1949, Phys. Rev. 76, 1259.

Mahanti S.D. and Das T.P., 1968, Phys. Rev. 170, 426.

McLachlan L.A., 1968, Can. J. Phys. 46, 871.

Pake G.E., 1956, Solid State Physics 2, (New York: Academic Press), p. 1.

Pearson W.B., 1967, A Handbook of Lattice Spacings and Structures of Metals and Alloys 2, (Toronto: Pergamon Press), p. 25.

Pople J.A., Schneider W.G. and Bernstein H.J., 1959, High Resolution Nuclear Magnetic Resonance, (Toronto: McGraw-Hill).

Purcell E.M., Torrey H.C. and Pound R.V., 1946, Phys. Rev. 69, 37.

Redfield A.G., 1957, IBM Journal 1, 19.

Roth L.M., Zeiger H.J. and Kaplan T.A., 1966, Phys. Rev. 149, 519.

Ruderman M.A. and Kittel C., 1954, Phys. Rev. 96, 99.

Schwind A.E., 1967, Ann. Physik 7, 22.

Sharma S.N., Williams D.L. and Schone H.E., 1969, Phys Rev. 188, 662.

Slichter C.P., 1963, Principles of Magnetic Resonance, (New York: Harper and Row).

Smith M.R. 1972, Ph.D. Thesis, University of Alberta.

Van Vleck J.H., 1948, Phys. Rev. 74, 1168.

Winter J., 1971, Magnetic Resonance in Metals, (Oxford: Clarendon Press), p. 67.

Appendix I The Time-averaged Values of C_{3n}^2

In this appendix we find the time-averaged values of C_{3n}^2, where C_{3n} is the direction cosine for the nth principal axis of a symmetric, second rank tensor $\underline{\underline{T}}$, with respect to the z axis (the steady magnetic field direction). $\underline{\underline{T}}$ could represent the Knight Shift tensor of β-tin for example. Suppose that the principal axes of $\underline{\underline{T}}$ are x'', y'' and z''. As we want to find the time variation of C_{3n} (in order to obtain the time averaged value of C_{3n}^2), we let x'', y'' and z'' rotate about an axis z' with angular speed Ω. The angle between z and z' is α_3. By determining the vectors x'', y'' and z'' in terms of the fixed laboratory coordinate system xyz, we can evaluate the time variation of C_{3n} (since the above vectors are unit vectors and thus C_{3n} is just the z component of the nth principal axis in the xyz coordinate system). In order to do this we introduce another coordinate system $x'y'z'$ where z' has been previously introduced and the $y'z'$ plane corresponds to the yz plane. The nth principal axis is the vector $(\sin\chi_n \sin(\Omega t+\psi_n), \sin\chi_n \cos(\Omega t+\psi_n), \cos\chi_n)$ in terms of the $x'y'z'$ coordinate system. Here χ_n is the angle between the nth principal axis and z', and ψ_n is the angle which is needed to fix the orientation of the nth principal axis at $t = 0$. A vector $\underline{A}'$ in the $x'y'z'$ coordinate system is the vector $\underline{A}$ in the xyz coordinate system where $\underline{A} = \underline{\underline{R}}.\underline{A}'$ and

$$\underline{\underline{R}} = \begin{bmatrix} 1 & 0 & 0 \\ 0 & \cos\alpha_3 & -\sin\alpha_3 \\ 0 & \sin\alpha_3 & \cos\alpha_3 \end{bmatrix}$$

Thus the nth principal axis is the vector

$$(\sin\chi_n \sin(\Omega t+\psi_n),\ \cos\alpha_3 \sin\chi_n \cos(\Omega t+\psi_n)-\sin\alpha_3 \cos\chi_n,$$
$$\sin\alpha_3 \sin\chi_n \cos(\Omega t+\psi_n)+\cos\alpha_3 \cos\chi_n)$$

in terms of the xyz coordinate system. Therefore

$$C_{3n} = \sin\alpha_3 \sin\chi_n \cos(\Omega t+\psi_n) + \cos\alpha_3 \cos\chi_n$$

and

$$\overline{C_{3n}^2} = \sin^2\alpha_3 \sin^2\chi_n/2 + \cos^2\alpha_3 \cos^2\chi_n$$

When α_3 satisfied the magic angle condition, $\sin^2\alpha_3 = 2/3$ and $\cos^2\alpha_3 = 1/3$ with the result that $\overline{C_{3n}^2} = 1/3$.

Appendix II: The Absorption Lineshape for the $\underline{X}AA'$ Resonance

In this sec[illegible] we include the expression for the absorption lineshape [illegible] $\underline{X}AA'$ resonance. This was obtained by solving (63) for $\underline{r}$ [illegible] substituting the solution into (65). The $\chi''(\omega)$ was determined from $\chi(\omega)$ by noting that $\chi''(\omega)$ is equal to the imaginary part of $\chi(\omega)$. The solution is

$$\chi''(\omega) = \frac{(\omega_X \gamma_X^2 \hbar^2/16kTW_A)\left[B\{\lambda JL+g(F-2D)-2A-4G\} + c^2\{B(2A+4G+g(2D-F))+J(EF-2ED-4H-2AK)+2Ab^4\} - 2A(bc)^4\right]}{B\{JC+4A-4gF+8G\}+ c^2\{B(4gF-8G-4A)+J(4AK+8H-4EF)-4Ab^4\}+ 4A(bc)^4}$$

where

$$A = (\lambda g-e)^2 + 4h^2d^2 \qquad G = d^2(\lambda^2+e)$$
$$B = (\lambda g-f)^2 + 4h^2d^2 \qquad H = d^2(\lambda^2+e)(\lambda^2+f)$$
$$C = (\lambda^2-e)^2 + 4\lambda^2d^2 \qquad J = g^2 + d^2$$
$$D = \lambda(\lambda g-e) + 2hd^2 \qquad K = \lambda^2 + d^2$$
$$E = \lambda(\lambda g-f) + 2hd^2 \qquad L = \lambda^2 + d^2 + a^2$$
$$F = (\lambda^2-e)(\lambda g-e) + 4\lambda hd^2 \qquad \lambda = 2(1 + W_X/W_A)$$

$$a = 2\pi(J_{AX}+J_{A'X})/2W_A \qquad e = d^2 - a^2$$
$$b = 2\pi\{4J_{AA'}^2+(J_{AX}-J_{A'X})^2\}^{\frac{1}{2}}/2W_A \qquad f = d^2 - b^2$$
$$c = (J_{AX}-J_{A'X})/\{4J_{AA'}^2+(J_{AX}-J_{A'X})^2\}^{\frac{1}{2}} \qquad g = 2 + \lambda$$
$$d = (\omega_X-\omega)/W_A \qquad h = 1 + \lambda .$$

Appendix III: Program to Calculate the $\underline{AA'X}$ Spectrum

Included in this section is the listing of the subprogram used to find the $\underline{AA'X}$ spectrum. To find this spectrum, we have to invert the 8×8 matrix given in table 2(b). To do this we have used the cofactor method. In general, this is an inefficient method of solving for the inverse of an 8×8 matrix. However, we have used this method for three reasons. The first is that, as described in the comment statements of the listing, we obtain the intensity of the spectrum as a function of frequency when using this program. This is important because, for this thesis, we need the derivative of the intensity with respect to frequency. This is easily obtainable here since we have the intensity as a function of frequency. If more usual methods of finding an inverse are used, one obtains an intensity value for a certain value of frequency, the result being that one has a discrete set of intensity values. The fact that we obtain the intensity as a function of frequency by one inversion of the matrix means that computer time is saved compared to the more usual methods which would require that the inverse be found for each frequency value. Finally, if certain elements of a matrix are zero, simplifications can be made when finding the inverse by the cofactor method. In our case, 24 out of the 64 elements of the 8×8 matrix are zero.

```
      SUBROUTINE FEED(WW,WWW,IZZZ,A54,N)
C     A DESCRIPTION OF SUBROUTINES USED TO CALCULATE AA'X SPECTRUM.
C
C
C     ALTHOUGH THERE ARE SEVERAL SUBROUTINES USED TO CALCULATE THE
C     AA'X SPECTRUM IT IS ONLY NECESSARY TO CALL THE SUBROUTINE FEED
C     AND ITS TWO ENTRY POINTS(FIRST AND SECOND) BY THE CALLING PROGRAM.
C     ALL OTHER SUBROUTINES ARE CALLED BY FEED.  A DESCRIPTION OF FEED
C     FOLLOWS(A DESCRIPTION OF FIRST AND SECOND FOLLOW THEIR ENTRY
C     STATEMENTS).
C     IT SHOULD BE NOTED THAT FEED IS CALLED ONCE, THEN FIRST IS CAL-
C     LED 36 TIMES, THEN SECOND IS CALLED ONCE FOR EACH AA'X SPECTRUM.
C
C     FEED:
C
C
C                                                             THE VEC-
C     TORS A,ABL,DETT ARE CALCULATED.  WHEN N IS NOT EQUAL TO ZERO, THEN
C     THE SUM OF TERMS A(N+1)*X**N DIVIDED BY THE SUM OF TERMS DETT(M+1)
C     *X**M GIVES THE INTENSITY AT FREQUENCY REAL(B) WHERE, N GOES FROM
C     0 TO 7; M GOES FROM 0 TO 8; AND X=-D-B, D BEING REAL AND B BEING
C     IMAGINARY.  TO OBTAIN THE INDIVIDUAL SPECTRA FOR THE A AND A' NUC-
C     LEI, N IS SET EQUAL TO ZERO.  THEN THE A AND A' SPECTA ARE OB-
C     TAINED BY REPLACING THE VECTOR A IN THE ABOVE SUM BY A AND ABL
C     VECTORS RESPECTIVELY.  THUS BY USING THE VECTORS WITH A CALLING
C     PROGRAM WHICH CALCULATES THE SUMS MENTIONED ABOVE, THE SPECTRA
C     CAN BE EVALUATED.  D SHOULD BE SET TO THE VALUE OF A54 UNLESS
C     THERE IS BROADENING DUE TO NUCLEI NOT IN THE GROUP AA'X SUCH AS IN
C     THE THESIS OF M. SMITH (1972).  FOR THAT THESIS D=BJ*SJI*SJI*.5
C     /WW +A54
C     IZZZ-THIS IS AN INTEGER.  WHEN IZZZ IS NOT EQUAL TO ZERO, THE
C     PRODUCT OF THE MATRIX OF THEORY AND ITS INVERSE IS PRINTED.  THIS
C     PRODUCT MATRIX IS NOT NORMALIZED AND THE FREQUNCY USED IN CALCU-
C     LATING THE MATRIX IS EQUAL TO A54.  IF IZZZ=0,THIS PRODUCT MATRIX
C     IS NOT PRINTED.  THIS IS ONLY USED AS A CHECK OF COMPUTATIONS.
C     A54-THIS IS A REAL NUMBER.  IT IS OF THE ORDER OF THE FREQUENCY
C     FOR WHICH THE RESONANCE INTENSITY IS EQUAL TO .5 TIMES THE MAXI-
C     MUM INTENSITY.
C     N-THIS IS AN INTEGER.  THE FUNCTION OF THIS VARIABLE IS DESCRIBED
C     ABOVE.
C     A DESCRIPTION OF THE PARAMETERS OF THE SUBROUTINE STATEMENT.
C     WW-THIS IS THE TRANSITION RATE FOR THE A OR A' NUCLEI.
C     WWW-THIS IS THE TRANSITION RATE FOR THE X NUCLEUS(WW,WWW ARE IN
C     1/SECONDS)
C     IN ADDITION TO THE ABOVE VARIABLES THE FOLLOWING VARIABLES MUST
C     APPEAR IN A COMMON STATEMENT OF THE CALLING PROGRAM. THE STATEMENT
C     TAKES THE FORM-COMMON/AREA/A(8),DETT(9),ABL(10),XJ1,XJ2,XJ3
C     A-THIS VECTOR IS DESCRIBED ABOVE.  THIS IS A COMPLEX VARIABLE OF
C     DOUBLE PRECISION(COMPLEX*16).
C     DETT-THIS VECTOR IS DESCRIBED ABOVE.  THIS IS A DOUBLE PRECISION
C     COMPLEX VARIABLE(COMPLEX*16)
C     ABL-THIS VECTOR IS DESCRIBED ABOVE.  THIS IS A COMPLEX DOUBLE
C     PRECISION VARIABLE(COMPLEX*16)
C     XJ1,XJ2,XJ3-THESE ARE THE INDIRECT COUPLING CONSTANTS OF THE
C     FIRST,SECOND, AND THIRD NEAREST NEIGHBOURS(IN HZ).
C     THIRTY-SIX RECORDS MUST BE READ FROM LOGICAL UNIT 2.  THE FOL-
C     LOWING 36 CARDS DISPLAY THE CONTENTS OF THE 36 RECORDS, EACH RE-
```

```
C      CORD CONSISTING OF 23 LETTERS.
C      BCDEFGHJKPILKLMINJIOOOC                           CARD1
C      ICDEFGHJKPILKLMINJINMPO                           CARD2
C      NBDEFGHILKJKPLMINJIIMPC                           CARD3
C      MGDEBCHLIJMNIJIKLPKPINO                           CARD4
C      PFEDBCHNMIILJKLJIPKMINO                           CARD5
C      BCEHFGOKPILKNINJIMPJILM                           CARD6
C      BCDEFGOJKIILNLMINMPPKJI                           CARD7
C      HACFDEGKJINMPILLIMNOOOO                           CARD8
C      AHFGDEOMFIJIPLIMNJKNKIL                           CARD9
C      KHFGADCINLJIKMLPMNIPIJO                           CARD10
C      AHCFDEONMIKJPILLIJKPIMN                           CARD11
C      PEFCADGJKIILNMLNIPMKIJO                           CARD12
C      AHGBDEFPIMIPJMNJKLIOOOC                           CARD13
C      IHBFAEGJLMPJIIKMIPNKNLO                           CARD14
C      LHFGDABINKJIPLMMPJIKINC                           CARD15
C      AHGBDEOPINIPKMNJKILMJLI                           CARD16
C      KEBFDAGPJIKINJILMMPLINC                           CARD17
C      BCEAFGHKIPLNKINMPJIOOOC                           CARD18
C      BCAHFGOIPJNKIMPJILMKLIN                           CARD19
C      LGAEBCHMIJPNIINKLPKMJIO                           CARD20
C      MFAEBCHPNIMIJINKLPKLJIO                           CARD21
C      JAFGEHCLMIMPNIJNILKIKPO                           CARD22
C      BCDAFGHJIPINKLMMPJIOOOC                           CARD23
C      IGADBCHMLJPMIINJIPKNKLO                           CARD24
C      NFADBCHPMIMLJINJIPKIKLC                           CARD25
C      BCADFGOIJKNILMPLMINPKJI                           CARD26
C      AHBCDEGINPPKIJKILMNOOOC                           CARD27
C      ADBCEHOINMJILKPLKIJPMNI                           CARD28
C      AHBCDEFINMPKJJKILLIOOOC                           CARD29
C      IECBADFKPJLKINIIJMLNPMO                           CARD30
C      JDGBAECIPKMJIPNIKNLLMIC                           CARD31
C      CBADFGENILIJKMPLMINOOOO                           CARD32
C      BCHDFGOPJIKINJILMMPKLIN                           CARD33
C      AHCGDEONPIKIPILMNJKMJLI                           CARD34
C      AHBFDEOIMNPJKJKLIIILPIMN                          CARD35
C      BCAEFGOIKJNLIMPINLMPKJI                           CARD36
C      THE ABOVE 36 RECORDS MUST BE READ EACH TIME VECTORS ARE REQUIRED
C      FOR AN AA'X SPECTRUM.  AFTER THE READING OF THE 36 RECORDS,LOGICAL
C      UNIT 2 IS REWOUND BY SUBROUTINE.
C
C
       COMPLEX*16 DETT,A,ABL
       COMPLEX*16 ALL(10),AXX,XRET(36,7),Z4,DDX,X2(40,8),F1(8,8),DX,DET
      $ (7,8),RX,Z(7),TT(8)
       REAL HACOS,HASIN
       COMPLEX XFAT
       COMPLEX CMPLX
       DIMENSION II(23),III(23)
       REAL*8 AL(8,8),STORE(36,16),X4(16)
       COMMON Z,X4
       COMMON TT
       COMMON XGAM1,XGAM2,XGAM3,XGAM4,XGAM5,XGAM6
       COMMON/AREA2/F1,XRET,STORE
       COMMON/AREA/A(8),DETT(9),ABL(10), XJ1,XJ2,XJ3
       DATA III/'A','B','C','D','E','F','G','H','I','J','K','L','M','N',
      $'P','Q','R','S','T','U','V','W','O'/
       DO 311 JKK=1,8
   311 ALL(JKK)=0.
       R9=-3.*WW-WWW
```

```
      PI=3.141593
      SPI=2.*PI
      XJ1=SPI*XJ1
      XJ2=SPI*XJ2
      XJ3=SPI*XJ3
      DD=.5*SQRT(.25*(XJ2-XJ3)**2+XJ1**2)
      RCOS=1.
      RSIN=0.
      IF(DD.NE.0.)RSIN=.5*XJ1/DD
      IF(DD.NE.0.)RCOS=.25*(XJ2-XJ3)/DD
      R1=(-2.*XJ1-XJ2-XJ3)/4.-DD
      R2=(-2.*XJ1+XJ2+XJ3)/4.-DD
      R3=(2.*XJ1-XJ2-XJ3)/4.-DD
      R4=(2.*XJ1+XJ2+XJ3)/4.-DD
      R5=R1+2.*DD
      R6=R2+2.*DD
      R7=R3+2.*DD
      R8=R4+2.*DD
      R1=R1+A54
      R2=R2+A54
      R3=R3+A54
      R4=R4+A54
      R5=R5+A54
      R6=R6+A54
      R7=R7+A54
      R8=R8+A54
      IF(N.NE.0)GO TO 309
      HACOS=SQRT(.5*(RCOS+1.))
      HASIN=SQRT(.5*(1.-RCOS))
      IF(RSIN.GT.0.)GO TO 308
      HACOS=-HACOS
  308 IF(HACOS.EQ.HASIN)GO TO 309
      IF(HACOS.EQ.-HASIN)GO TO 309
      DUM1=HACOS+HASIN
      DUM2=HACOS-HASIN
      ALL(1)=CMPLX(HACOS/DUM2,0.)
      ALL(2)=CMPLX(-HASIN/DUM2,0.)
      ALL(3)=CMPLX(HACOS/DUM1,0.)
      ALL(4)=CMPLX(HASIN/DUM1,0.)
      ALL(5)=ALL(4)
      ALL(6)=ALL(3)
      ALL(7)=ALL(2)
      ALL(8)=ALL(1)
  309 CONTINUE
      I11=0
      DO 1 I1=1,36
      I11=I11+1
      READ(2,1000)(II(L1),L1=1,23)
      DO 1 M1=1,23
      M2=M1-7
      IF(M1.EQ.1)M2=M1
      IF(M1.EQ.1)XRET(I11,1)=(0.,0.)
      IF(II(M1).EQ.III(1))XRET(I11,M1)=CMPLX(R9,R1)
      IF(II(M1).EQ.III(2))XRET(I11,M1)=CMPLX(R9,R2)
      IF(II(M1).EQ.III(3))XRET(I11,M1)=CMPLX(R9,R3)
      IF(II(M1).EQ.III(4))XRET(I11,M1)=CMPLX(R9,R4)
      IF(II(M1).EQ.III(5))XRET(I11,M1)=CMPLX(R9,R5)
      IF(II(M1).EQ.III(6))XRET(I11,M1)=CMPLX(R9,R6)
      IF(II(M1).EQ.III(7))XRET(I11,M1)=CMPLX(R9,R7)
      IF(II(M1).EQ.III(8))XRET(I11,M1)=CMPLX(R9,R8)
```

```
      IF(II(M1).EQ.III( 9))STORE(I11,M2)=WWW*RSIN
      IF(II(M1).EQ.III(10))STORE(I11,M2)=WW*RCOS
      IF(II(M1).EQ.III(11))STORE(I11,M2)=WWW*RCOS
      IF(II(M1).EQ.III(12))STORE(I11,M2)=WW*RSIN
      IF(II(M1).EQ.III(13))STORE(I11,M2)=-WWW*RCOS
      IF(II(M1).EQ.III(14))STORE(I11,M2)=-WW*RCOS
      IF(II(M1).EQ.III(15))STORE(I11,M2)=-WW*RSIN
      IF(M1.NE.1)GO TO 25
      CC=AIMAG(XRET(I11,1))
      XYY=STORE(I11,1)
      IF(CC.EQ.0.)  XRET(I11,1)=CMPLX(       XYY    ,0.)
   25 CONTINUE
      IF(M1.GT.15)GO TO 12
      IF(II(M1).EQ.III(23))XRET(I11,M1)=(0.,0.)
      GO TØ 1
   12 IF(II(M1).EQ.III(23))STORE(I11,M2)=0.
    1 CONTINUE
      JK=0
      KKK=2
 1000 FORMAT(23(A1))
      CALL REWIND(2)
      RETURN
      ENTRY FIRST(I11)
C
C
C
C     FIRST:
C
C
C     I11-THIS IS AN INTEGER.  WHEN FIRST IS CALLED FOR THE FIRST TIME
C     FOR EACH AA'X SPECTRUM, I11=1.  EACH ADDITIONAL TIME I11 IS INCRE-
C     MENTED BY 1.  THUS ON THE LAST CALL TO FIRST FOR EACH AA'X
C     SPECTRUM I11=36.
      Z4=(1.,0.)
      RX=(1.,0.)
      JK=0
      DO 3 M2=1,7
      Z(M2)=XRET(I11,M2)
    3 CONTINUE
      DO 14 M2=1,16
   14 X4(M2)=STORE(I11,M2)
      CC=AIMAG(XRET(I11,1))
      IF(CC.EQ.0.)GO TO 10
      CC=AIMAG(XRET(I11,7))
      IF(CC.EQ.0.)GO TO 11
      JK=1
      CALL ZERO(JK)
      DO 31 I=1,8
   31 TT(I)=TT(I)*(-1.,0.)
      GO TO 6
   10 CALL NZERO(KKK)
      GO TO 6
   11 CALL ZERO(JK)
      GO TO 6
    6 CONTINUE
      DO 27 I=1,8
   27 X2(I11,I)=TT(I)
      Z4=TT(1)
      IF(I11.GT.5)GO TO 4
      DO 20 I=1,8
```

```
   20 DET(I11,I)=TT(I)
    4 IF(I11.NE.8)GO TO 5
      DO 15 I=1,8
      RX=(0.,0.)
      IF(I.NE.1) RX=DET(1,I-1)
      DETT(I)=DET(1,I)*XRET(8,2)+RX
      DO 15 M2=2,5
      M1=M2+1
   15 DETT(I)=DET(M2,I)*STORE(8,M1)+DETT(I)
      DETT(9)=DET(1,8)
    5 CONTINUE
      RETURN
      ENTRY SECOND
      DO 22 I=1,8
      F1(1,1)=X2(1 ,I)
      F1(1,2)=X2(2 ,I)
      F1(1,3)=X2(3,I)
      F1(1,4)=X2(6,I)
      F1(1,6)=X2(4,I)
      F1(1,7)=X2(5,I)
      F1(1,8)=X2(7,I)
      F1(2,2)=X2(8,I)
      F1(2,3)=X2(9,I)
      F1(2,5)=X2(10,I)
      F1(2,7)=X2(11,I)
      F1(2,8)=X2(12,I)
      F1(3,3)=X2(13,I)
      F1(3,4)=X2(14,I)
      F1(3,5)=X2(15,I)
      F1(3,6)=X2(16,I)
      F1(3,8)=X2(17,I)
      F1(4,4)=X2(18,I)
      F1(4,5)=X2(19,I)
      F1(4,6)=X2(20,I)
      F1(4,7)=X2(21,I)
      F1(2,4)=X2(22,I)
      F1(5,5)=X2(23,I)
      F1(5,6)=X2(24,I)
      F1(5,7)=X2(25,I)
      F1(5,8)=X2(26,I)
      F1(6,6)=X2(27,I)
      F1(6,7)=X2(28,I)
      F1(7,7)=X2(29,I)
      F1(7,8)=X2(30,I)
      F1(6,8)=X2(31,I)
      F1(8,8)=X2(32,I)
      F1(1,5)=X2(33,I)
      F1(2,6)=X2(34,I)
      F1(3,7)=X2(35,I)
      F1(4,8)=X2(36,I)
      DO 13 N2=1,8
      DO 13 N1=1,8
   13 F1(N1,N2)=F1(N2,N1)
      IF(I.NE.1) GO TO 21
      CALL CHECK(IZZZ)
      D1=1.-RSIN
      D2=1.+RSIN
      D3=RCOS
      AL(1,1)=D1
      AL(1,2)=-D1
```

```
      DO 300 J1=3,6
  300 AL(1,J1)=-D3
      AL(1,7)=D1
      AL(1,8)=-D1
      AL(3,1)=-D3
      AL(3,2)=D3
      DO 301 J1=3,6
  301 AL(3,J1)=D2
      AL(3,7)=-D3
      AL(3,8)=D3
      DO 304 J2=4,6
      DO 304 J1=1,8
  304 AL(J2,J1)=AL(3,J1)
      DO 302 J1=1,8
      D4=AL(1,J1)
      AL(7,J1)=D4
      AL(8,J1)=-D4
      AL(2,J1)=-D4
  302 CONTINUE
   21 CONTINUE
      A(I)=(0.,0.)
      ABL(I)=(0.,0.)
      DO 303 J1=1,8
      AXX=ALL(J1)
      DO 303 J2=1,8
      IF(N.NE.0)GO TO 305
      ABL(I)=AL(J1,J2)*P1(J1,J2)*AXX+ABL(I)
  305 A(I)=AL(J1,J2)*P1(J1,J2)+A(I)
  303 CONTINUE
   22 CONTINUE
      IF(N.EQ.0)GO TO 306
      RETURN
  306 CONTINUE
      IF(ABS(HACOS).NE.HASIN)GO TO 313
      DO 314 JKK=1,8
  314 ABL(JKK)=A(JKK)/2.
  313 CONTINUE
      DO 307 I=1,8
  307 A(I)=A(I)-ABL(I)
      RETURN
      END
C
C
C
      SUBROUTINE NZERO(KKK)
C
C
C
      REAL*8 H,I,J,K,L,M,N,P,Q,R,S,T,U,V,W,X
      REAL*8 XGAM1,XGAM2,XGAM3,XGAM4,XGAM5,XGAM6,A1,A2,A3,A4,A5,A6,A7,
     $A8,A9,A10,A11,A12,A13,A14,A24,A16,A17,A18,A19,A20,A21,A22,A23,A
      COMPLEX*16 Y,B,C,D,E,F,G,XX(8),TT,ZZ(8),C1,C2
      COMMON Y,B,C,D,E,F,G,H,I,J,K,L,M,N,P,Q,R,S,T,U,V,W,X
      COMMON ZZ
      COMMON XGAM1,XGAM2,XGAM3,XGAM4,XGAM5,XGAM6
      COMMON/AREA1/C1(10,8),C2(10,8),XX,TT
      A=Y
      XGAM5=N*R-P*Q
      XGAM6=N*T-P*S
      A1=H*U-K*A
```

```
      A2=R*S-Q*T
      A3=M*R-L*T
      A5=L*S-M*Q
      A6=N*M-K*S
      A7=M*A-J*U
      A8=P*M-K*T
      A9=S*W-V*T
      A10=-A2
      A11=Q*W-V*R
      A12=W*L-U*R
      A13=W*M-T*U
      A14=A9
      A16=W*N-V*P
      A17=L*P+K*R
      A18=I*M-L*J
      A19=I*U-L*A
      A20=L*N-K*Q
      A23=K*J-M*H
      A24=I*K-L*H
      TT=(0.,0.)
      DO 58 II=1,8
   58 XX(II)=(0.,0.)
      DO 4 II=1,10
      DO 4 JJ=1,8
      C2(II,JJ)=(0.,0.)
    4 C1(II,JJ)=(0.,0.)
      C1(1,1)=F
      C1(2,1)=D
      C1(3,1)=E
      C1(4,1)=C
      C1(5,1)=G
      C1(6,1)=B
      DO 21 II=1,6
   21 C1(II,2)=(1.,0.)
      DO 9 II=1,8
    9 XX(II)=(0.,0.)
      CALL CALC(2,3,2,10)
      DO 10 II=1,8
   10 C1(10,II)=C2(10,II)*Y
      DO 1 II=1,8
    1 XX(II)=(0.,0.)
      XGAM1=-K*A2-L*XGAM6+M*XGAM5
      XGAM2=U*XGAM6+V*A8-W*A6
      XGAM3=-U*A2+V*A3+W*A5
      TT=A2*K*(A1*A2 +A*(P*A5+N*A3) +H*(M*A11-A9*L))+XGAM5*(M*A*(2.*L*
     $ XGAM6-R*A6)+A3*(J*N*U+H*V*M)+J*S*U*A17+Q*A7*A8)+XGAM6*L*(A*(A17*S
     $-T*A20)+I*U*XGAM6+I*(K*A14-M*A16))+A3*N*(Q*(      -A13*H)+A12*H*S)
      TT=TT+XGAM1*(J*(K*A11-L*A16      )-XGAM2*I)-I*L*XGAM2*XGAM6+
     $XGAM3*S*L*P*H+M*P*Q*H*(-W*A5+U*A2)
      TT=TT+A3*(-H*L*N*V*T)
      XX(1)=TT
      TT=A6*(S*A1+N*A7+V*A23)
      CALL CALC(1,2,2,1)
      TT=A8*(T*A1+P*A7+W*A23)
      CALL CALC(3,2,2,2)
      TT=-A5*(S*A19+Q*A7-V*A18)
      CALL CALC(1,4,2,3)
      TT=A3*(T*A19+R*A7-W*A18)
      CALL CALC(3,4,2,4)
      TT=A20*(Q*A1-N*A19+V*A24)
```

```
      CALL CALC(1,5,2,5)
      TT=A2*(A*A2-I*A14+J*A11)
      CALL CALC(6,4,2,6)
      TT=A17*(R*A1+W*A24-P*A19)
      CALL CALC(3,5,2,7)
      TT=XGAM6*(A*XGAM6+H*A14-J*A16)
      CALL CALC(6,2,2,8)
      TT=XGAM5*(XGAM5*A+H*A11-I*A16)
      CALL CALC(5,6,2,9)
      DO 5 II=1,9
      DO 5 JJ=1,8
    5 C1(II,JJ)=C2(II,JJ)
      TT=A19*L
      CALL CALC(3,7,4,2)
      TT=A1*[illegible]
      CALL CALC(1,7,4,1)
      TT=(J*V-S*A)*S
      CALL CALC(1,6,4,3)
      TT=(J*W-T*A)*T
      CALL CALC(2,6,4,4)
      TT=(V*I-Q*A)*Q
      CALL CALC(5,6,4,5)
      TT=(I*W-R*A)*R
      CALL CALC(7,6,4,6)
      TT=(H*V-N*A)*N
      CALL CALC(5,8,4,7)
      TT=-A7*M
      CALL CALC(2,3,4,8)
      TT=(W*H-P*A)*P
      CALL CALC(9,2,4,9)
      DO 3 II=1,8
    3 C1(5,II)=C2(5,II)
      TT=(1.,0.)
      CALL CALC(5,10,6,1)
      DO 2 II=1,8
    2 ZZ(II)=XX(II)*(-1.,0.)
      RETURN
      END
C
C
C
      SUBROUTINE ZERO(JK)
C
C
C
      REAL*8 H,I,J,K,L,M,N,P,Q,R,S,T,U,V,W,X
      COMPLEX*16 C1,C2,X1,X2,X3,X4,X5,X6,XX(8),TT,ZZ(8),A,B,C,D,E,F,G
      REAL*8 XGAM1,XGAM2,XGAM3,XGAM4,XGAM5,XGAM6,A1,A2,A3,A4,A5,A6,A7,
     $A8,A9,A10,A11,A12,A13,A14,A15,A16,A17,A18,A19,A20,A21,A22,A23,A24
      REAL*8 A25,A26 A27,A28,A29,A30,A31,A32,XGAM7
      COMMON A,B,C,D,E,F,G,H,I,J,K,L,M,N,P,Q,R,S,T,U,V,W,X
      COMMON ZZ
      COMMON XGAM1,XGAM2,XGAM3,XGAM4,XGAM5,XGAM6
      COMMON [illegible]C1(10,8),C2(10,8),XX,TT
      XGAM5=[illegible]
      A1=T*N[illegible]
      A5=C*T-R[illegible]
      A15=L*T-M[illegible]
      A16=M*P-K*T[illegible]
      A17=L*S-M*Q
```

```
      A18=M*N-K*S
      A22=H*S-J*N
      A24=P*J-H*T
      A26=I*T-R*J
      A28=J*K-H*M
      A30=I*M-J*L
      A32=I*S-J*Q
      IF(JK.EQ.0.)GO TO 1
      U=J
      V=M
      W=S
      X=T
      A4=-A5
      A6=-A15
      A7=A17
      A8=-A18
      A9=A16
      A10=A1
      A11=-A26
      A12=-A32
      A13=A24
      A14=-A22
      A23=A13
      A25=A26
      A29=A28
      A31=A30
    1 CONTINUE
      A2=L*P-K*R
      A3=K*Q-N*L
      A19=R*H-P*I
      A21=Q*H-I*N
      A27=H*L-I*K
      IF(JK.EQ.1)GO TO 2
      A4=R*W-Q*X
      A6=V*R-L*X
      A7=L*W-V*Q
      A8=K*W-V*N
      A9=V*P-K*X
      A10=X*N-P*W
      A11=R*U-I*X
      A12=U*Q-I*W
      A13=U*P-H*X
      A14=U*N-H*W
      A23=U*P-H*X
      A25=I*X-U*R
      A29=U*K-H*V
      A31=I*V-U*L
    2 CONTINUE
      A20=-A10
      XGAM1=-U*A2-H*A6+I*A9
      XGAM2=H*A7-I*A8+U*A3
      XGAM3=-Q*A13-I*A10+R*A14
      XGAM6=-J*A2+H*A15+I*A16
      XGAM7=H*A17+I*A18+J*A3
      TT=(0.,0.)
      DO 58 II=1,8
   58 XX(II)=(0.,0.)
      DO 20 II=1,10
      DO 20 JJ=1,8
      C1(II,JJ)=(0.,0.)
```

```
   20 C2(II,JJ)=(0.,0.)
      C1(1,1)=C
      C1(2,1)=D
      C1(3,1)=A
      C1(4,1)=B
      C1(5,1)=E
      C1(6,1)=F
      C1(7,1)=G
      DO 21 II=1,10
   21 C1(II,2)=(1.,0.)
      CALL CALC(3,4,2,1)
      CALL CALC(6,3,2,2)
      CALL CALC(3,5,2,3)
      CALL CALC(6,4,2,4)
      CALL CALC(5,4,2,5)
      CALL CALC(6,5,2,6)
      CALL CALC(3,2,2,9)
      CALL CALC(6,2,2,10)
      X1=L*A1*(W*A2+X*A3-V*XGAM5)+A5*K*(K*A4-N*A6-P*A7)+M*XGAM5*(-R*A8
     $-Q*A9-L*A10)
      X2=XGAM3*XGAM5*J+H*A5*(H*A4-N*A11+P*A12)+I*A1*(-I*A10-Q*A13+R*A14)
      X3=-XGAM1*XGAM6
      X4=-XGAM2*XGAM7
      DO 52 II=1,8
   52 XX(II)=(0.,0.)
      XX(1)=X1*A+X2*B+X3*E+X4*F
      XX(2)=X1+X2+X3+X4
      X1=-A20*A1
      X2=-A18*A8
      X3=A16*A9
      X4=-A22*A14
      X5=A23*A24
      X6=A28*A29
      DO 26 JJ=1,8
   26 C1(10,JJ)=X1*C2(1,JJ)+X2*C2(2,JJ)+X3*C2(3,JJ)+X4*C2(4,JJ)+X5*C2
     $ (5,JJ)+X6*C2(6,JJ)
      TT=(1.,0.)
      CALL CALC(2,10,3,7)
      X1=-A4*A5
      X2=A17*A7
      X3=-A6*A15
      DO 27 JJ=1,8
   27 C1(10,JJ)=X1*C2(1,JJ)+X2*C2(2,JJ)+X3*C2(3,JJ)
      TT=(1.,0.)
      CALL CALC(1,10,3,7)
      DO 7 II=9,10
      DO 7 JJ=1,8
    7 C1(II,JJ)=C2(II,JJ)
      DO 8 II=4,6
      DO 8 JJ=1,8
    8 C1(II,JJ)=C2(II,JJ)
      TT=-A32*A12
      CALL CALC(1,4,3,8)
      TT=A25*A26
      CALL CALC(1,5,3,9)
      TT=A30*A31
      CALL CALC(1,6,3,10)
      DO 9 II=1,8
    9 C1(3,II)=C2(9,II)
      X1=M*V
```

```
      X2=S*W
      X3=T*X
      X4=U*J
      DO 10 II=1,8
   10 C1(4,II)=C2(10,II)*X1+C2(8,II)*X2
      TT=(-1.,0.)
      CALL CALC(4,9,5,7)
      DO 11 II=1,8
   11 C1(5,II)=C1(9,II)*X3+C1(10,II)*X4
      TT=(-1.,0.)
      CALL CALC(3,5,5,7)
      IF(JK.EQ.0)GO TO 22
      X1=A2*A2
      X2=A19*A19
      X3=A3*A3
      X4=A21*A21
      X5=XGAM5*XGAM5
      X6=A27*A27
      DO 12 II=1,8
   12 C1(4,II)=X1*C2(3,II)+X2*C2(5,II)+X3*C2(2,II)+X4*C2(4,II)+X5*
     $C2(1,II)+C2(6,II)*X6
      TT=(1.,0.)
      CALL CALC(4,7,3,7)
      DO 13 II=1,8
   13 ZZ(II)=XX(II)
      X1=N*N
      X2=P*P
      X3=K*K
      DO 14 II=1,8
   14 C1(5,II)=X1*C2(4,II)+X2*C2(5,II)+X3*C2(6,II)
      CALL CALC(5,9,4,7)
      X1=R*R
      X2=Q*Q
      X3=L*L
      DO 44 II=1,8
   44 C1(3,II)=(0.,0.)
      C1(3,1)=A
      C1(3,2)=(1.,0.)
      DO 15 II=1,8
   15 C1(5,II)=C2(9,II)*X1+X2*C2(8,II)+C2(10,II)*X3
      CALL CALC(5,3,4,6)
      CALL CALC(9,1,3,4)
      DO 38 II=1,8
   38 C1(10,II)=C2(5,II)
      C1(6,1)=F
      C1(6,2)=(1.,0.)
      C1(6,3)=(0.,0.)
      CALL CALC(6,10,3,10)
      DO 40 II=1,8
   40 C1(10,II)=C2(10,II)
      X1=H*H
      X2=I*I
      DO 16 II=1,8
   16 C1(5,II)=(-1.,0.)*C2(4,II)+C1(2,II)*X1+C1(1,II)*X2
      CALL CALC(5,10,6,5)
      DO 17 II=1,8
   17 C1(4,II)=C2(5,II)+C2(7,II)+C2(6,II)
      DO 23 II=1,8
   23 XX(II)=ZZ(II)
      TT=(-1.,0.)
```

```
      CALL CALC(4,7,7,4)
   22 CONTINUE
      DO 25 II=1,8
   25 ZZ(II)=XX(II)*(-1.,0.)
      RETURN
      END
C
C
C
      SUBROUTINE CALC(L,K,M,KK)
C
C
C
      COMPLEX*16 C1,C2,XX,TT
      COMMON/AREA1/C1(10,8),C2(10,8),XX(8),TT
      DO 4 I=1,8
    4 C2(KK,I)=(0.,0.)
      KR=M+2
      DO 2 N=2,KR
      DO 1 I=1,8
      DO 3 J=1,8
      IF(I.GE.N) GO TO 2
      IF(I+J.NE.N)GO TO 3
      C2(KK,N-1)=C2(KK,N-1)+C1(L,J)*C1(K,I)
      GO TO 1
    3 CONTINUE
    1 CONTINUE
    2 XX(N-1)=C2(KK,N-1)*TT+XX(N-1)
      RETURN
      END
C
C
C
      SUBROUTINE CHECK(I)
C
C
C
      COMPLEX*16 DX
      COMPLEX*8 DDX
      REAL*8 STORE
      COMPLEX*16 F1,XRET,F2(8,8)
      COMMON/AREA2/F1(8,8),XRET(36,7),STORE(36,16)
      IF(I.EQ.0) GO TO 6
      DO 12 N1=1,8
      DO 12 N2=1,8
   12 F2(N1,N2)=(0.,0.)
      F2(1,1)=XRET(8,2)
      F2(1,2)=STORE(1,4)
      F2(1,3)=STORE(1,10)
      F2(1,6)=STORE(1,8)
      F2(1,7)=STORE(1,3)
      F2(2,4)=STORE(1,1)
      F2(2,5)=STORE(1,2)
      F2(2,8)=F2(1,7)
      F2(3,4)=F2(1,2)
      F2(3,5)=STORE(1,5)
      F2(3,8)=F2(2,5)
      F2(4,6)=F2(3,5)
      F2(4,7)=F2(1,6)
      F2(5,6)=F2(1,2)
```

```
           F2(5,7)=F2(1,3)
           F2(6,8)=F2(2,4)
           F2(7,8)=F2(1,2)
           F2(8,8)=XRET(1,7)
           DO 16 N2=1,6
           N3=N2+1
      16   F2(N3,N3)=XRET(7,N2)
           DO 13 N2=1,8
           DO 13 N1=1,8
      13   F2(N1,N2)=F2(N2,N1)
           DO 14 N1=1,8
           DO 14 N2=1,8
           DX=(0.,0.)
           DO 15 N3=1,8
      15   DX=DX+F2(N1,N3)*F1(N3,N2)
           DDX=DX
           CX=AIMAG(DDX)
           EX=REAL(DDX)
      14   WRITE(6,2002)CX,EX
    2002   FORMAT(' ',E14.7,3X,E14.7)
       6   RETURN
           END
END OF FILE
```

Appendix IV The Effect of More Distant Nuclei in the Ruderman-Kittel Model

We use the approximate lineshape of an XA configuration for the determination of the effect of more distant nuclei. If $J_{AX} << W_X$, the XA spectrum is Lorentzian and is equal to (43) of section II except that $2W_X$ is replaced by

$$2W_X + 7(\pi J_{AX})^2/20W_X \qquad (1)$$

(D.G. Hughes, private communication). To take into account the effect of the more distant nuclei we assume that the apparent increase in the relaxation rate of the observed nucleus due to each of the more distant unlike magnetic nuclei is equal to $7(J_{AX}\pi)^2/40W_X$ and that the increases add linearly. This is equivalent to assuming that the more distant nuclei are independent of each other. Then the apparent increase in the relaxation rate of a Sn^{117} nucleus is

$$(7/40W_X)\sum_i(\pi J_{iX})^2 p_{un} \qquad (2)$$

$$(7/40W_X)\pi^2 J_1^2 \sum_i F(k_f|R_{iX}|)^2 p_{un}/.7705\times10^{-6} = 3.3825 J_1^2 p_{un}/2$$

Here the sum $\sum_i$ is over all nuclear sites outside the 3 inner shells. Also J_1 is the magnitude of the Ruderman-Kittel interaction for nearest neighbours, $F(x)$ is given in equation (34) and p_{un} is the probability of a magnetic nucleus (other than a Sn^{117} nucleus) being found at a lattice site. The result is that the apparent increase in the relaxation rate is

$$0.3054 J_1^2/2W_X \qquad (3)$$

We have not taken into account the effect of like nuclei nor the mutual interactions between the more distant nuclei in the calculations leading to (3). Because (3) is an approximate expression for the effect of more distant nuclei, we multiply this expression by ξ and obtain for the apparent increase in W_X

$$\xi\{.3054 J_1^2 / 2W_X\} \qquad (4)$$

Here ξ is a fitting parameter and its magnitude is found by minimizing (2) of section IV.

NATIONAL LIBRARY
OTTAWA

CANADA

BIBLIOTHÈQUE NATIONALE
OTTAWA

NAME OF AUTHOR .... TAPPER ....

TITLE OF THESIS ....THE SPATIAL ORGANISATION OF PIKAS (OCHOTONA) AND ITS EFFECT ON POPULATION RECRUITMENT ....

UNIVERSITY .... ALBERTA ....

DEGREE FOR WHICH THESIS WAS PRESENTED .... Ph. D ....

YEAR THIS DEGREE GRANTED .... 1973 ....

Permission is hereby granted to THE NATIONAL LIBRARY OF CANADA to microfilm this thesis and to lend or sell copies of the film.

The author reserves other publication rights, and neither the thesis nor extensive extracts from it may be printed or otherwise reproduced without the author's written permission.

(Signed) .... [signature] ....

PERMANENT ADDRESS:

Dept of Zoology
Univ. of Alberta
....

DATED .... May 23 1973

NL-91 (10-68)

THE UNIVERSITY OF ALBERTA

THE SPATIAL ORGANISATION OF PIKAS (OCHOTONA), AND ITS EFFECT ON POPULATION RECRUITMENT

by

(C) STEPHEN CHARLES TAPPER

A THESIS

SUBMITTED TO THE FACULTY OF GRADUATE STUDIES AND RESEARCH
IN PARTIAL FULFILLMENT OF THE REQUIREMENTS FOR THE DEGREE
OF DOCTOR OF PHILOSOPHY

DEPARTMENT OF ZOOLOGY

EDMONTON, ALBERTA

FALL, 1973

THE UNIVERSITY OF ALBERTA

FACULTY OF GRADUATE STUDIES AND RESEARCH

The undersigned certify that they have read, and recommend to the Faculty of Graduate Studies and Research, for acceptance, a thesis entitled "The Spatial Organisation of Pikas (Ochotona), and its Effect on Population Recruitment" submitted by Stephen Charles Tapper in partial fulfilment of the requirements for the degree of Doctor of Philosophy.

Fred C. Zwickel
Supervisor

J. O. Murie

Lawrence C. Bliss

W. M. Samuel

Lee H. Metzgar
External Examiner

Date May 18, 1973

ABSTRACT

Home range, dispersion, and dispersal patterns of pikas were studied for three summers in S. W. Alberta.

Home ranges of adults consisted mainly of talus adjacent to areas of vegetation used for grazing. With the construction of haypiles in late summer (July - September), pikas used the central portions of these home ranges more intensively than they did in early summer (May - June). Home ranges of males were larger than those of females in early summer, but not in late summer. Home range size varied from area to area and was associated with changes in population density, and with amounts of vegetation on feeding areas.

Pika populations were organised into pairs of males and females with members of the pairs sharing much of their home range with each other, but the degree to which this occurred varied with density and season. There was little overlap between home ranges of females, whereas in males overlap was considerable in early summer but declined to about the same level as in females in late summer. Home range overlap increased at higher densities. Relative dominance between neighbouring males was apparent

and some were pushed to marginal areas where they generally remained unpaired.

Dispersal of juveniles between populations occurred in animals of both sexes. Within populations, males moved little in the year of their birth, whereas females moved various distances; young males, however, were apparently forced to move again the following spring. Settlement patterns of young pikas suggested that adult females that were lost were replaced directly by dispersal of juvenile females, whereas males that were lost were replaced in spring by yearlings, or by unpaired neighbouring males.

In three years, the population on the main study area showed an increase. Most of this was due to a greater number of marginal unpaired males rather than an increase in the number of breeding pairs.

It is concluded that social behaviour affects both the number and location of new recruits settling on rock-slides, and that this sets an upper limit on the number of breeding pairs in pika populations.

ACKNOWLEDGEMENTS

I am very grateful to Dr. F. C. Zwickel for supervising this study and for his constant advice and assistance throughout. Thanks are also due to members of my supervisory and examining committees, Dr. L. C. Bliss, Dr. J. O. Murie, Dr. W. M. Samuel and Dr. A. L. Steiner for their help at various stages of the research.

Thanks are also due to Michael Boyd and Lorne Fisher who provided valuable assistance during the summers of 1970 and 1971 respectively, to Mrs. B. Chernik who provided advice on some of the statistical analyses and to Dr. J. S. Millar who kindly allowed the inclusion of some unpublished data for comparison.

I should like to acknowledge the cooperation and help given by various members of the Alberta Forest Service, particularly those associated with the Crowsnest Forest, and the financial support given by the N.R.C. of Canada and the R. B. Miller Biological Research Station.

Finally, special thanks are due to Jan Tapper for her help, advice and encouragement throughout, and also to many graduate students in the Zoology Department for heir ideas and arguments about many aspects of this study.

TABLE OF CONTENTS

TABLE OF CONTENTS (continued)

LIST OF TABLES

LIST OF TABLES (continued)

LIST OF FIGURES

LIST OF FIGURES (continued)

LIST OF FIGURES (continued)

INTRODUCTION

Most vertebrate populations appear to possess some form of social organisation which not only determines the relationship of one individual to another, but also serves to organise the population in space and time. Wynne-Edwards (1962) suggested that these systems whatever their other functions may be, also serve to restrict the uncontrolled growth of the population in terms of numbers. This may be done by displacing surplus individuals or by restricting the number that breed each year. Thus, important resources such as food supply would be utilized more efficiently over the long term. Wynne-Edwards went even further and suggested that this was the primary reason for these systems developing, and defined a society as an "organisation capable of providing conventional competition."

Such an hypothesis is not readily testable with field experiments since it would require experimental manipulation of behaviour. Although this has been done to a limited extent with the injection of hormones (Watson 1970), such methods are not of wide practical use at this time. An alternative approach is to study the relationship between social behaviour and population dynamics in both undisturbed and experimentally manipulated populations, and accumulate new evidence which can be evaluated for or against this hypothesis. This was the approach used her

. . . (*Ochotona princeps*) are particularly well suited to this type of study since they are diurnal, habituate readily to humans, can be easily marked, and individuals are very local with small home ranges. This makes their behaviour relatively easy to document. However, activity under the rocks cannot be studied by direct observation, but MacArthur (personal communication) using radio-transmitters implanted into the body cavity of wild pikas had no evidence that they move more than a few metres under the rock surface. His data also agree with the observations of Krear (1965) which suggest little activity at night. Also they live in areas of restricted habitat (rock-slides) and many populations can be considered as discrete units.

The objectives of my study could be set out as two questions -

1. Do pikas have a social system which could operate as a regulatory mechanism?

2. If so, does it operate in this way?

To answer the first question it had to be shown that a form of conventional competition existed which either limited the total number of animals living within the population or restricted the number that bred. Prior to my study, there was some evidence that pikas are territorial (Kilham 1958, Broadbooks 1965, Krear 1965) and competition for space appeared likely. Therefore, a thorough documentation of spatial relationships among pikas was undertaken, so that the exact nature of any spacing system could be evaluated.

If pikas were shown to have a territorial system, a demonstration of its operation as a regulatory mechanism would require that surplus animals be shown to be displaced, at least from the breeding population. In order to do this, young animals were individually marked, and their dispersal and settlement patterns studied with respect to dispersion of adults. The settlement of young animals was observed on; (a) areas which appeared saturated with adults; (b) areas where vacancies were known to exist (established animals having died or been removed), and (c) on areas where all individuals had been removed. If territoriality was limiting the population, permanent recruitment would be expected to correspond directly with vacancies in the established population.

This study began in May 1969 and continued during the summers of 1970 and 1971, with some additional data collected in May 1972. The study populations were in the Livingstone Range of the Canadian Rockies in South Western Alberta.

STUDY AREAS

Since pikas are restricted to rockslides, the specific study areas consisted mainly of talus interspersed with vegetation. Four study sites were used, and they were designated Areas I-IV inclusive.

Areas I-III were chosen because they were discrete units of habitat all within 3 kilometres (2 miles) of each other (Fig. 1) and were at elevations between 1500-1800 metres (5000-6000 ft) in the Sub-alpine Forest Zone (Rowe 1959). The surrounding forest consisted mainly of immature lodgepole pine (Pinus contorta), and meadow areas and forest clearings were dominated by lush mixtures of grasses and herbs. These three rockslides were also inhabited by other medium-sized mammals, particularly wood rats (Neotoma cinerea), golden-mantled ground squirrels (Spermophilus lateralis), red squirrels (Tamiasciurus hudsonicus), and yellow pine chipmunks (Eutamias amoenus). Abundant carnivores were badgers (Taxidea taxus), coyotes (Canis latrans), long-tailed weasels (Mustela frenata) and short-tailed weasels (Mustela erminea).

Area IV, in a large mountain basin about 16 kilometres (10 miles) to the north of Areas I-III, was between 2300 - 2500 metres (7000-7500 ft) in elevation and just

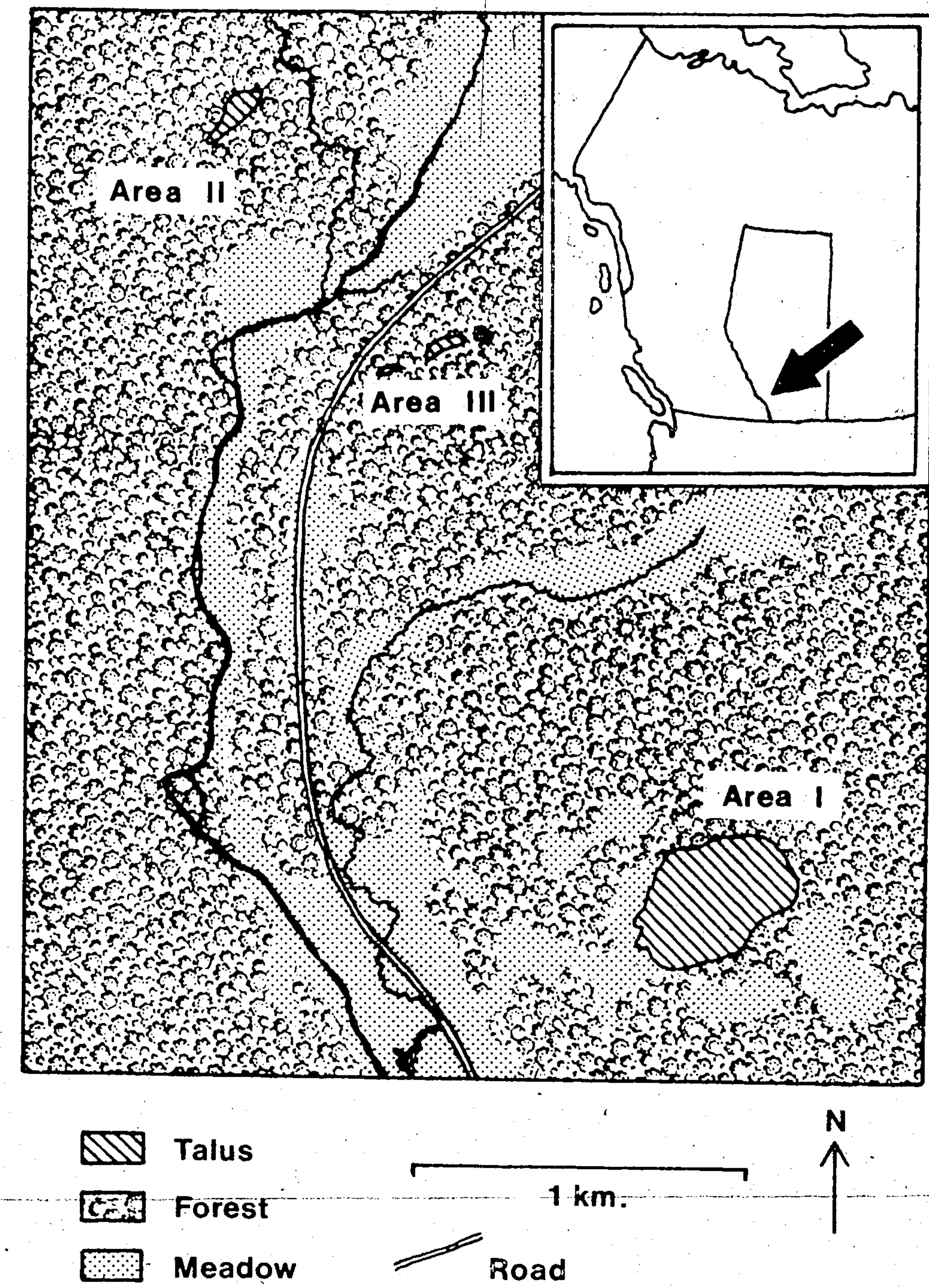

Fig. 1. Map showing geographical location of study areas (inset), and their relative positions in the Livingstone River Valley.

above tree-line. The fauna was alpine in character with Eutamius minimus replacing E. amoenus, and the rocky slopes were inhabited by hoary marmots (Marmota caligata).

Area I

This was a large rockslide of about 10 hectares (Fig. 2). The talus, of well weathered rock with a heavy lichen covering, was interspersed with stands of lodgepole pine, and with scattered white spruce (Picea glauca) alpine fir (Abies lasiocarpa) and limber pine (Pinus flexilis). Under the forest canopy and on the upper sections of the slide the ground vegetation was sparse. The lowermost portion of the slide adjoined a meadow of plentiful grasses and herbs where springs kept the meadow moist for most of the summer.

The rockslide was situated on a slope with a mainly southerly aspect. Hence, most parts of the slide were free of snow relatively early in the year, usually by early May. Some of the upper sections of talus, where extensive drifting occurred, remained snow-covered for several weeks longer.

This area, on which most of the behavioural work was done, had an average population of 25 adult pikas, and was studied intensively for three summers (1969-71). Complete censuses were obtained in 1970 and 1971, and a

Fig. 2. General habitat types on Area I. Axes show grid of 20 X 20 metre squares.

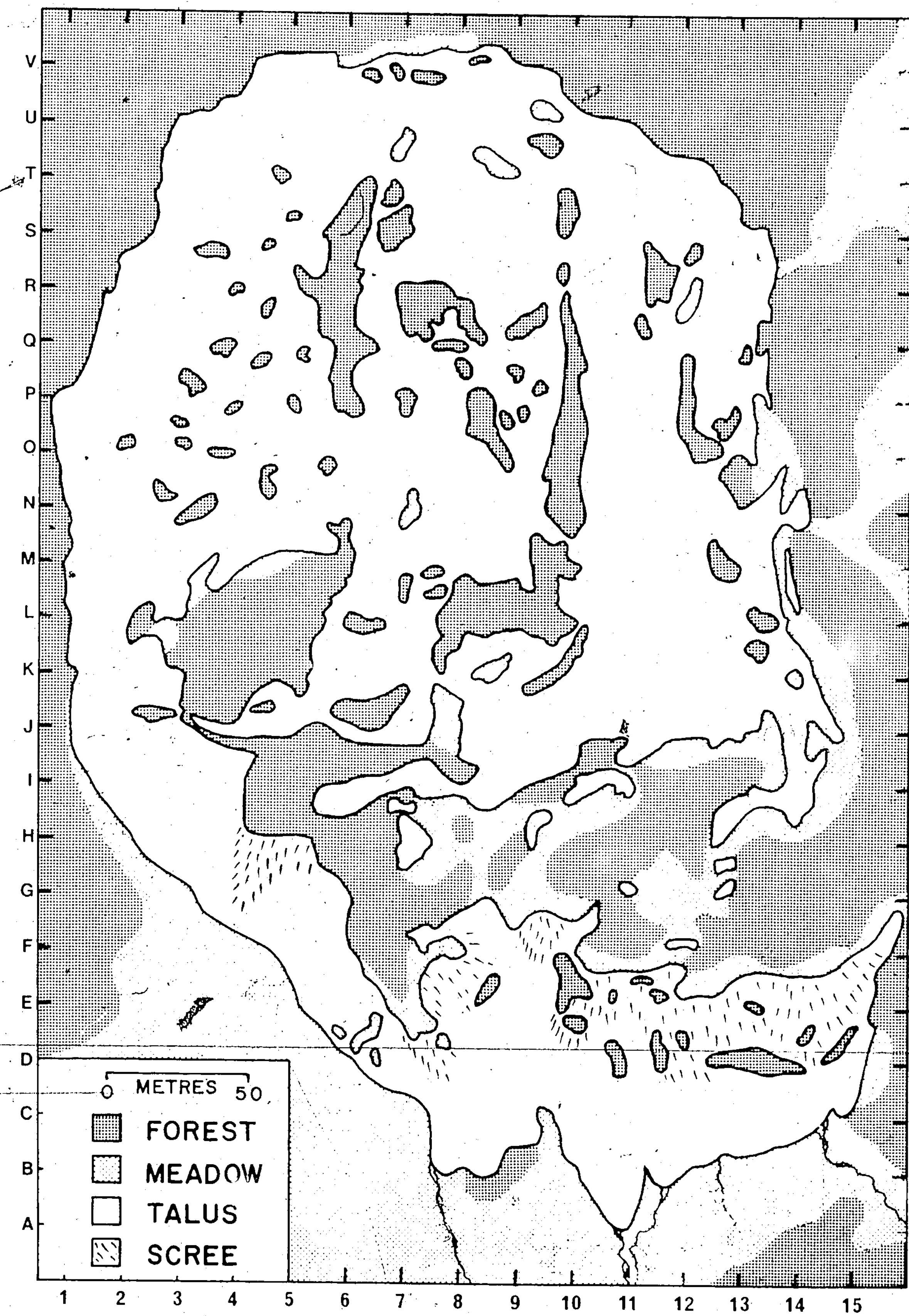
V
U
T
S
R
Q
P
O
N
M
L
K
J
I
H
G
F
E
D
C
B
A
1
2
3
4
5
6
7
8
9
10
11
12
13
14
15
0 METRES 50
FOREST
MEADOW
TALUS
SCREE

good estimate of the adult population was made in 1969.

Area II

This was a small rockslide with about 1.5 hectares of talus surrounded by forest. It sloped in a westerly direction away from the base of a cliff and ground vegetation was generally sparse.

This slide had an average population of only 8 adults. Complete censuses were made during all three summers of study. All pikas were removed from it in May 1971 as part of a recolonisation study.

Area III

This area consisted of a small rockslide of about 1 hectare surrounded by mature spruce forest under which ground vegetation was very sparse. The slide sloped in a northerly direction away from the base of a cliff.

There were 8 adults here in the spring of 1971 and they were used for a replacement study in that year. The area was not used during the other years.

Area IV

This rockslide was in a large mountain basin facing generally northeast. The basin (measuring 1000 metres in length and about 500 metres in breadth) had continuous talus at the base of the surrounding cliffs. The area was not discrete since other basins adjoined to the north and south.

This population was used mainly for experimental purposes, food stores of some pikas being manipulated in 1969 (Appendix I), and one section of talus cleared of pikas in 1971, as part of a recolonisation study.

Meteorological records were not kept for each study area, but general weather changes during the study are shown in Appendix II -- these are from the Highwood River Ranger Station (6·5 kilometres north of Area IV).

METHODS

Capturing and Handling

In order to determine home ranges and population levels I used a colour ear-tagging system so that individual animals could be recognised in the field without repeated recaptures.

Galvanised metal Sherman traps (10 X 10 X 36 cm) were used for initial capture and were usually prebaited a day or two in advance with willow (Salix) and other green shoots. Traps were set in talus areas and were checked every hour, since animals tended to exhaust themselves rapidly or become overheated in warm weather.

After capture, a pika was dropped into a polythene bag and weighed. The weight of a juvenile was used to estimate the animal's age in days (Millar 1971). The animal was manipulated within the bag so that the anal region protruded through the opening and sex was determined by everting the cloaca and checking for a penis or clitoris (Duke 1951). Juveniles were often difficult to sex in this manner until they were approximately two months old, hence sexing of juveniles was often omitted until they were almost adult size. However, beginning in 1971, I attempted to sex the younger animals by classifying those which had a rounded tip to their genital organ as males, and those with a flattened tip as females. This proved fairly accurate, since of ten animals which were recaptured when larger, only one had had its sex incorrectly determined. Another criterion used to establish sex in juveniles was the 'long' call. This call is given almost exclusively by males (Krear 1965), though there is some evidence that adult females may give it, or a similar call, on rare occasions (Severaid 1955; Sharp 1973). No marked females in my study were heard to give this call. Once sex had been determined, the animal was reversed in the bag so that the head region was exposed. Two metal eartags with coloured discs were applied to each ear. Thus an animal was assigned a two colour code which was recognisable from either side. Using different colours and different positions of the tags on the ear, up to 100 animals could be distinctively marked which was sufficient on all study areas.

Observations

Since juvenile pikas remained in the general area of the nest site prior to dispersal, it was usually possible to attribute recently emerged juveniles to a particular female.

Home ranges, dispersal movements, and a periodic nsus of the populations were all determined by direct observations on individually marked animals. All study areas, except Area IV were staked out in 20 X 20 metre squares, with a marked post at each point. Positions of animals were then noted relative to these stakes. In most cases it was possible to estimate an animal's position to within 3 or 4 metres. Locations were noted in the field and later plotted onto base maps of the study area, on a daily basis. Activities such as feeding, calling, and carrying vegetation were also recorded. If an animal was seen running from one location to another the movement was plotted as a line on the map. The data from these maps were later transformed into a series of individual observation points which could be represented by a number from each axis of the grid. Linear movements of animals were considered as single observation points every five metres (ie. an animal running 10 metres was considered to have been observed three times at three locations, the beginning, the middle and the end of its run). This approach enabled quantification of the data and made analysis of the spatial use of home ranges simpler.

No attempt was made to randomise either periods or locations of watching; instead every effort was made to maximise the number of observations for all individuals known to be in the population. Thus more time was spent attempting to observe animals which were seen less frequently. Hours of watching were variable but were concentrated during periods when animals were most active, which was generally morning and evening.

In making observations, an observer patrolled the study area pausing to note the activities and locations of marked animals. Most animals quickly habituated to humans and appeared undisturbed even if an observer approached to within a few metres. If animals were frightened, they usually darted out of sight beneath the talus. Hence, they were not chased out of their normal areas of activity. Most observations were made with binoculars at distances between 10 and 50 metres.

Analysis of Data

Home ranges were analysed using an IBM 360 computer. Data in the form of a matrix were entered and using a specially designed APL programme, home ranges were plotted for each animal during specified time periods. These plots showed not only the shape and extent of the home range but also intensity of use of different parts -- based on the percentage of observations in different areas. The programme also calculated the centres of activity (Hayne 1949). These home range maps were overlaid and the spatial relationships between animals studied.

Because many of the data were not normally distributed, most of the statistical analyses are non-parametric. The various tests used are described in Siegel (1956) and/or Sokal and Rohlf (1969). A probability value of ≤ 0.05 was considered significant, but actual probability levels are given where appropriate.

HOME RANGE

Concepts and Problems

Jewell (1966) reviewed many of the concepts and problems associated with home range. He restated Burt's definition of home range as follows: "Home range is the area over which an animal normally travels in pursuit of its routine activities." Burt (1943) specifically excluded dispersal, exploratory, and migratory movements from his definition. Although this is probably the commonest use of the term home range, as a definition it lacks objectivity since it is difficult to specify what activities are routine and what are not For the purposes of this study, home range is defined as: "The area in which an individual spends all of its time, for a specified time period." Weeden (1965) used a similar definition for tree sparrows and referred to it as the total activity space.

Another problem associated with home range is a realistic method for plotting it graphically. Many methods have been used depending on the type and quantity of data analysed. Several methods which are specifically designed for use with a live trapping grid, and certain mathematical methods such as those used by Dice and Clark (1953), and Jennrich and Turner (1969), which make assumptions of circularity or bivariate normality, are ignored since they are not applicable to the type of data obtained. Perhaps the simplest method is a line surrounding all the observations or trapping points of an animal, as used by Brown (1969). A more objective adaptation is to join the most peripheral points with straight lines to form the smallest convex polygon -- as used for deer (Bramley 1970). This method has been modified to include re-entrant angles (Harvey and Barbour 1965), which eliminates some of the error developed where large areas containing no records are included.

The above methods have the advantage of being quickand easy and are generally simple to interpret. They have several major disadvantages however, two of which are: (1) they imply a specific boundary which may not exist -- in fact animal may only be aware of a gradual decrease in its familiarity with the terrain at the edges of its range; and (2) they often enclose large areas where there are no records, which may lead to entirely false impressions of the spatial relationships among animals. Hence, these methods are not useful for looking at details of home range.

Another frequently used technique is to plot location records in the form of scattered points on a map; this is often done in observational or radio-telemetric studies, examples being Schaller (1961), Grubb and Jewell (1966), Ables (1969), and Siniff and Tester (1965). Sometimes this technique is extended to plotting runways and paths used by an animal, eg. Kaufman (1962) and Altman (1962). This method is ideal where individual animals are considered in detail, but graphically, becomes messy when several animals with overlapping ranges are plotted. Also, it is very difficult to quantify the data in terms of area without resorting to one of the earlier methods as well.

In my study an attempt is made both to characterise and quantify home ranges and the spatial relationships between animals, so that they can be analysed statistically. To do this an objective, yet reasonably realistic method was required.

The method used depicts the home range on the basis of 5 X 5 metre squares. The criterion for inclusion of a square in an animal's home range is based on the animal being observed at least once within that square during the specified time period. The 25 square metre unit was chosen as a useful size for several reasons: (1) it was a small enough distance to be easily estimated in the field (the study areas being marked with numbered stakes in 20 X 20 metre squares); (2) a reasonable graphical picture of the home range was obtained using the average quantity of data; (3) five metres seemed from casual observation to approximate the usual minimum individual distance between animals; and (4) it was the largest area which could reasonably be expected to be in the view of a pika at most times, given the nature of the terrain.

Using this method it was possible to show details of shape and use of home range, and at the same time enabled home range overlap to be measured in an objective fashion. This technique was used to establish the nature of the spatial organisation of pikas. After general spatial relationships were determined, other methods were used to show changes in dispersion pattern of the populations with time.

General Topography of Home Range

Home ranges of 10 pikas (5 males and 5 females) are shown in Fig. 3. Home ranges of pikas usually included a large area of talus adjacent to meadow areas which were used in feeding and gathering vegetation. Between July and September most of an animal's activity was concentrated around the haypile site and this area may be termed a core area (Kaufman 1962). These haypile sites were used in successive years by the same or different pikas and appeared to be fairly traditional. This

Fig. 3. Home ranges of five adult males (pp. 21-25) and five adult females (pp. 26-30) on Area I during 1970. Home ranges are drawn on the basis of 5 X 5 metre squares; co-ordinates on the maps are part of the 20 metre grid system (see Fig. 2). Graphs show intensity of use of home range along its long and short axes - these are based on the percentage of observations within each 10 metre strip at right angles to these axes (see p. 37).

- (hatched) Home range
- (cross-hatched) Home range - core area (3% of observations in each square)
- ▲ Haypile site
- ● Nest site of female
- (open box) Talus
- (box) Scree
- (box) Forest
- (box) Sparse meadow
- (box) Lush meadow
- ·······△ May - June 1970
- —● July - September 1970
- N1 Number of observations, May - June 1970
- N2 Number of observations, July - September 1970.

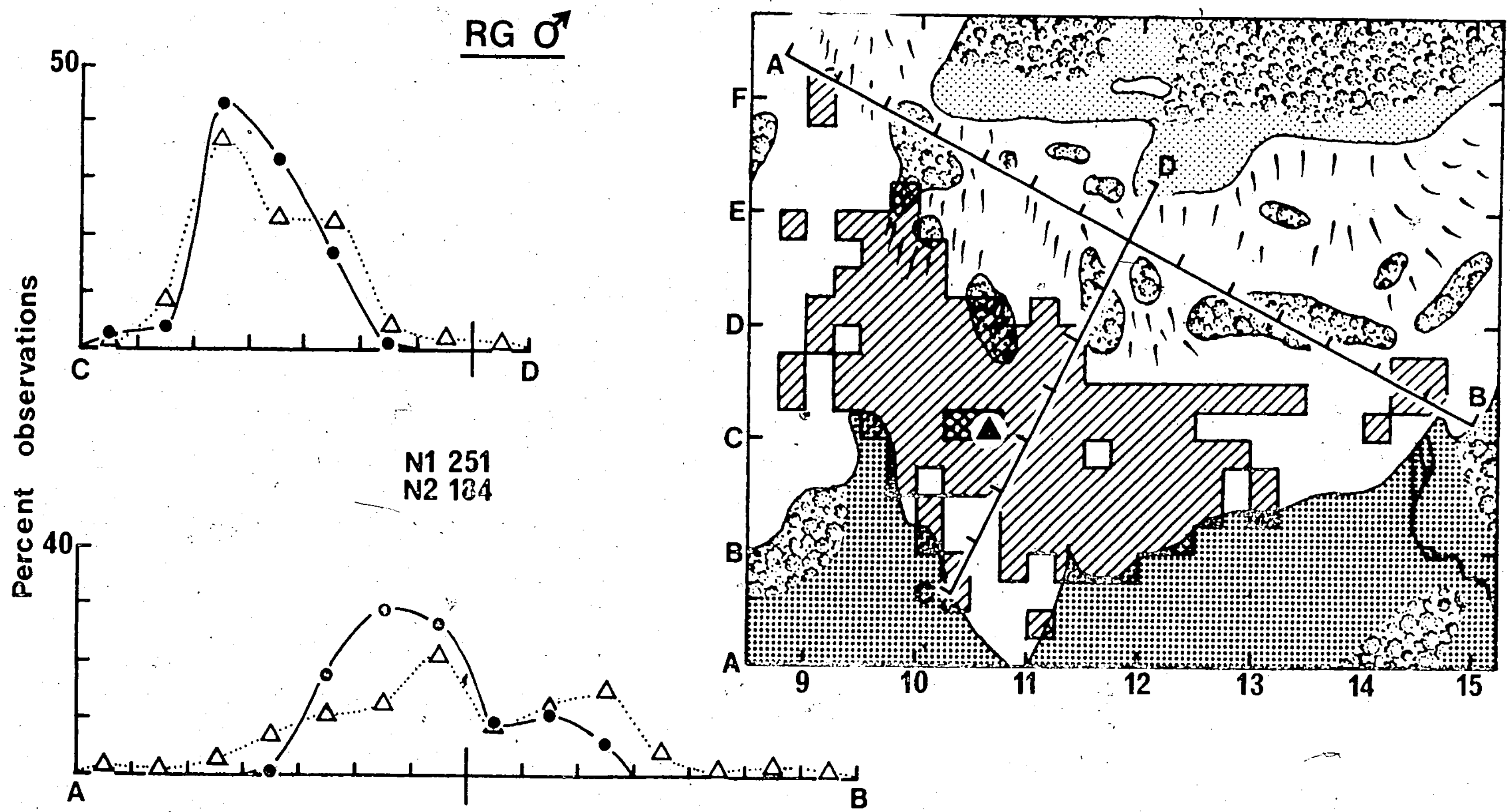
RG ♂
50
C
D
Percent observations
N1 251
N2 184
40
A
B
F
E
D
C
B
A
9
10
11
12
13
14
15

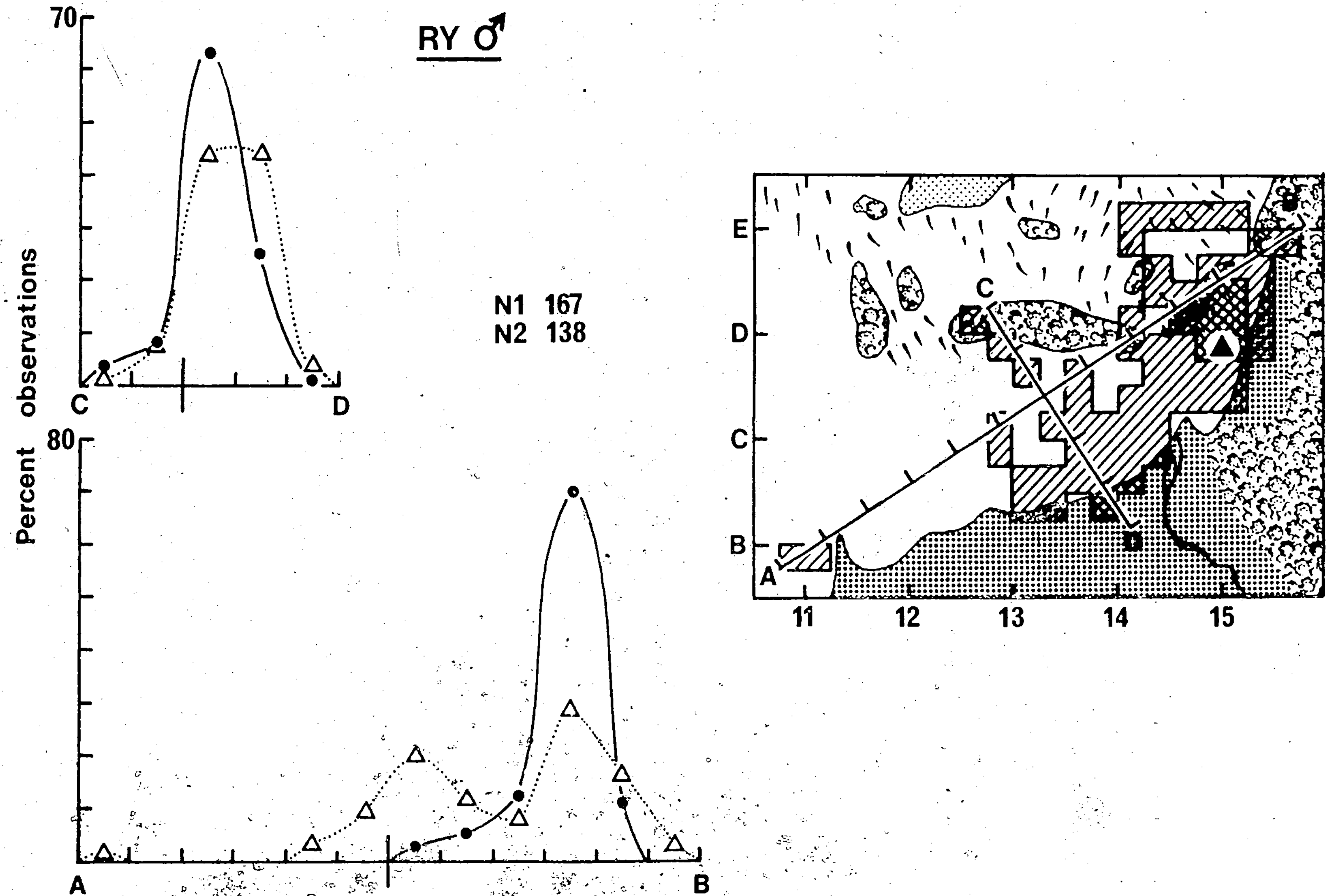
RY ♂
N1 167
N2 138
Percent observations
70
80
C
D
A
B
E
D
C
B
A
C
D
11
12
13
14
15

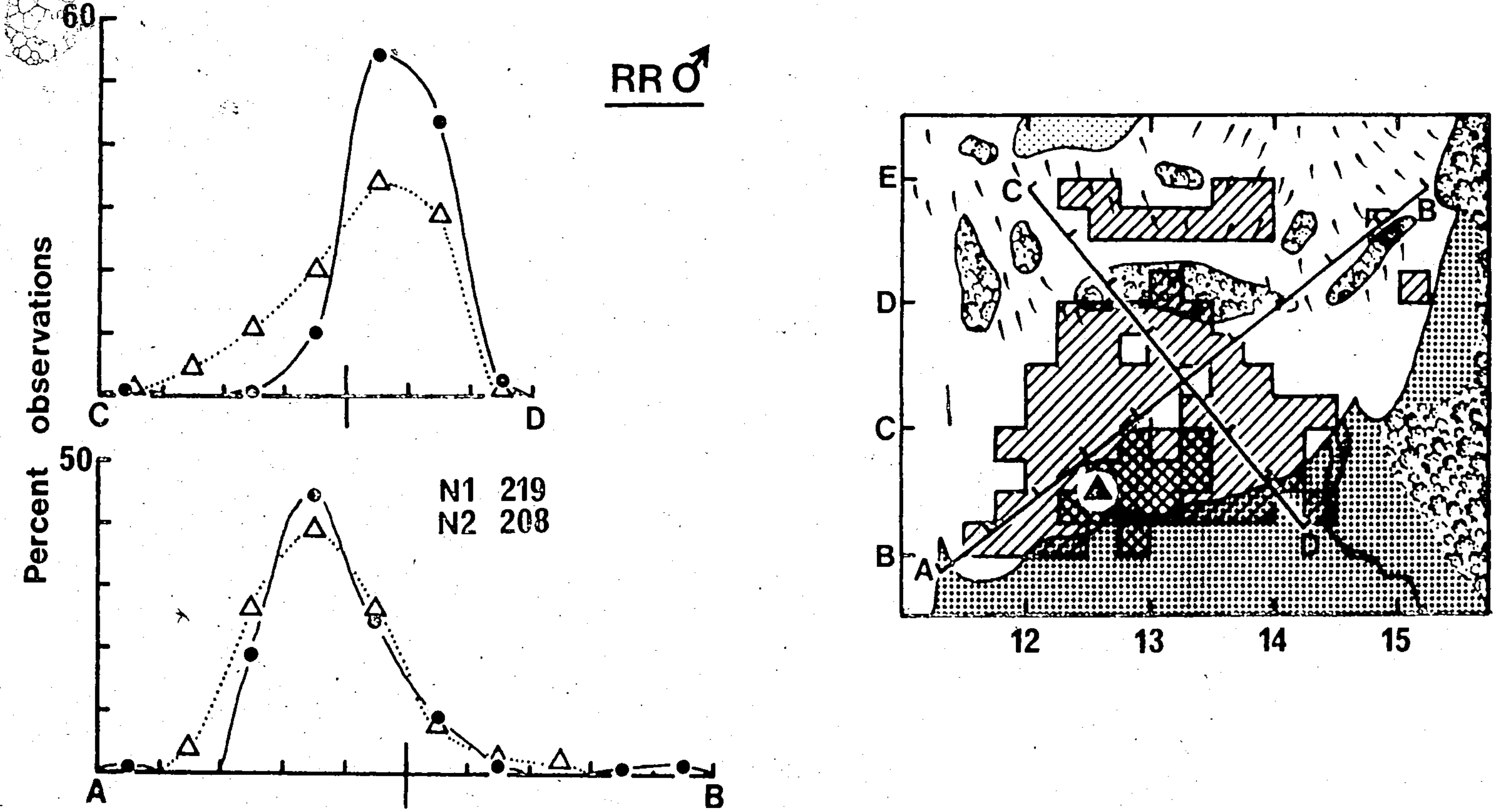
RR ♂
60
Percent observations
C
D
50
N1 219
N2 208
A
B
E
D
C
B
C
B
A
D
12
13
14
15

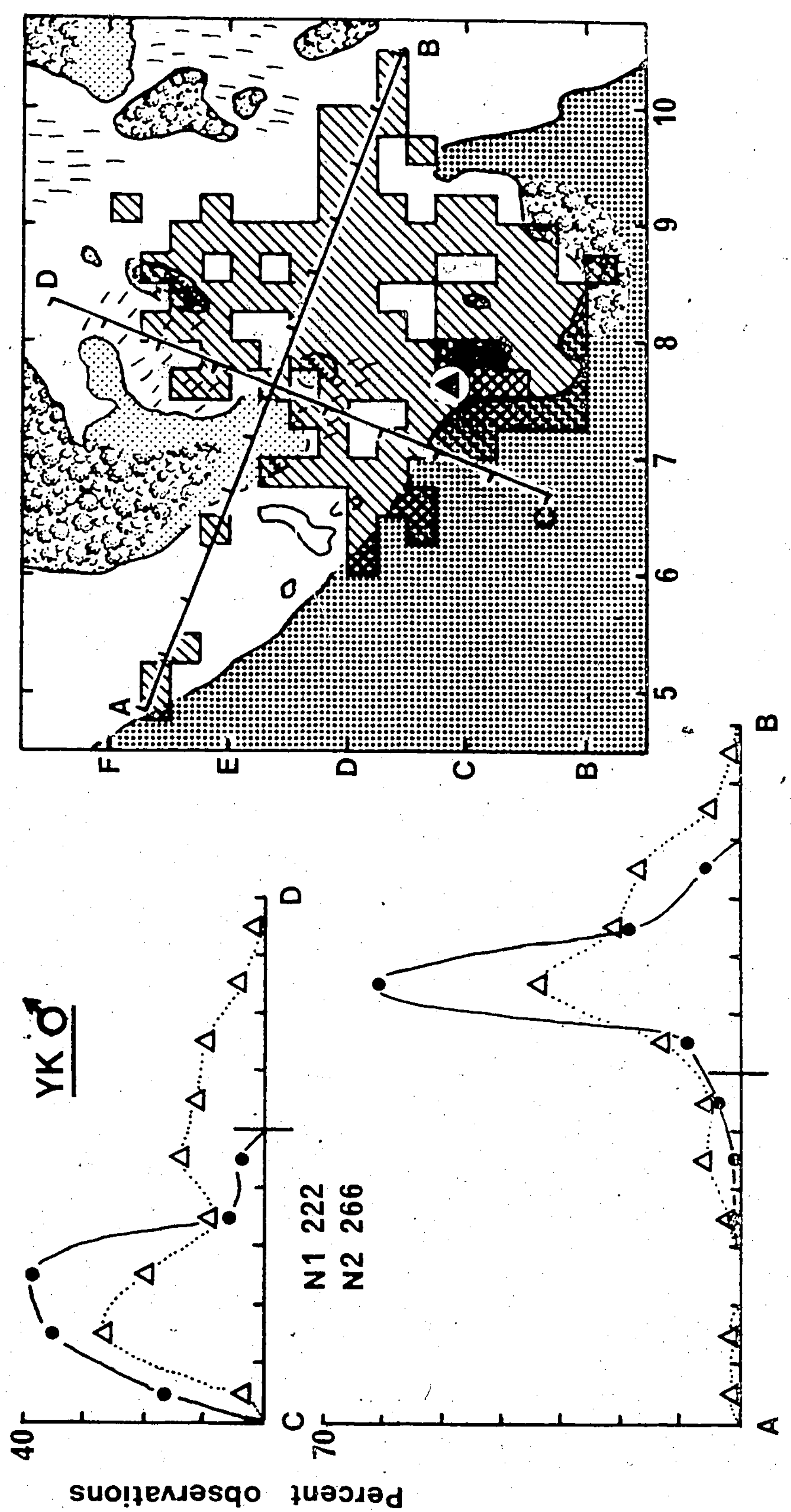
YK ♂
N1 222
N2 266
Percent observations
40
70
A
B
C
D
E
F
5
6
7
8
9
10

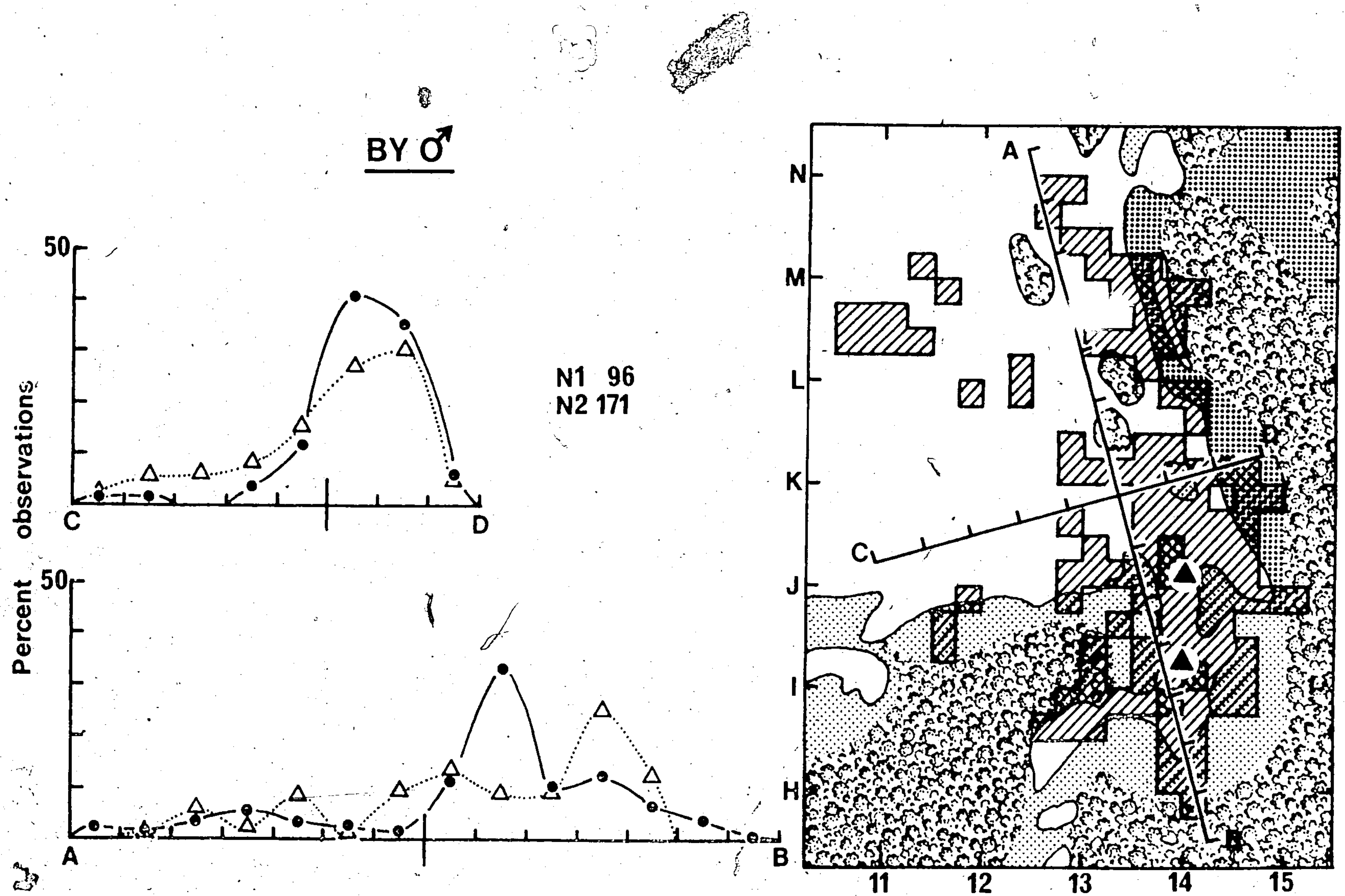
BY ♂
50
observations
Percent
C
D
50
A
B
N1 96
N2 171
A
N
M
L
K
J
I
H
C
D
B
11
12
13
14
15

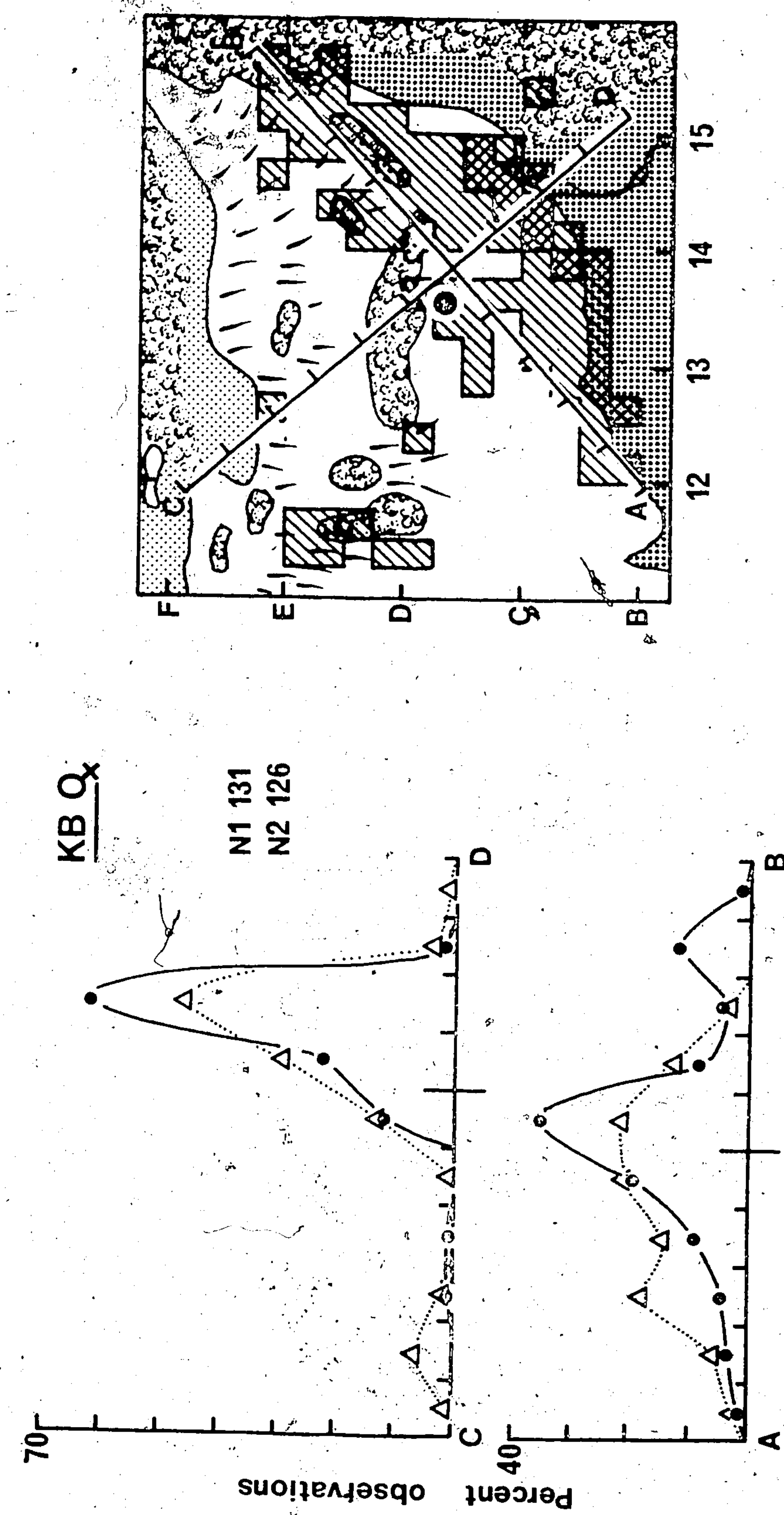

KB Qx
N1 131
N2 126
70
40
Percent observations
C
D
A
B
F
E
12
13
14
15

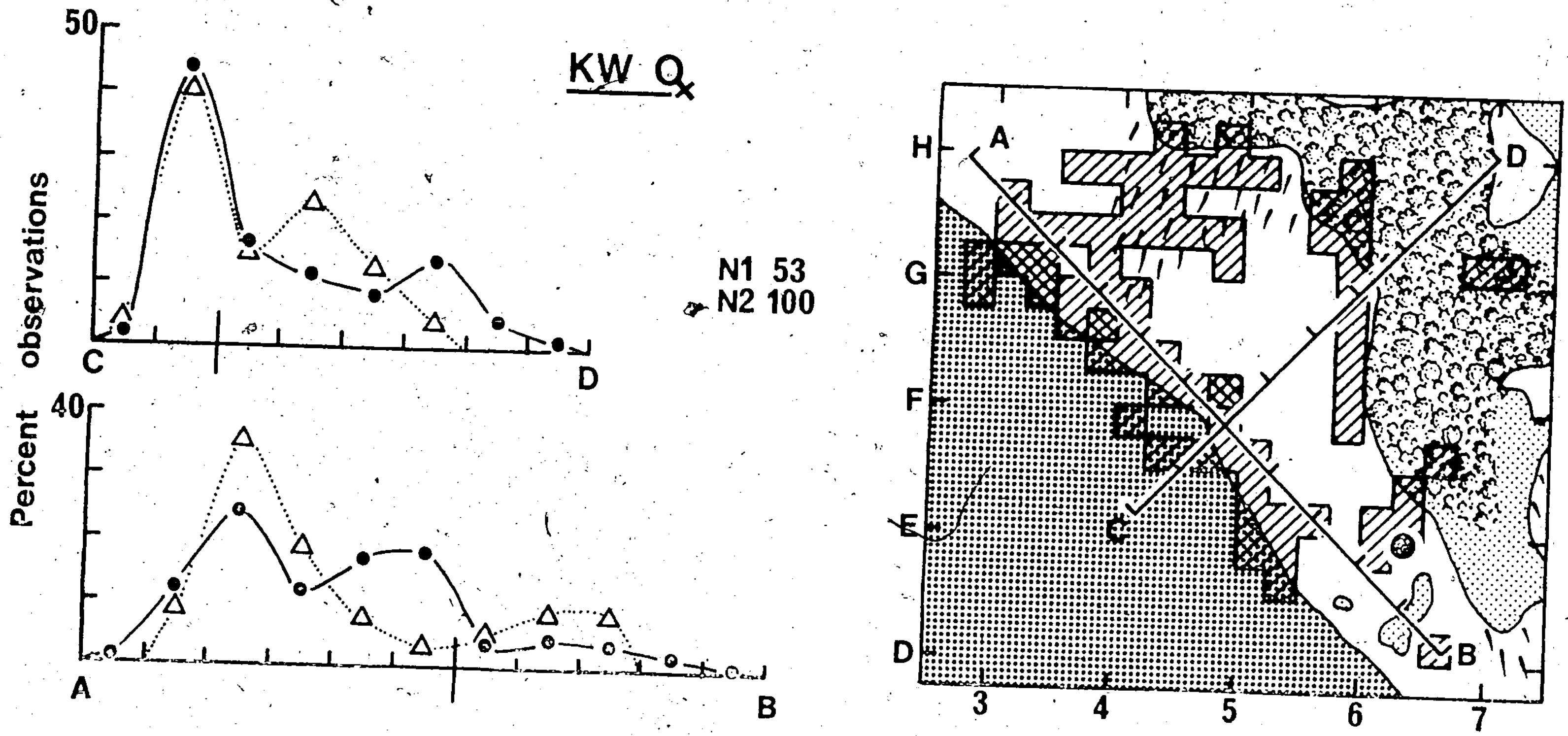
KW Q
N1 53
N2 100
50
40
Percent observations
C
D
A
B
H
G
F
E
D
3
4
5
6
7

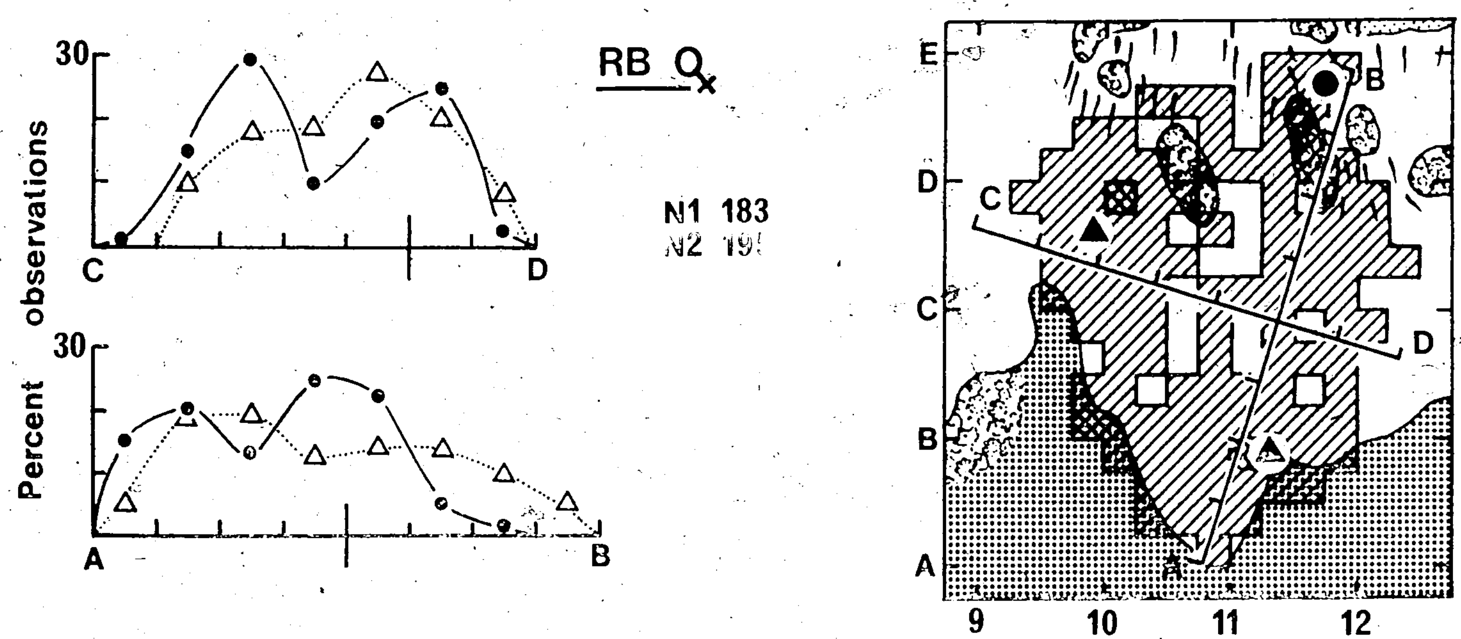

RB ♀
N1 183
N2 19
30
Percent observations
C
D
30
A
B
E
D
C
B
A
9
10
11
12

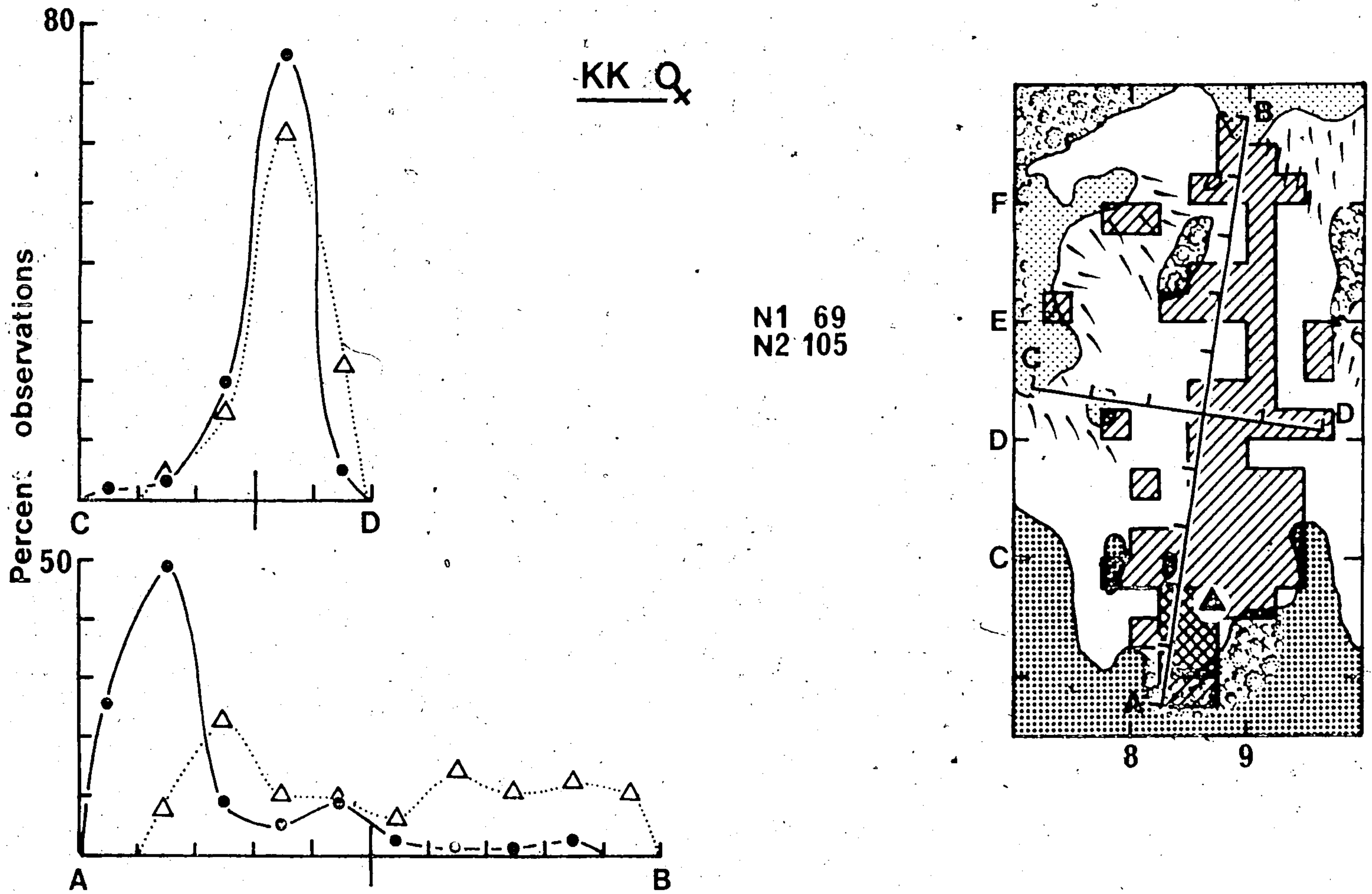
KK ♀
N1 69
N2 105
80
50
Percent observations
C
D
A
B
F
E
D
C
8
9

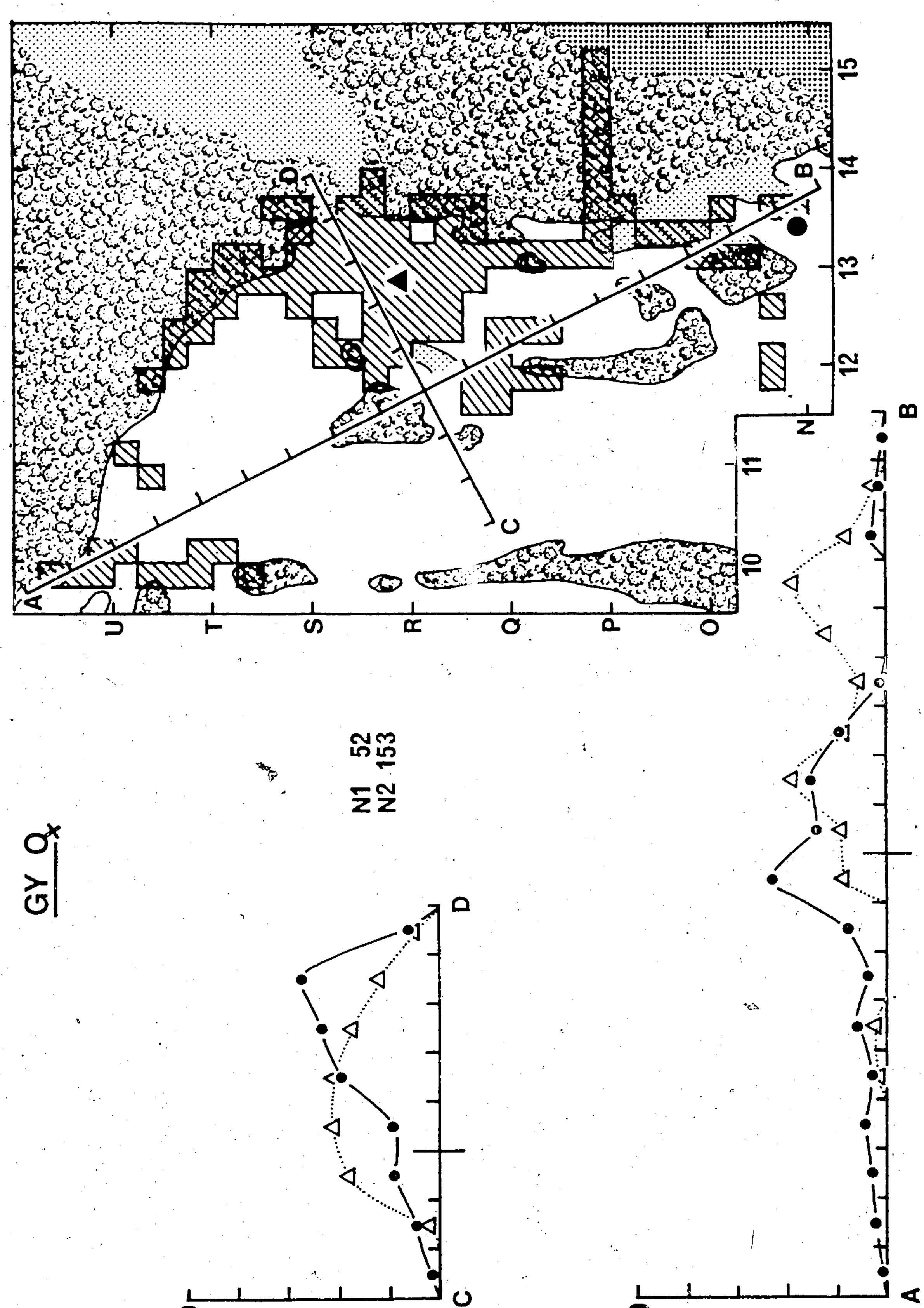
GY ♀
N1 52
N2 153
U
T
S
R
Q
P
O
N
10
11
12
13
14
15
A
B
C
D
Percent observations
50
50

was noticed also by Sharp (1973). In males, the nest site is probably close to the haypile site since, on most days, activity appeared to start in this region. Note that, in females, a separate breeding nest was usually constructed at the periphery of the female's home range.

The distribution of observations within home ranges showed little evidence of the use of traditional runways as described for the Japanese pika (Kawamichi 1969); perhaps because runways would be unnecessary in a situation where broken talus provided an overall network of escape routes.

Among males, several aspects of home range were found to be variable, both seasonally and from area to area. These seasonal and regional differences in home range will be examined using the data from Area I in 1970, under the headings of: habitat use, intensity of use, and size. Data from 1970 were used since a large number of records was obtained for that year, and the area was studied more intensively than in other years. Data from 1969 and 1971, however, showed similar trends.

The early summer period (May - June) was the breeding season. Millar (1972) found that 100 percent of the males were fertile throughout May, 83 percent in the first half of June and 56 percent in the second half of

June; but in July very few males were fertile (9 percent and 3 percent), and none were in August. He found that two litters were produced, the first being conceived around May 9 and the second about June 12.

Haypiles were constructed in late summer (July-September). In 1969, on Area I, haypiling was not observed at all during May and only on two occasions in June, whereas it was seen 19 times in July and 15 times in August. Sharp (1973) found that adult males and females spent < 1 percent of their observed time haypiling between April and June, but in July this rose to about 20 percent for males and 5 percent for females, and in August to about 35 percent for males and 23 percent for females.

Because of these seasonal differences in behaviour, most of the temporal comparisons will be made between early summer (May - June) and late summer (July-September).

Use of Habitat within Home Range

For this analysis the study area was divided into five habitat types.

1. Talus - refers to large areas of broken rock fragments. The fragments varied in size from about 20 centimetres across to some of one or two metres.

2. Scree- refers to small loose fragments

of rock usually less than 20 centimetres in diameter. Talus was generally stable to walk on, whereas scree tended to be loose and mobile. More important, pikas could live and move amongst the talus whereas they were not able to penetrate the interstices of the rock on the scree.

3. Forest - varied from continuous stands of immature lodgepole pine with little or no ground vegetation, to small clumps of white spruce and occasional alpine fir. Ground vegetation in these areas was generally sparse, though variable, depending on the density of the trees.

4. Sparse meadows - were dry areas with bearberry (*Arctostaphylos*), juniper (*Juniperus*), and sedges (*Carex*) being dominant.

5. Lush meadows - were wet or moist areas which contained a rich abundance of grasses and herbs.

Home ranges of all adults on Area I in 1970 (except two females not observed during spring) were analysed to determine the area of each habitat within them. These areas were then expressed as percentages of the total home range, since the size of the home range was dependent on the number of times the animals had been observed. These results (Tables 1 and 2) clearly indicate a much greater proportion of rocky areas within home ranges, in

Table 1. The amount of different habitat types used by individual male pikas on Area I during summer of 1970.

Pika	Talus	Scree	Forest	Sparse meadow	Lush meadow	No. of observations
	Percent of home range in each habitat					
			Early summer			
NK	85	8	-	7	-	26
YR	64	13	3	5	15	109
NN	72	4	-	7	17	65
BY	71	2	2	16	9	96
BR	66	2	21	11	-	45
RR	77	14	2	-	7	219
GG	80	8	3	4	5	146
YW	76	3	3	2	16	43
WN	24	66	-	10	-	58
RY	80	2	10	1	7	167
GW	43	40	1	16	-	108
RG	88	4	3	-	5	251
YK	79	8	1	1	11	222
Mean	69.61	13.38	3.77	6.15	7.08	
			Late summer			
NK	43	6	17	34	-	156
YR	58	20	-	2	20	135
NN	61	5	2	9	23	128
BY	58	7	11	18	6	171
BR	73	-	20	7	-	112
RR	82	2	-	-	16	208
GG	81	5	3	-	11	226
YW	74	-	8	9	9	180
WN	20	61	7	12	-	84
RY	69	17	8	-	6	138
GW	46	30	4	19	1	94
RG	86	3	3	-	8	184
YK	62	7	3	2	26	266
Mean	62.53	12.53	6.62	8.62	9.69	

Table 2. The amount of different habitat types used by individual female pikas on Area I during summer of 1970.

	Percent of home range in each habitat					
Pika	Talus	Scree	Forest	Sparse meadow	Lush meadow	No. of observations
			Early summer			
GK	58	-	4	38	-	14
GY	46	-	22	32	-	52
BB	84	-	4	12	-	32
RW	78	4	-	9	9	48
RK	81	-	2	-	17	70
KY	19	75	2	6	-	55
KK	86	9	-	4	1	69
GB	70	4	-	6	20	97
RB	75	9	5	-	11	183
KB	70	12	2	-	16	133
KW	60	21	-	-	19	53
Mean	66.09	12.18	3.73	9.73	8.45	
			Late summer			
GK	90	2	4	4	-	43
GY	74	1	13	12	-	153
BB	64	-	2	34	-	76
RW	74	-	-	16	10	161
RK	80	-	11	-	9	86
KY	6	68	-	26	-	80
KK	79	5	2	-	14	105
GB	61	9	-	1	29	216
RB	85	1	2	-	12	195
KB	82	4	7	-	7	127
KW	57	12	12	1	18	100
Mean	68.36	9.27	4.82	8.55	9.00	

comparison with vegetated areas. This was consistent for nearly all animals.

To test whether or not there were any significant differences between the sexes and seasonally with respect to habitat use, a Chi-square analysis was used; first on individual animals, and secondly on the pooled data between groups -- since there were no significant differences within groups. For this analysis the habitats were lumped into two types: rocky areas (talus and scree) and vegetated areas (forest and meadow); and the number of 5 X 5 metre squares in each type compared. This was done for simplicity and because it circumvented some of the more subjective divisions, as between sparse and lush meadow areas.

Among males, only two (NK and YK) showed a significant change in the proportion of rocky to vegetated areas from early to late summer ($P < 0.01$ for NK, and $P < 0.02$ for YK). However, when the data for all males were pooled the difference was highly significant ($P < 0.001$), due to a high proportion of rocky areas used in early summer.

Analysis of the home ranges of females showed two animals with significantly different seasonal use of habitat (GK, $P < 0.05$ and GY, $P < 0.005$); both of these showed a higher proportion of rocky areas in late summer. However, when the data were pooled, females showed no statistical differences between early and late summer. Comparison between males and females revealed a significant difference ($P < 0.05$) in early summer, but no difference in late summer. These data are summarised in Fig. 4. Home ranges of males in early summer showed a significantly higher proportion of rocky areas to vegetated areas than did any of the other three categories.

This difference in habitat useage of males in the spring is probably due to an increase in [illegible] of rocky areas rather than a decrease in use of vegetated areas, since on the average males used 37.86 squares in rocky areas and 7.06 squares in vegetated areas per 100 observations during early summer, compared to 26.17 squares in rock and 9.17 squares in vegetation in late summer.

<u>Intensity of use within Home Range</u>

The distribution of observations within home ranges changed seasonally, with animals spending more time at the periphery of their home ranges in early summer and more time centrally in late summer. In order to evaluate these changes, 'intensity of use' graphs were constructed for all animals which had been observed frequently enough to estimate the size of their homes ranges. (Ref. Size of Home Range).

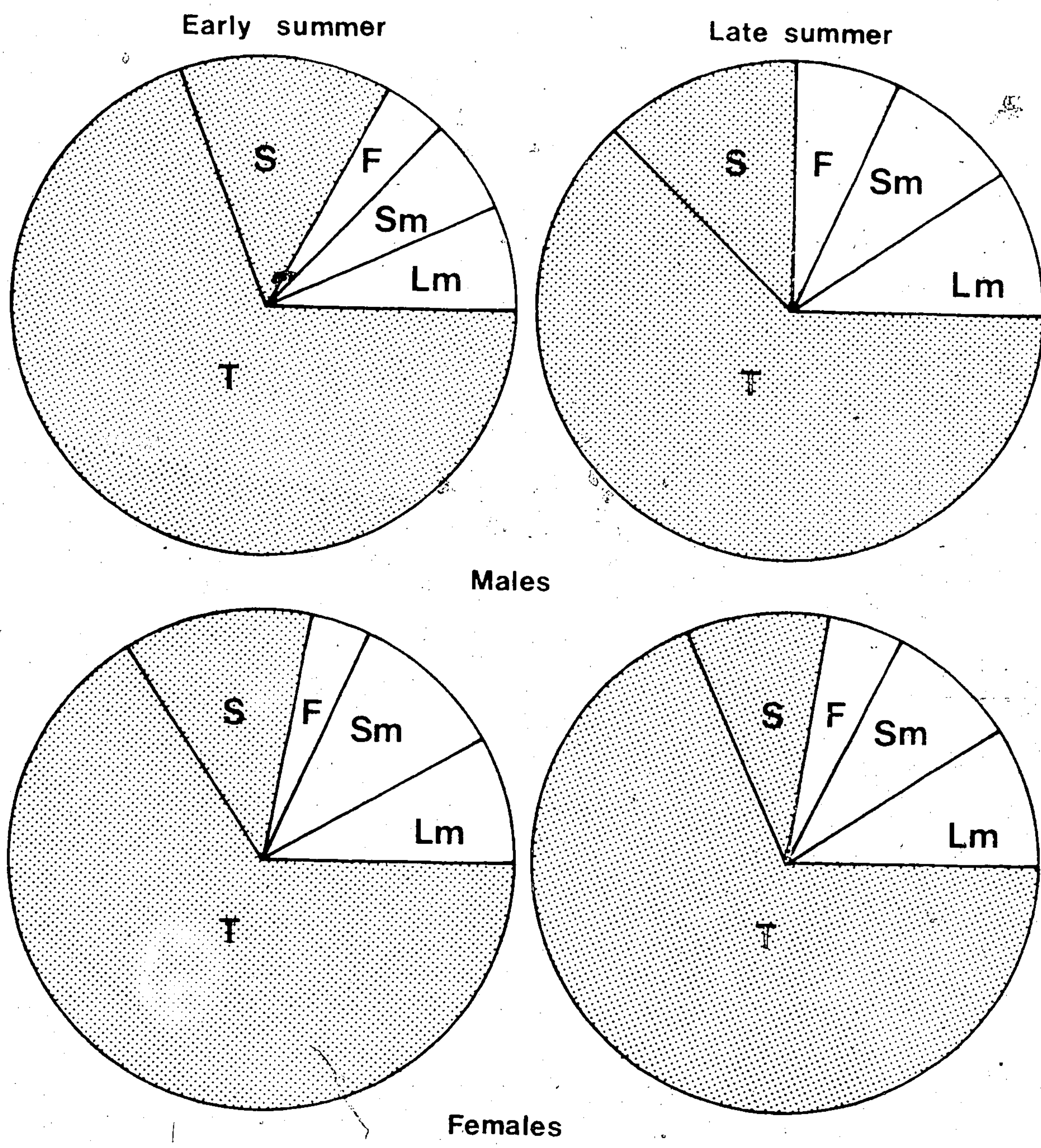

Fig. 4. A schematic representation of habitat use by male and female pikas during the early and late summer of 1970.
T = talus; S = scree; F = forest; Sm = sparse meadow; Lm = lush meadow.

A 'long axis" (AB - Fig. 3) was plotted for each home range on the line between the two most distant observation points. At right angles to this, a series of strips 10 metres wide were drawn and the number of observations occurring within each strip counted and expressed as a percentage of the total. This was also done for the 'short axis' (CD). These data, plotted seasonally, are shown in Fig. 3 for the ten animals referred to earlier. In order to make statistical comparisons, the heights of the tallest peaks on each axis were tabulated and compared seasonally with respect to sex. The results for all animals on Area I in 1970 are shown in Table 3. Using a Wilcoxon's signed-ranks test it was found that peaks were higher, indicating greater clustering of observations, in late summer than in early summer. The difference was significant for both males and females ($P < 0.01$). Males were then compared with females in the early and late summer, and no significant differences were found.

These results indicate that both males and females tend to utilize their home ranges more evenly in early summer and tend to use particular areas more intensively during late summer. This is probably caused by animals constructing haypiles in late summer producing increased activity at a haypile site. However, such things as patrolling home range boundaries in the breeding season could also account for these differences.

Table 3. Intensity of use of home ranges on Area I in 1970.

Percent of observations in highest peak along each axis

Pika	Long axis Early summer	Long axis Late summer	Short axis Early summer	Short axis Late summer
		Males		
RY	28	70	44	63
YR	28	52	38	61
RG	21	29	37	43
GG	24	43	35	51
RR	39	45	34	55
BY	26	33	30	41
GW	66	42	41	28
YK	33	61	27	38
		Females		
KB	21	36	46	62
KK	22	48	61	74
GY	19	23	21	27
KW	36	24	41	44
RB	19	24	27	29
RW	35	33	50	54

As noted later, males have larger home ranges in early summer than in late summer. Hence this might cause the differences in intensity of use just shown. Although this must be true in part, females did not show any seasonal differences in size of home ranges, yet did show a significant difference in their use of home ranges. Thus it is likely that use intensity differences shown for males are not dependent only on differences in home range size.

Size of Home Range

With increasing amounts of data the calculated size of home ranges increases until a level is reached after which further observations do not cause a corresponding increase. The standard method for estimating home range size is, therefore, to plot size against the cumulative numbers of observations or trappings etc., and when the curve reaches an asymptote the actual home range is assumed to be represented (eg. Stickel 1954, Odum and Kuenzler 1955, Weeden 1965, Ables 1969, Stoddart 1970).

In this study, area, as measured by number of squares occupied did not produce a curve from which any reasonable estimate could be made. Instead when the dimensions of the home range (length plus breadth) were plotted with increasing observations, the curves for some animals did reach an asymptote (Figs. 5 and 6). Even in these cases a high number of observations was required for any particular time period. In order to estimate the level of the final asymptote when sufficient observations were not available, Stenger and Falls (1959) developed a method using the slope of the initial part of the curve to derive an estimate of territory size in ovenbirds (*Seiurus aurocapillus*). But the initial slopes of the curves produced from pika ranges appeared unrelated to the final asymptote, and this was probably because the observations were not sufficiently independent of each other. However, if the level at which the home range remains constant for three consecutive points on the graph is taken as an index of home range size, a constant relationship is found with the final asymptote. This index will be referred to as the 'sub-asymptote' and its relationship to the final asymptote (using animals in Figs. 5 and 6) is shown in Fig. 7.

Although the data are too few in number (and are not normally distributed) for statistical analysis they suggest that this index is very nearly the same as the final asymptote for females but is definitely lower for male pikas. This may indicate that male pikas are more likely to make exploratory excursions than females. All home range sizes used in analysis are sub-asymptotic levels.

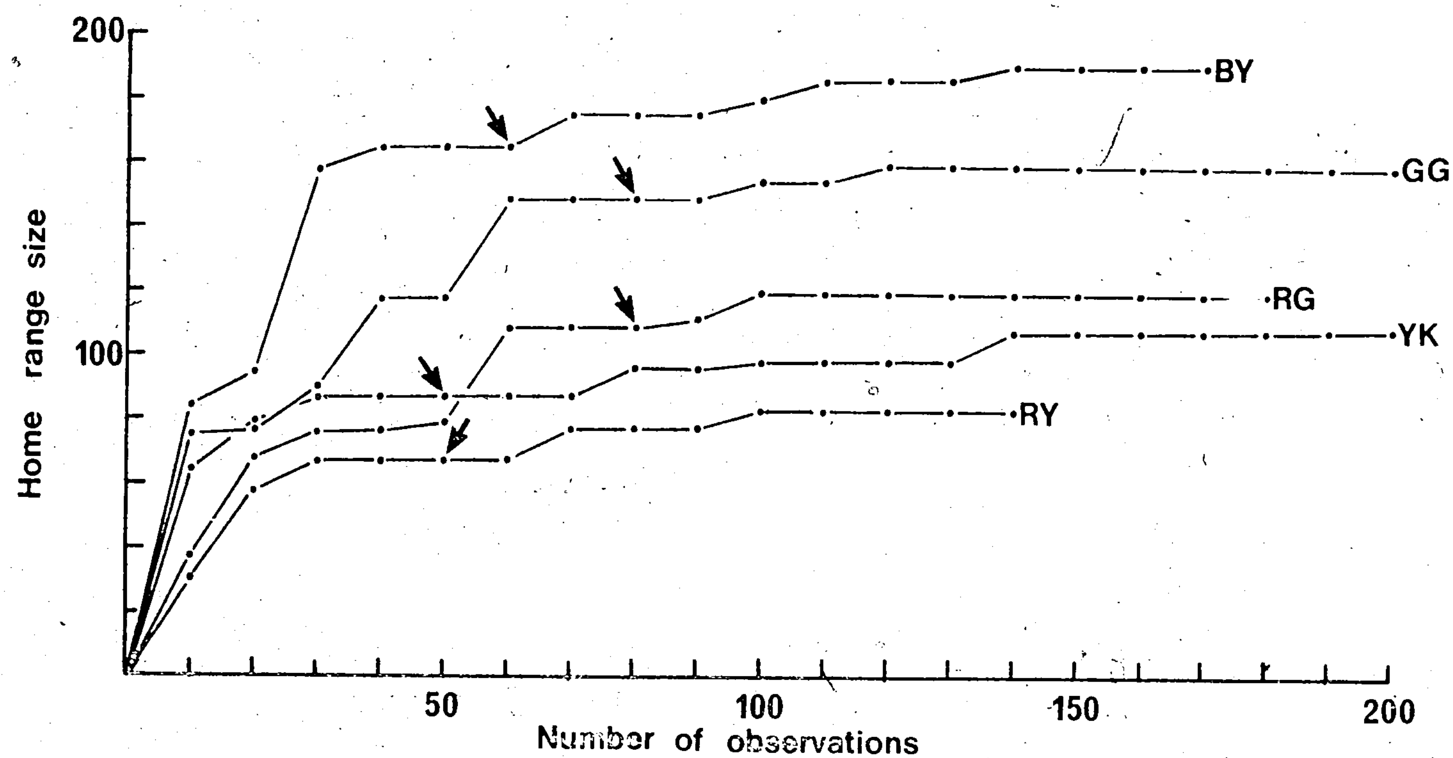

Fig. 5. Size of home range (in metres) versus number of observations for five males during late summer 1970. Animals were selected on the basis that the curves for home range size appeared to reach an asymptote. Arrows indicate sub-asymptote.

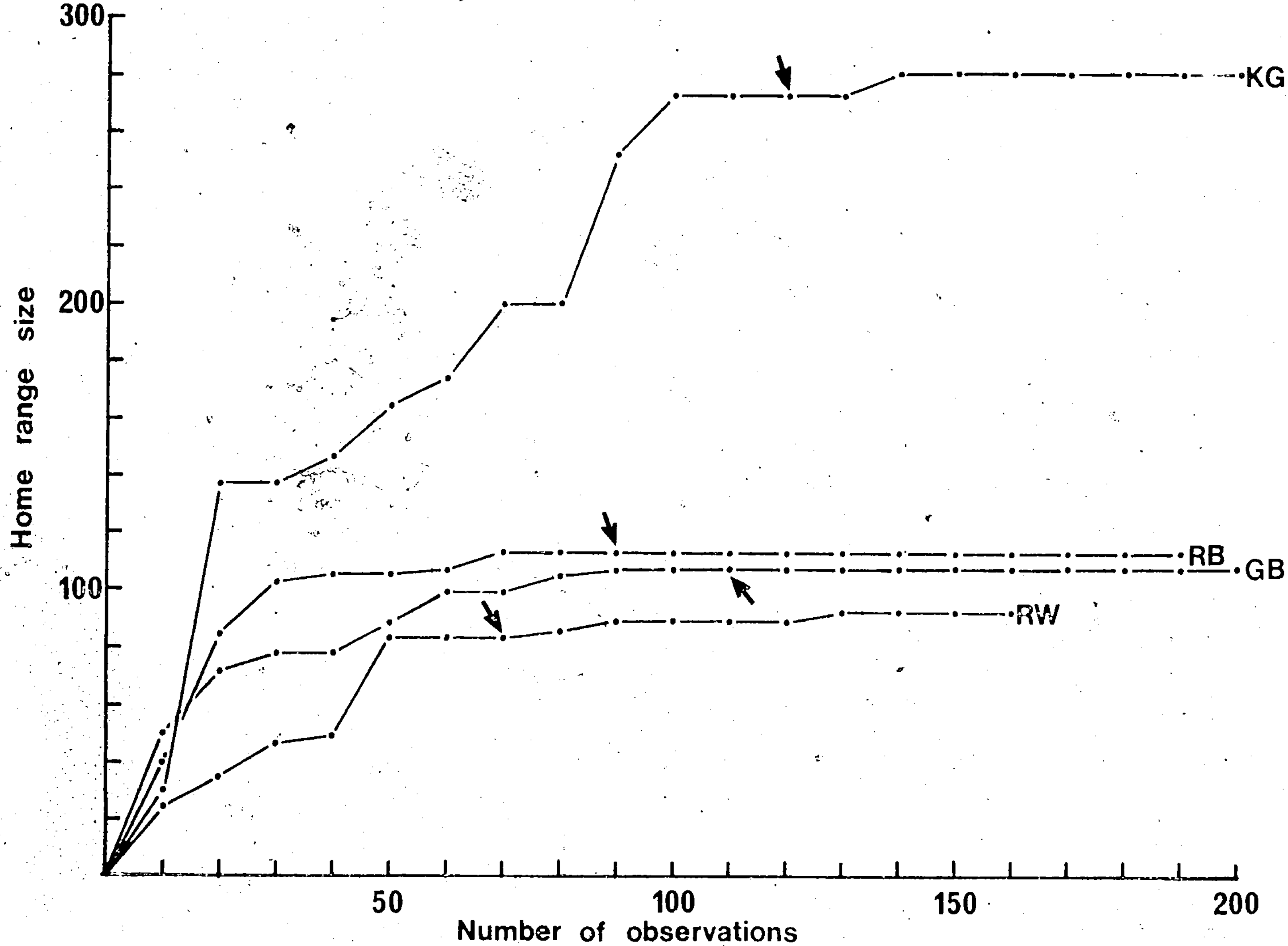

Fig. 6. Size of home range (in metres) versus number of observations for four females during late summer 1970. Animals were selected on the basis that the curves for home range size appeared to reach an asymptote. Arrows indicate sub-asymptote.

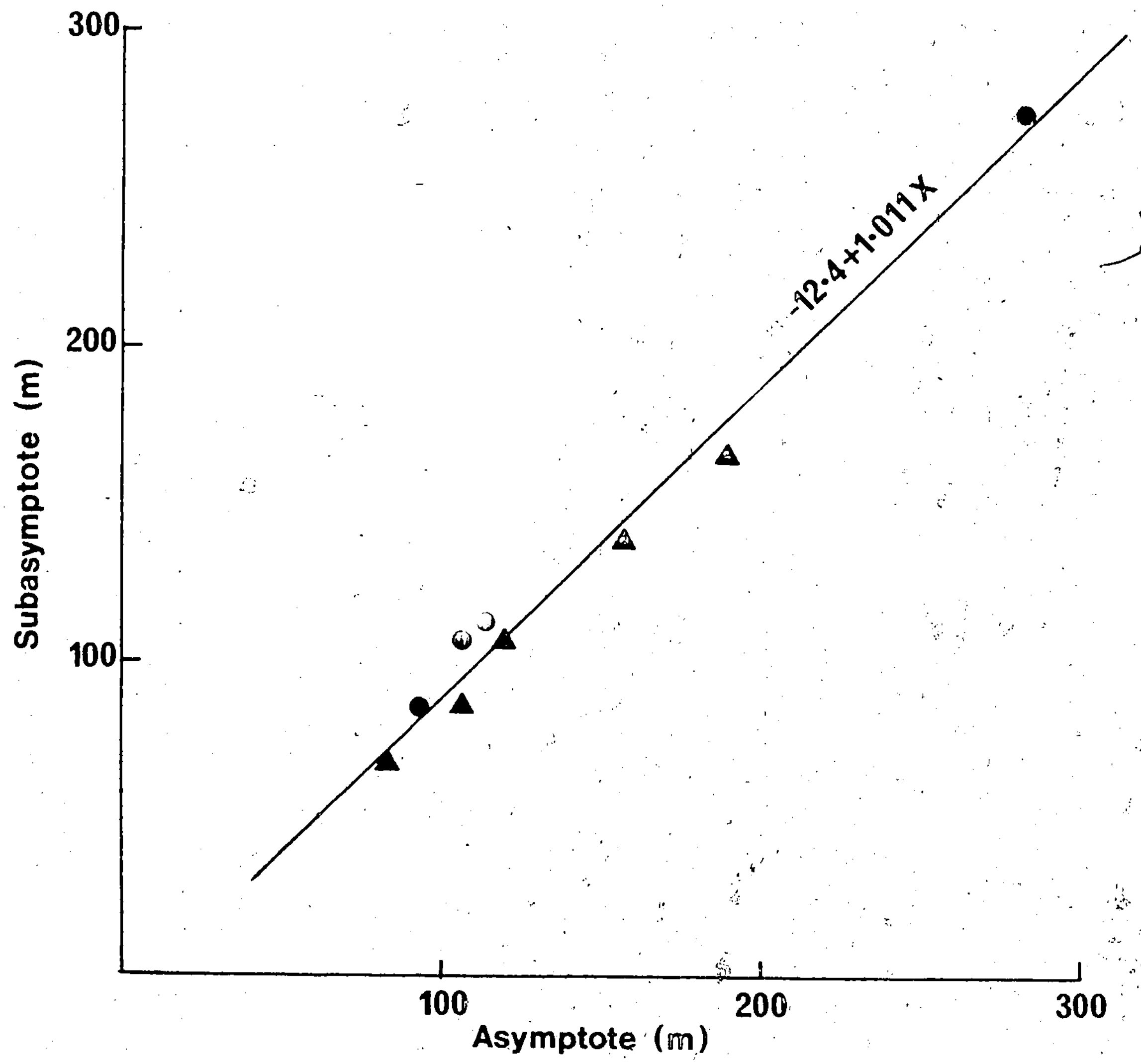

Fig. 7. Relationship between sub-asymptotes and asymptotes of home ranges of five males and four females shown in Figs. 5 and 6.

▲ Males.

● Females.

Seasonal Variation

Sizes of home ranges of all adults on Area I in 1970 are shown in Table 4. In this table, figures in brackets are home range sizes below the sub-asymptote; they are included only for comparative inspection and were not used in statistical calculations. Where sufficient data are available, an estimate for each month is given -- otherwise months are combined as early or late summer. Where estimates are made for both months in one season the final figure is given by the average of the two months. Seasonal changes in home range size were examined using a Wilcoxon signed-ranks test. This meant that only animals for which there were figures for both seasons were included in the analysis.

In males, home ranges were significantly larger in early than in late summer ($P < 0.025$). This decrease in size with the progression of summer appears to be a gradual shrinkage rather than a rapid switch since the August-September figures are also significantly lower than those in July ($P < 0.05$). Unfortunately sample sizes were too small to make comparisons between May and June, and June and July.

This change in size of home range correlates with the change in use of habitat described earlier, which suggests that expansion of home ranges in early summer is

Table 4. Home range sizes of all adult pikas on Area I during the summer of 1970. Ranges are measured in metres (length + breadth) and are 'sub-asymptotes.'

Pika	May	June	Early Summer	July	Aug-Sept	Late Summer
			Males			
YR	–	–	145	–	–	140
BY	–	–	192	–	–	164
RG	116	149	132	108	96	102
RR	–	–	110	98	84	91
RY	155	87	121	67	–	67
YK	–	–	165	87	81	84
GG	122	–	122	149	124	136
GW	–	–	132	–	–	124
NK	–	–	(>181)	151	–	151
NN	–	–	(>123)	–	–	109
WN	–	–	(>110)	–	–	116
YW	–	–	(>236)	251	245	248
			Females			
BB	–	–	(>189)	–	–	150
GB	–	–	(>136)	107	71	89
GK	–	–	(>83)	–	–	(>125)
GY	–	205	205	–	–	219
KB	–	–	139	–	–	151
KG	–	–	–	–	–	273
KK	–	–	111	–	–	134
KW	–	–	112	–	–	154
KY	–	–	–	–	–	93
RB	–	–	129	–	–	112
RK	–	–	–	–	–	–
RW	–	–	89	83	74	78
WB	–	–	–	–	–	(>191)

accomplished by the inclusion of larger areas of talus.

In females, there was no significant change in the home range size from season to season. Although the sample sizes are small, it is clear that there are no seasonal trends.

Sizes of home ranges were compared between males and females during both seasons using paired and non-paired non-parametric statistical tests. No significant differences were found although males appeared to have generally larger home ranges than females in early summer when adjacent males and females were considered. It is probable that the wide variation in home range sizes and the small sample sizes account for this lack of significance.

Regional Variation

Apart from the seasonal variation in size of home ranges and a general variability between individuals there appeared to be marked regional differences in home range size within and between study areas. This was apparent on Area I where animals on the upper section of the slide (above grid line 'H') had large home ranges while those on the lower section (below grid line 'H') had smaller ranges (Table 5). This difference was significant among males ($P = 0.005$ - Mann Whitney U test), but not among

Table 5. Comparison of home range sizes from upper and lower sections of Area I.

Sub-asymptotes - measured in metres			
Lower section		Upper section	
Males	Females	Males	Females
116	89	248	150
109	151	151	219
124	134	164	273
136	154		
84	93		
67	112		
91	78		
102			
140			

females; probably due to small sample size.

Associated with this were two other variables which could be important in explaining the difference. (1) The density of individuals was lower on the upper section of talus. (2) The amount of food available, as indicated by the standing crop of herbaceous vegetation, seemed to be much lower on the upper section of talus. These aspects were examined in more detail.

Centres of activity were calculated for all adult animals on Area I during late summer 1970, using the method described by Hayne (1949). The distance from the centre of activity of one animal to the centre of activity of its nearest neighbour of the same sex was taken as an index of relative density. These indices for all adults on Area I are shown in Table 6. Indices for males on the upper section of talus were significantly higher than those on the lower section ($P < 0.005$ - Mann Whitney U test). This was also true for females ($P < 0.001$).

In order to evaluate the relative amounts of food available in different areas, all observations of feeding and haying behaviour made during July - September 1970 were plotted on a map of Area I (Fig. 8). From these observations, ten feeding areas were chosen; five from the upper section of slide and five from the lower (Fig. 8). Feeding areas were sampled by clipping all ground vegeta-

Table 6. Comparison of densities from upper and lower sections of Area I.

Distance to nearest neighbour (metres) of same sex			
Lower section		Upper section	
Males	Females	Males	Females
32	14	105	93
32	14	105	93
42	35	188	85
45	44	128	85
45	20		92
14	20		
14	52		
56	52		
68			

Fig. 8. Observations of feeding and haying behaviour on Area I from July to September 1970. Closed circles - observations of pikas feeding; arrows - movements of pikas carrying vegetation; I - V feeding areas on lower section of slide; VI - X feeding areas on upper section of slide.

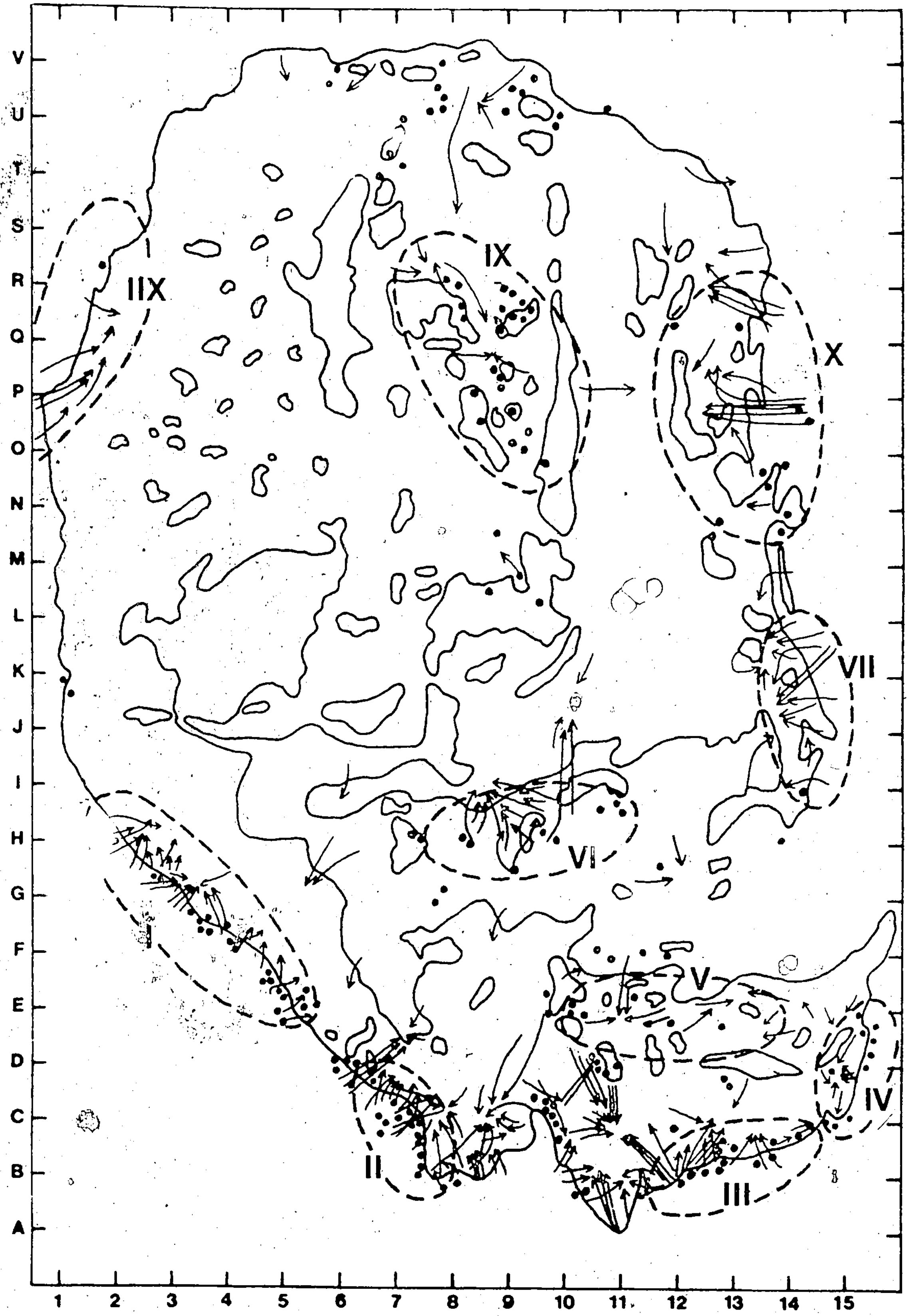
V
U
T
S
R
Q
P
O
N
M
L
K
J
I
H
G
F
E
D
C
B
A
1
2
3
4
5
6
7
8
9
10
11
12
13
14
15
IIX
IX
X
VII
VI
I
V
IV
II
III

tion (excluding mosses and lichens) from five 1/10 square metre plots on each feeding area. However, one species, juniper (Juniperus), was excluded since it was extremely widespread and abundant but was almost never used by pikas (Millar 1971). Because of the nature of the terrain (often only clumps of vegetation between broken rocks), plots were subjectively chosen within these feeding areas so that only the densest patches of vegetation were sampled. Hence the weights are maxima rather than random samples. These results are shown in Table 7. The mean weights from the upper section of the slide were significantly smaller than from the lower section ($P < 0.001$ - t test).

These results have to be viewed with caution since they do not show any cause and effect relationship. However, they suggest two principles which could be important in the dispersion of pikas. (1) Size of home range appears related to density, suggesting the use of space tends to be exclusive between individuals of the same sex. (2) Size of home range and, therefore density, appears related to the relative abundance of an accessible source of food.

Table 7. Comparison of weights of vegetation from upper and lower sections of Area I

Feeding area	Dry wgt. (grams) of vegetation on 1/10 sq. metre plot					Mean
	Lower section					
I	34.5	33.8	32.2	53.1	37.0	38.12
II	29.1	34.5	40.3	57.0	23.5	36.88
III	35.5	35.8	40.1	36.3	29.1	35.36
IV	8.0	27.8	14.1	32.6	28.5	22.20
V	10.6	1.5	74.1	82.9	7.0	35.22
	Upper section					
VI	6.8	9.1	14.2	10.0	8.3	9.68
VII	13.2	9.4	14.0	13.9	8.9	11.88
VIII	5.2	15.2	9.3	5.0	4.3	7.80
IX	5.3	12.3	6.5	3.4	5.3	6.56
X	13.8	23.0	24.1	9.5	4.9	15.06

SPATIAL ORGANISATION OF ADULTS

This section deals with dispersion of adult pikas and with the social factors which appear to give rise to it; the movement and settlement of juveniles being considered later.

Although the spatial organisation should be considered as an interrelated system with variations in one aspect causing compensatory changes in other aspects, it is dealt with here in three separate subsections: (1) male - female spacing, (2) male - male spacing, (3) female - female spacing. Only data from Area I during 1970 and 1971 are used in this analysis.

Male - Female Spacing

At birth the sex ratio in pikas was found by Millar (1971) to be almost 1:1. On Area I the sex ratio of adults is shown in Table 8. While none of these figures differed significantly from a 1:1 sex ratio (using Chi-square analysis), there was a slight bias in favour of males, especially during 1971.

When centres of activity of adults were plotted (Fig. 9), there appeared to be a close association between

Table 8. Number of adults by sex on Area I, 1969 - 1972

		Males	Females
1969	Early summer	12	11
	Late summer	10	10
1970	Early summer	14	4
	Late summer	14	13
1971	Early summer	19	13
	Late summer	17	10
1972	Early summer	13	9

Fig. 9. Calculated centres of activity for adult pikas on Area I, July - September 1970

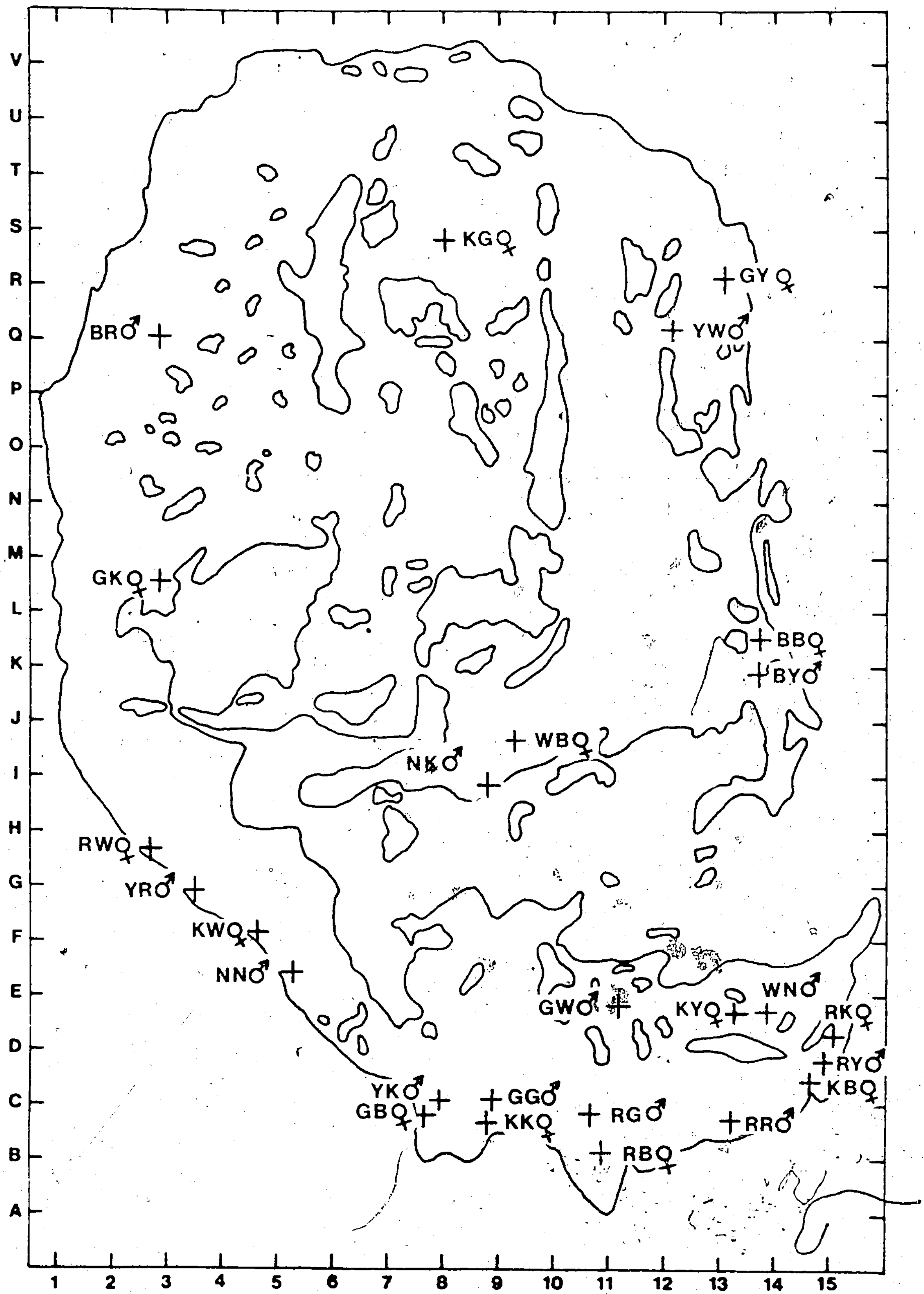
V
U
T
S
R
Q
P
O
N
M
L
K
J
I
H
G
F
E
D
C
B
A
1 2 3 4 5 6 7 8 9 10 11 12 13 14 15
KG♀
GY♀
BR♂
YW♂
GK♀
BB♀
BY♂
WB♀
NK♂
RW♀
YR♂
KW♀
NN♂
GW♂
KY♀
WN♂
RK♀
RY♂
KB♀
YK♂
GB♀
GG♂
KK♀
RG♂
RR♂
RB♀

males and females. With few exceptions adults seemed to occur in pairs. When home ranges were plotted for individual pairs this association was even more striking. An example is shown in Fig. 10, where the female's home range varied little seasonally. During the late summer both animals appeared to have almost exactly the same outer limits to their home ranges, however there were areas used exclusively by each.

Another pair is shown in Fig. 11 where the home ranges were almost entirely separate, perhaps indicating little association unless one refers back to Fig. 9 and considers the centers of activity relative to the other members of the population. This separation was more noticeable at low than at high densities.

These same principles are illustrated in Fig. 12 but with a slight variation. Here two pairs of animals (BY:BB, and GY:YW) showed a clear boundary between pairs, especially along the edge of the rock slide, and yet in both pairs, the males and females used different areas most intensively. This situation was further complicated by a third female (KG) which seemed to be unpaired, although YW extended his home range right across hers. In this situation there was still a clear boundary between the two adjacent females, indicating that females may maintain their own boundaries irrespective of males. In

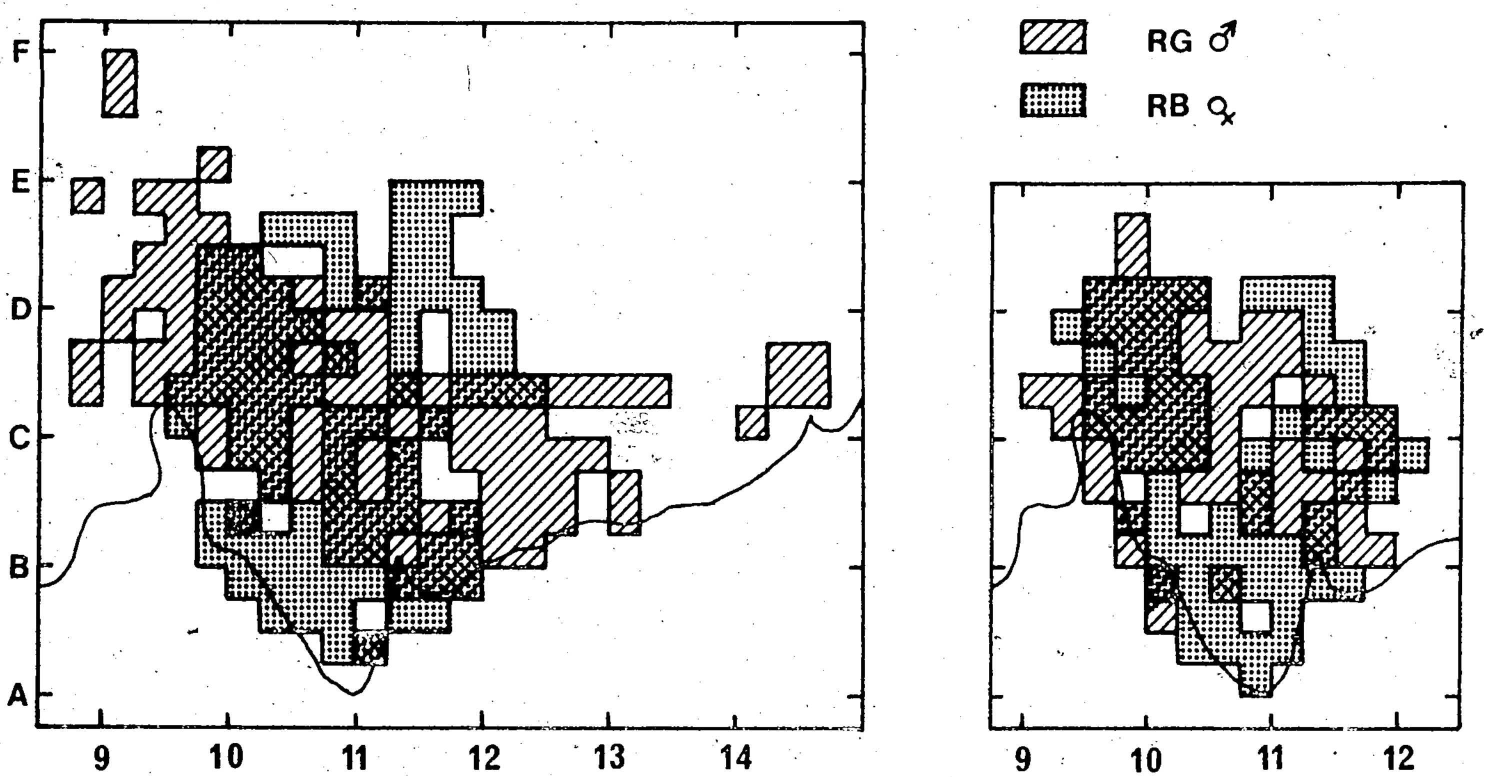

Fig. 10. Home ranges of a pair of pikas during early summer (left) and late summer (right) on Area I in 1970. Number of observations: Early summer, RG = 255, RB = 183. Late summer, RG = 184, RB = 197

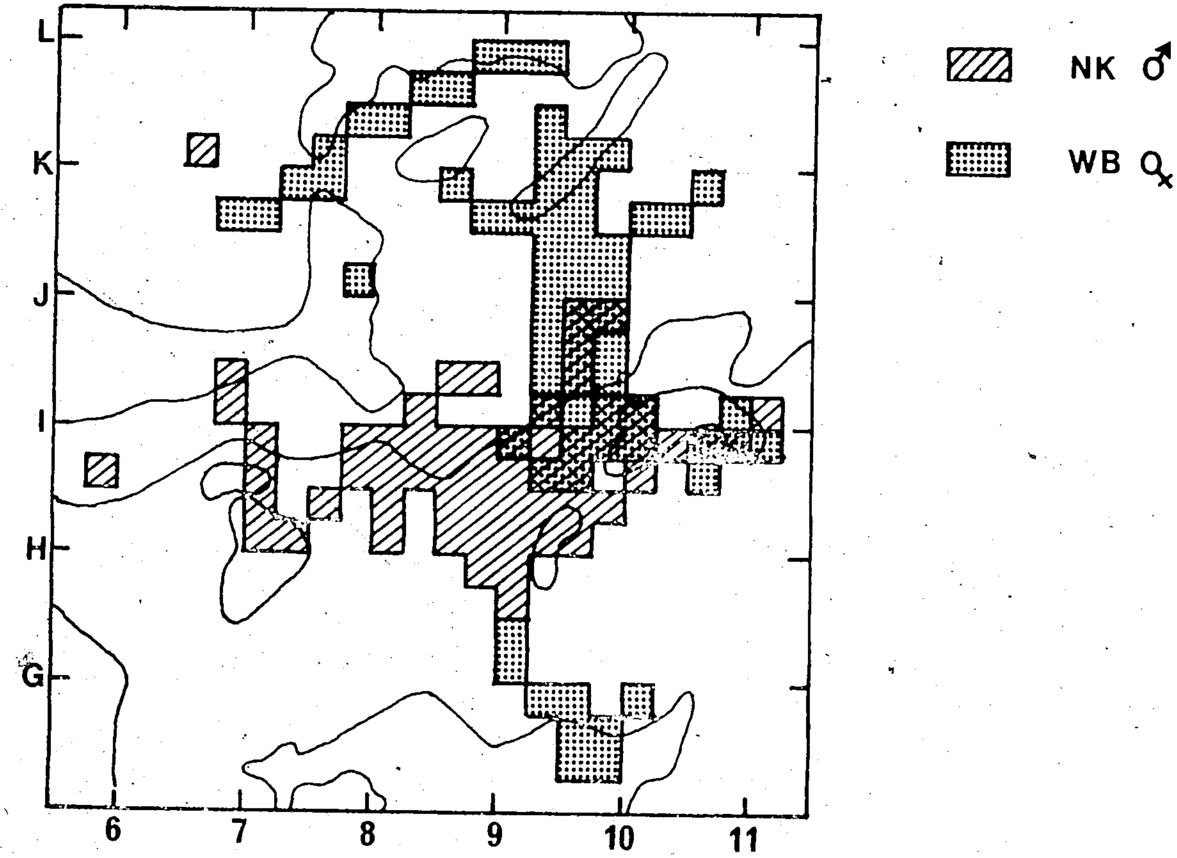

Fig. 11. Home ranges of a pair of pikas during late summer on Area I in 1970, number of observations: NK = 156, WB = 89.

Fig. 12. Home ranges of five pikas during summer on Area I in 1970.

Number of observations: BY = 267, YW = 223, BB = 108, GY = 206, KG = 202.

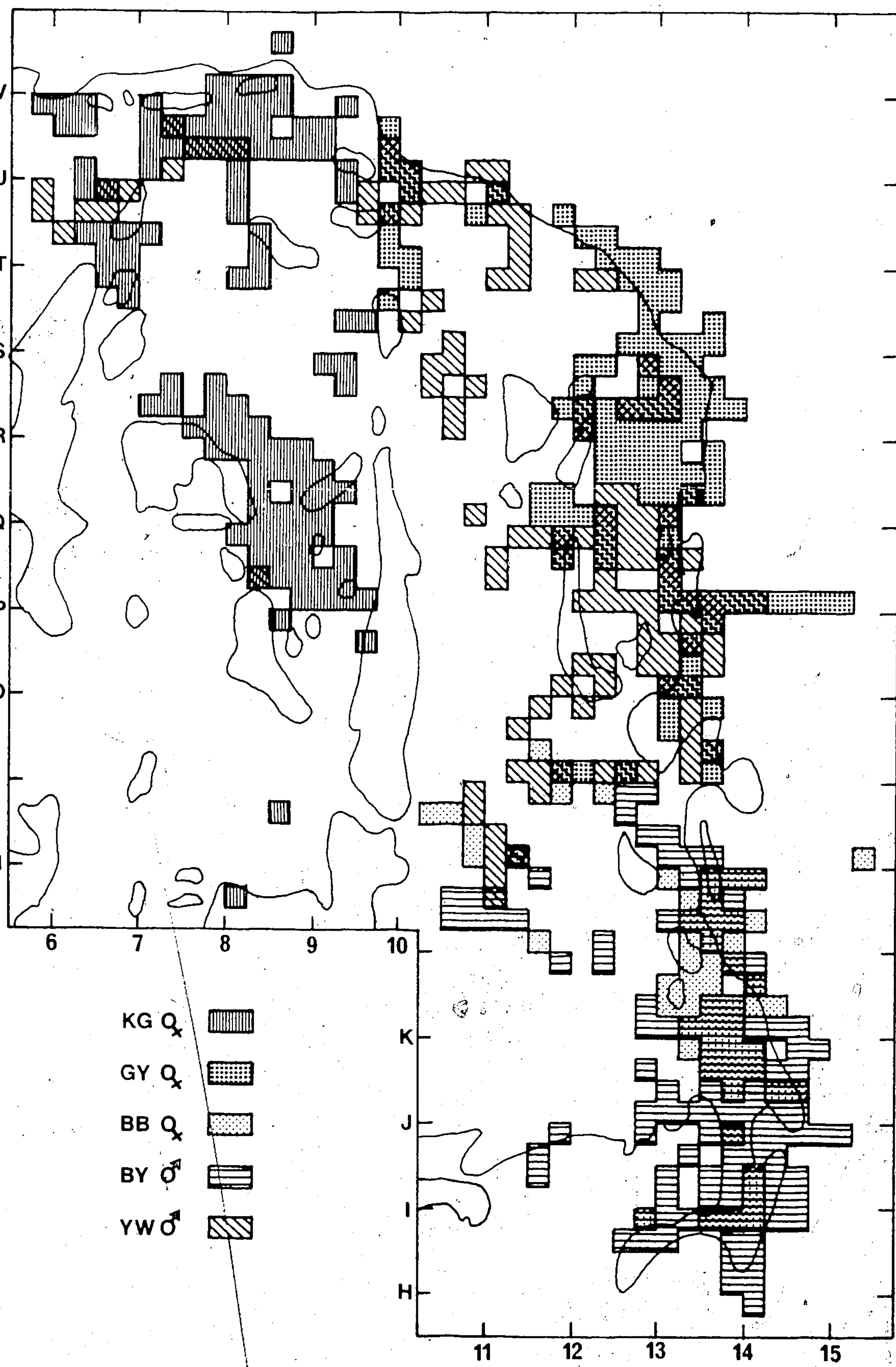
V
U
T
S
R
Q
P
O
N
M
6
7
8
9
10
K
J
I
H
11
12
13
14
15
KG ☿
GY ☿
BB ☿
BY ♂
YW ♂

general, however, paired animals seemed to have similar outer limits to their ranges. This particular situation could be explained in two ways: (1) that there was originally another pair present, the male of which died leaving female KG, and YW's range extension merely exploited this vacancy; (2) that YW in fact had an exceptionally large home range which was of sufficient size to include two females. This latter explanation appeared to be more likely since the situation remained largely unaltered in three years, except KG replaced a female lost in 1969 (trap mortality), and a male was present near KG in the spring of 1971 but failed to survive the summer.

Since there was much variation in spatial relationships among adults it is difficult to extrapolate general principles from selected examples. Therefore, the whole adult population on Area I for 1970 and 1971 was analysed with respect to overlap between home ranges of males and females.

These results are shown in Tables 9 and 10. Overlap is expressed as a percentage of a female's home range overlapped by all other males, and this is based on the total number of 5 X 5 metre squares in a female's home range and the number shared with each male. Clearly no home range of one male can overlap a female's home range more than 100 percent, but including all males, a female's

Table [illegible]. Matrix showing relative amounts of home range overlap between individual males and females on Area [illegible] 1970.

Male — Percent of female's home range overlapped by male

Early summer

Male	RK	KB	KY	RB	KK	GB	KW	RW	GK	KG	GY	BB	WB
RY	86	47	4	3	–	–	–	–	–	–	–	–	–
RR	24	33	27	6	–	–	–	–	–	–	–	–	–
WN	–	–	42	3	–	–	–	–	–	–	–	–	–
GW	–	11	23	10	4	–	–	–	–	–	–	–	–
RG	21	25	–	55	16	2	–	–	–	–	–	–	–
GG	–	–	–	–	71	32	–	–	–	–	–	–	–
YK	–	–	–	7	44	68	6	–	–	–	–	–	–
NN	–	–	–	–	–	–	19	–	–	–	–	–	–
YR	–	–	–	–	–	–	25	38	–	–	–	–	–
BR	–	–	–	–	–	–	–	–	25	–	–	–	–
YW	–	–	–	–	–	–	–	–	–	–	10	4	–
BY	–	–	–	–	–	–	–	–	–	–	–	48	–
RN	–	–	–	–	–	–	–	–	–	–	–	–	–*
NK	–	–	–	–	–	–	–	–	–	–	–	–	–
Total squares occupied by female	29	57	26	87	45	50	36	24	12	*	41	25	*

Late summer

Male	RK	KB	KY	RB	KK	GB	KW	RW	GK	KG	GY	BB	WB
RY	62	44	3	–	–	–	–	–	–	–	–	–	–
RR	14	35	3	3	–	–	–	–	–	–	–	–	–
WN	10	9	55	–	–	–	–	–	–	–	–	–	–
GW	–	–	9	13	–	–	–	–	–	–	–	–	–
RG	–	2	–	51	–	–	–	–	–	–	–	–	–
GG	–	–	–	–	71	27	–	–	–	–	–	–	–
YK	–	–	–	–	39	69	2	–	–	–	–	–	–
NN	–	–	–	–	–	12	19	–	–	–	–	–	–
YR	–	–	–	–	–	–	31	24	–	–	–	–	–
BR	–	–	–	–	–	–	–	–	7	–	–	–	–
YW	–	–	–	–	–	–	–	–	–	5	12	–	–
BY	–	–	–	–	–	–	–	–	–	–	1	43	–
RN	–	–	–	–	–	–	–	–	–	–	–	–	–?
NK	–	–	–	–	–	–	[illegible]	–	–	–	–	–	23
Total squares occupied by female	29	45	34	67	31	65	54	38	27	108	84	42	66

* Insufficient data. ? animal disappeared from population

Table 10. Matrix showing relative amounts of home range overlap between individual males and females on Area I, 1971

Males	Percent of female's home range overlapped by males												
	Early summer												
	RK	KB	KY	RB	KW	RW	$\overline{NN}$	KG	GY	NG	BB	$\overline{YY}$	WB
YB1	63	30	–	–	–	–	–	–	–	–	–	–	–
RY	95	33	–	4	–	–	–	–	–	–	–	–	–
RR	21	79	–	4	–	–	–	–	–	–	–	–	–
WN	–	–	52	–	–	–	–	–	–	–	–	–	–
GW	–	3	15	13	4	–	–	–	–	–	–	–	–
RG	–	3	4	65	–	–	–	–	–	–	–	–	–
BW	–	15	4	46	–	–	–	–	–	–	–	–	–
GG	–	–	–	1	–	–	–	–	–	–	–	–	–
YK	–	–	–	–	42	12	–	–	–	–	–	–	–
$\overline{YB}$	–	–	–	–	2	–	–	–	–	–	–	–	–
$\overline{YR}$	–	3	–	13	19	44	–	–	–	–	–	–	–
BR	–	–	–	–	–	9	5	–	–	–	–	–	–
WK	–	–	–	–	–	–	–	–	13	–	–	–	–
YW	–	–	–	–	–	–	–	12	13	11	–	–	4
BY	–	–	–	–	–	–	–	–	–	–	65	17	–
WY	–	–	–	–	–	–	–	–	–	–	8	26	4
NK	–	–	–	–	–	–	–	–	–	–	–	–	22
YN	–	–	–	–	–	–	–	–	–	–	–	–	–
WW1	–	–	–	–	2	–	–	–	–	–	–	–	–
Total squares occupied by female													
	19	33	27	78	52	34	19	25	47	9	26	30	23

(continued)

Table 10, continued

Males	Percent of female's home range overlapped by males												
	Late summer												
	RK	KB	KY	RB	KW	RW	$\overline{NN}$	KG	GY	NG	BB	$\overline{YY}$	WB
YB1	–	–	–	–	–	–	–	–	–	–	–	–	–
RY	–	–	–	–	–	–	–	–	–	–	–	–	–
RR	–	–	10	–	–	–	–	–	–	–	–	–	–
WN	–	–	21	–	–	–	–	–	–	–	–	–	–
GW	–	–	–	–	–	–	–	–	–	–	–	–	–
RG	–	–	–	33	–	–	–	–	–	–	–	–	–
BW1	–	–	3	36	–	–	–	–	–	–	–	–	–
GG	–	–	–	6	–	–	–	–	–	–	–	–	–
YK	–	–	–	–	–	–	–	–	–	–	–	–	–
$\overline{YB}$	–	–	–	–	–	–	–	–	–	–	–	–	–?
$\overline{YR}$	–	–	–	–	38	24	–	–	–	–	–	–	–
BR	–	–	–	–	–	–	10	–	–	–	–	–	–
WK	–	–	–	–	–	–	–	–	–	–	–	–	–?
YW	–	–	–	–	–	–	–	–	5	–	–	–	–
BY	–	–	–	–	–	–	–	–	–	–	28	6	–
WY	–	–	–	–	–	–	–	–	–	–	–	9	–
NK	–	–	–	–	–	–	–	–	–	–	–	–	6
YN	–	–	–	–	–	–	–	–	–	–	–	–	3
WW1	–	–	–	–	–	–	–	–	–	–	–	–	–
Total squares occupied by female													
	?	?	29	33	34	33	39	17	20	?	18	35	32

?Animal disappeared from population

home range may be overlapped by a factor greater than 100 percent.

These figures, besides showing general trends, also point out interesting details and variations among individual animals. For example, in 1970, RG by expansion of his home range in early summer was able to overlap the ranges of three other females besides his 'mate' (RB); by late summer however he only overlapped one other. Conversely GW appeared to be an unpaired male since, although his home range did overlap other females, none of them were strongly associated with him. In 1971 the proportion of males was much higher relative to the females and more of these males appeared to be unpaired -- examples were WW1, YN, YB1, and GW. Others were left single because of the death of the female they were paired with previously. GG illustrated this situation in 1971 as did YK, except that the latter managed to temporarily pair with a neighbouring female (KW) who had lost her mate.

An examination of these data shows three major trends in the use of space between males and females.

1. There is a much greater degree of overlap between males and females in early compared with late summer. This can be clearly seen in the tables. Using a Wilcoxon's signed ranks test, the percentage of overlap was found to be statistically greater in early summer;

$P = 0.001$ for 1970, and $P < 0.005$ for 1971. This is in part a reflection of larger sizes of home ranges in males early in the season.

2. If the above relationship is examined using paired males and females only, there is also a significant decrease in the amount of space shared in late summer when compared with early summer; animals which could not be associated with one male or female were not used in the calculations. Using a Wilcoxon's signed ranks test the overlap was significantly greater in the early summer compared with the late summer ($P < 0.05$ for 1970 and $P < 0.005$ for 1971).

3. In Tables 9 and 10, animals are plotted in an order of approximately decreasing density (ie. from the bottom of the slide to the top); density decreasing from left to right for females and top to bottom for males. It then becomes clear that with increasing density the amount of overlap by males increases also. This situation might be expected where neighbouring males contribute to a lot of the overlap but not necessarily when members of pairs only are considered. To examine this statistically an index of relative density was correlated with the amount of overlap. This index was the distance from one female to the nearest female neighbour, against which was correlated (a) the percentage overlap by all males, and (b) by the paired male only. The results are shown graphically in Fig. 13. Only

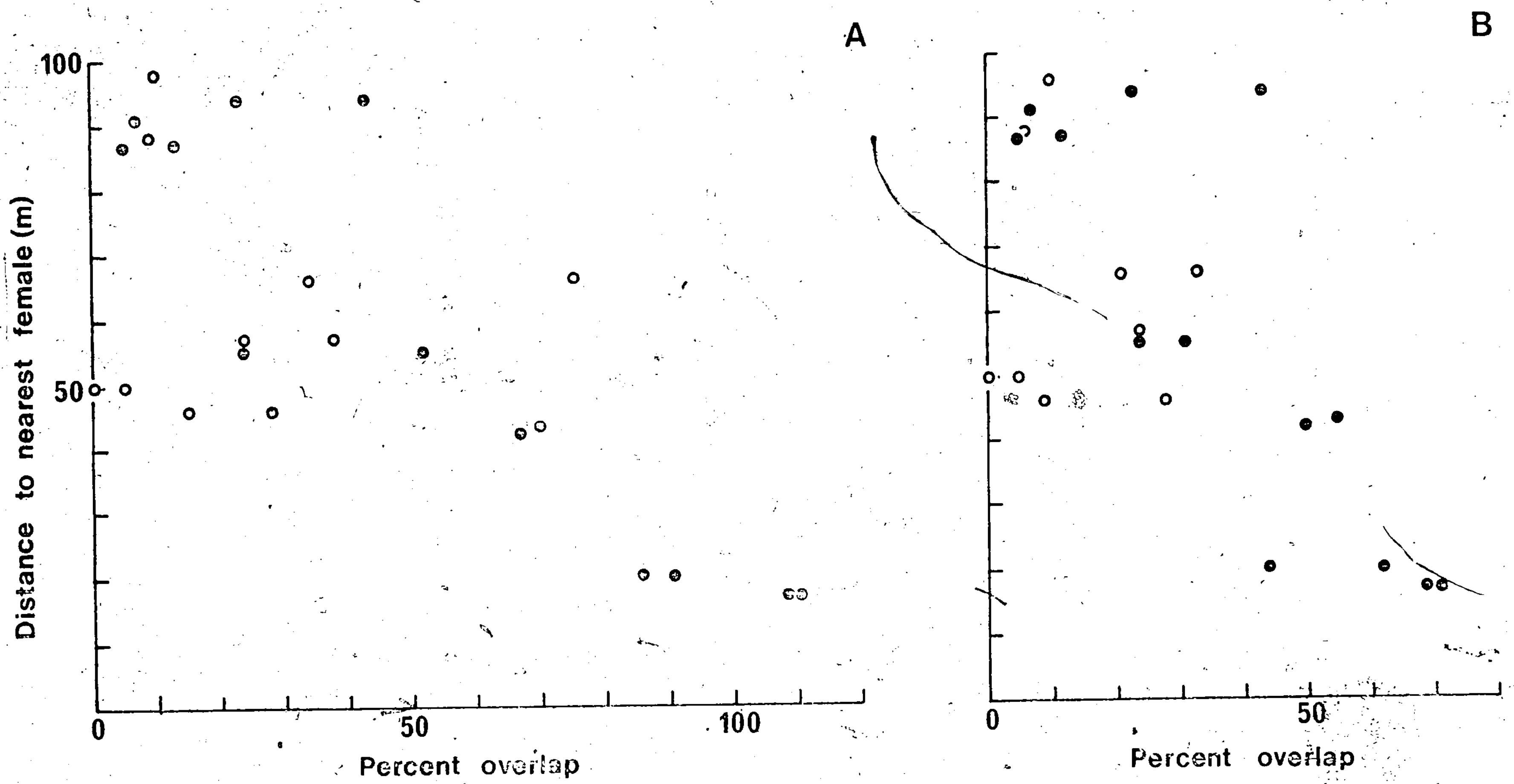

Fig. 13. Scattergrams show the relationship between an index of density (distance to nearest female) and the amount of the female's home range which it shares with (a) all neighbouring males, (b) only the male with which she appeared to be paired.

- Data for late summer 1970
- Data for late summer 1971.

data from late summer was used since this was when there was least overlap and when the effect of large home ranges of males was minimal. Using Spearman's rank correlation it was found that there was a significant correlation in 1970 for all males, and paired males only. There were no significant correlations in 1971, but when the data for the two years were pooled the correlation was again significant.

The correlation coefficients and levels of significance for these analyses are shown in Table 11. The reason for the lack of correlation in 1971 is probably due to the sex ratio being skewed in favour of males, meaning that the distance to the nearest female gave a poor index of density for that year; also several of the paired females had died by that time and had not been replaced.

In summary, pikas appear to have a spatial organisation which disperses the adults in pairs. These pairs maintain relatively exclusive home ranges with respect to neighbouring animals. During the breeding season, adult males have a greater propensity to intrude into neighbouring ranges, and as a result, females may come into contact with more males during the breeding season than at other times of the year. There is a tendency for males and females to use separate parts of a mutually shared range,

Table 11. Spearman's rank correlation statistics on data from [illegible]

		No. of pairs.	Correlation coeff.	T value.	df	Probability.
1970	Overlap between females and all males.	13	0.855	5.486	11	<0.001
	Overlap between females and paired male only.	13	0.806	4.521	11	<0.001
1971	Overlap between females and all males.	10	0.079	0.21	8	Not Sig.
	Overlap between females and paired male only.	9	0.095	0.25	7	Not Sig.
Total Both Years	Overlap between females and all males.	23	0.604	3.393	21	<0.01
	Overlap between females and paired male only.	22	0.581	3.199		<0.01

and this becomes more pronounced later in the summer and also at lower densities. This suggests that at higher densities they are forced to share space more than at lower densities. It appears that there may be a separate class of unpaired males, but this was not true for females. Variations from this general pattern, described earlier, suggest that the system can be modified if the circumstances (such as mortality) permit.

Male - Male Spacing

There were fourteen males on Area I during 1970 but by spring 1971 the number had risen to nineteen. The amount of overlap between these animals is shown in Tables 12 and 13. The matrices (set out for seasonal comparison) reflect a decrease in density from left to right and top to bottom. These data show the following trends. (1) There appears to be a steady decrease in the area of overlap with decreasing density. (2) The amount of overlap both in actual and percentage of area appears to be higher in 1971 than in 1970. (3) There is clearly a greater amount of overlap in early summer, as compared with late summer. These three trends were examined statistically in further detail.

Using the distance to the nearest male as an index of density, the percentage overlap of each male's home

Table 12. Matrix showing relative amounts of overlap between home ranges of individual males on Area I, 1970.

Percent of home range overlapped by other males

Early summer

	RY	RR	WN	GW	RG	GG	YK	NN	YR	BR	YW	BY	RN	NK
RY	**	23	–	–	7	–	–	–	–	–	–	–	–	–
RR	25	**	46	–	19	–	–	–	–	–	–	–	–	–
WN	–	21	**	5	3	–	–	–	–	–	–	–	–	–
GW	–	–	8	**	3	1	–	–	–	–	–	–	–	–
RG	15	39	11	8	**	19	15	–	–	–	–	–	–	–
GG	–	–	–	3	12	**	29	–	–	–	–	–	–	–
YK	–	–	–	–	13	39	**	2	–	–	–	–	–	–
NN	–	–	–	–	–	–	1	**	8	–	–	–	–	–
YR	–	–	–	–	–	–	–	10	**	–	–	–	–	–
BR	–	–	–	–	–	–	–	–	–	**	–	–	–	–
YW	–	–	–	–	–	–	–	–	–	–	**	–	–	–
BY	–	–	–	–	–	–	–	–	–	–	–	**	–	5
RN	–	–	–	–	–	–	–	–	–	–	–	2	**	–
NK	–	–	–	–	–	–	–	–	–	–	–	–	–	**
Total squares occupied by male	52	57	26	39	113	74	99	41	52	33	34	62	+	20

Late summer

	RY	RR	WN	GW	RG	GG	YK	NN	YR	BR	YW	BY	RN	NK
RY	**	10	17	2	–	–	–	–	–	–	–	–	–	–
RR	14	**	2	–	6	–	–	–	–	–	–	–	–	–
WN	19	2	**	2	–	–	–	–	–	–	–	–	–	–
GW	–	–	2	**	10	2	–	–	–	–	–	–	–	–
RG	–	8	–	15	**	2	–	–	–	–	–	–	–	–
GG	–	–	–	2	2	**	31	–	–	–	–	–	–	–
YK	–	–	–	–	–	26	**	9	–	–	–	–	–	–
NN	–	–	–	–	–	–	10	**	3	–	–	–	–	–
YR	–	–	–	–	–	–	–	2	**	–	–	–	–	–
BR	–	–	–	–	–	–	–	–	–	**	–	–	–	–
YW	–	–	–	–	–	–	–	–	–	–	**	–	–	–
BY	–	–	–	[illegible]	–	–	–	–	–	–	–	**	–	–
RN	–	–	–	[illegible]	[illegible]	–	–	–	–	–	–	–	**	–
NK	–	–	–	[illegible]	[illegible]	–	–	–	–	–	–	–	–	**
Total squares occupied by male	36	48	40	47	62	60	51	53	35	64	96	85	7	59

+Insufficient data

Table 13. Matrix showing relative amount of overlap between home ranges of individual males on Area I, 1971.

Percent of home range overlapped by other males

Early summer

	YB1	RY	RR	WN	GW	RG	BW1	GG	YK	ȲB	WW1	ȲR	BR	WK	YW	BY	WY	NK	YN
YB1	**	48	11	-	-	-	3	-	-	-	-	-	-	-	-	-	-	-	-
RY	48	**	17	5	14	6	9	-	-	-	-	3	-	-	-	-	-	-	-
RR	5	23	**	-	16	15	23	-	-	-	-	11	-	-	-	-	-	-	-
WN	-	2	-	**	7	-	-	-	-	-	-	-	-	-	-	-	-	-	-
GW	-	12	10	14	**	18	18	-	-	-	-	6	-	-	-	-	-	-	-
RG	-	10	17	-	32	**	60	3	-	-	-	21	-	-	-	-	-	-	-
BW1	4	13	25	-	32	58	**	5	-	-	-	12	-	-	-	-	-	-	-
GG	-	-	-	-	-	3	4	**	20	33	33	-	-	-	-	-	-	-	-
YK	-	-	-	-	-	-	-	25	**	33	24	18	-	-	-	-	-	-	-
ȲB	-	-	-	-	-	-	-	5	4	**	-	1	-	-	-	-	-	-	-
WW1	-	-	-	-	-	-	-	18	11	-	**	-	-	-	-	-	-	-	6
ȲR	-	4	11	-	9	19	12	-	18	11	-	**	10	-	-	-	-	-	-
BR	-	-	-	-	-	-	-	-	-	-	-	3	**	-	-	-	-	-	-
WK	-	-	-	-	-	-	-	-	-	-	-	-	-	**	7	-	-	-	-
YW	-	-	-	-	-	-	-	-	-	-	-	-	-	18	**	-	-	-	-
BY	-	-	-	-	-	-	-	-	-	-	-	-	-	-	-	**	27	-	-
WY	-	-	-	-	-	-	-	-	-	-	-	-	-	-	-	15	**	8	-
NK	-	-	-	-	-	-	-	-	-	-	-	-	-	-	-	-	15	**	-
YN	-	-	-	-	-	-	-	-	-	-	3	-	-	-	-	-	-	-	**
Total squares occupied by male	52	52	71	21	44	79	77	61	73	9	33	72	20	22	59	60	33	64	15

(continued)

Table 13, continued

Percent of home range overlapped by other males

Late summer

	YB1	RY	RR	WN	GW	RG	BW1	GG	YK	$\overline{Y}$B	WW1	$\overline{Y}$R	BR	WK	YW	BY	WY	NK	YN
YB1	**	18	14	7	-	-	-	-	-	-	-	-	-	-	-	-	-	-	-
RY	43	**	10	11	-	-	-	-	-	-	-	-	-	-	-	-	-	-	-
RR	29	9	**	18	-	-	-	-	-	-	-	-	-	-	-	-	-	-	-
WN	14	9	17	**	-	-	-	-	-	-	-	-	-	-	-	-	-	-	-
GW	-	-	-	-	**	4	-	-	-	-	-	-	-	-	-	-	-	-	-
RG	-	-	-	-	11	**	6	3	-	-	-	-	-	-	-	-	-	-	-
BW1	-	-	-	-	-	7	**	-	-	-	-	-	-	-	-	-	-	-	-
GG	-	-	-	-	-	4	-	**	17	-	46	-	-	-	-	-	-	-	-
YK	-	-	-	-	-	-	-	18	**	-	23	-	-	-	-	-	-	-	-
$\overline{Y}$B	-	-	-	-	-	-	-	-	-	**	-	-	-	-	-	-	-	-	-
WW1	-	-	-	-	-	-	-	15	7	-	**	-	-	-	-	-	-	-	3
$\overline{Y}$R	-	-	-	-	-	-	-	-	-	-	-	**	-	-	-	-	-	-	-
BR	-	-	-	-	-	-	-	-	-	-	-	-	**	-	-	-	-	-	-
WK	-	-	-	-	-	-	-	-	-	-	-	-	-	**	-	-	-	-	-
YW	-	-	-	-	-	-	-	-	-	-	-	-	-	-	**	-	-	-	-
BY	-	-	-	-	-	-	-	-	-	-	-	-	-	-	-	**	13	-	-
WY	-	-	-	-	-	-	-	-	-	-	-	-	-	-	-	6	**	-	-
NK	-	-	-	-	-	-	-	-	-	-	-	-	-	-	-	-	-	**	-
YN	-	-	-	-	-	-	-	-	-	-	8	-	-	-	-	-	-	-	**
Total squares occupied by male	14	33	29	27	9	28	35	39	40	?	13	40	52	?	30	51	23	22	30

?Animal disappeared from population.

range was plotted against this index (Fig. 14). This was done using data from 1970 and 1971 taken during late summer when overlap was minimal. Spearman's rank correlations were found to be significant in each year and combined years (Table 14). This indicates that with increasing density home ranges become less and less exclusive, however no animals were overlapped more than 100 percent indicating that in late summer, all animals were able to maintain at least part of their home range for their exclusive use (with respect to other males). Since there is this difference in overlap with density one would expect a greater amount of overlap in 1971 than 1970, the population of males being higher in 1971. Indeed, using a Mann-Whitney U test a significant difference was found in the amount of overlap between males in early summer ($P < 0.025$), but not during late summer. The lack of significance for late summer is probably due to a small sample size since examination of Fig. 14 shows that the animals with the four highest amounts of overlap are all from 1971. Additionally, the two animals on the extreme right of the graph, with the overlap of 77 and 86 percent were both yearling unpaired males born in 1970.

Seasonal differences in the degree of home range overlap were significant also. Home ranges of males overlapped significantly more in early summer than late summer

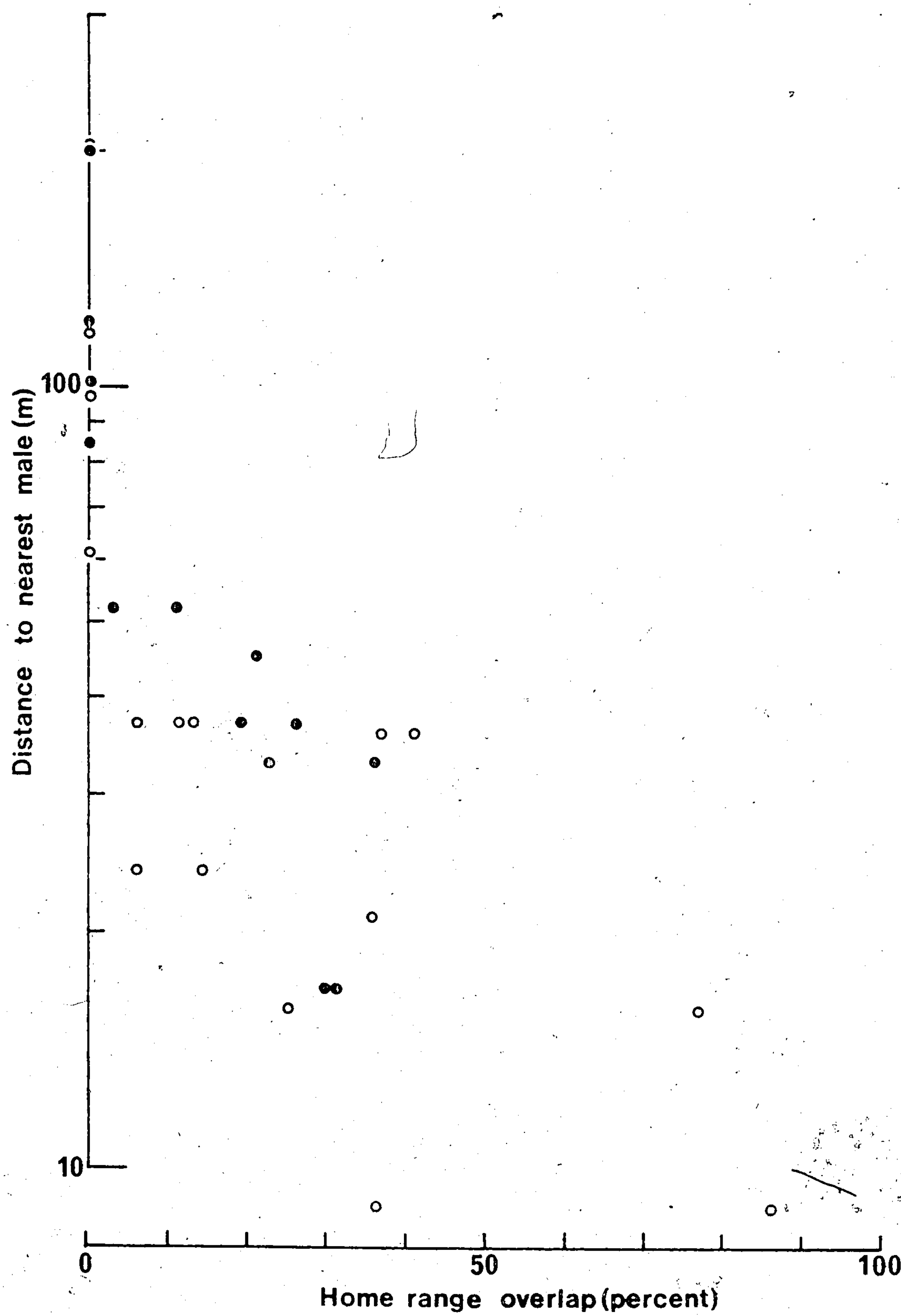

Fig. 14. Scattergram showing relationship between overlap of male home ranges and density. Late summer on Area I.

● Data for 1970

○ Data for 1971

Table 14. Spearman's rank correlation statistics on data from Fig. 14.

	No. of animals in sample	Correlation coeff.	T value	df	Probability
1970 Overlap among males	13	0.901	6.892	11	<0.001
1971 Overlap amcng males	17	0.829	5.755	15	<0.001
Both Years	30	0.841	8.273	28	<0.001

(1970, $P < 0.005$; 1971, $P = 0.01$ - Wilcoxon's signed ranks test). These differences corresponded with the larger size of home ranges of males in early summer. One interesting feature here is that there were four males which did not show a decrease in home range overlap later in the summer, and of these four, three were unpaired yearling males. This suggests that unpaired males might show different seasonal changes in use of space than do paired males.

Among mature paired males relative dominance between animals may be reflected in their home range characteristics. This is illustrated in Figs. 15 and 16. Home ranges of five adjacent males on Area I in late summer are shown in Fig. 15 and overlap was generally small, although in one case quite large (YK v GG). The situation in early summer (Fig. 16) showed a much larger amount of overlap. However examination of the ranges showed almost all the overlap was a result of range extensions by three of the males - RY, RG, and YK. These three not only overlapped their neighbours completely but maintained larger exclusive areas than RR and GG; the latter showed almost no range extension. All these animals were paired and all at least two years of age. Further, the same pattern was apparent in 1969 though the number of observations are fewer and GG and RR were unpaired at that time. This suggests that if pikas are considered as being territorial, there may be relative dominance among them, giving some

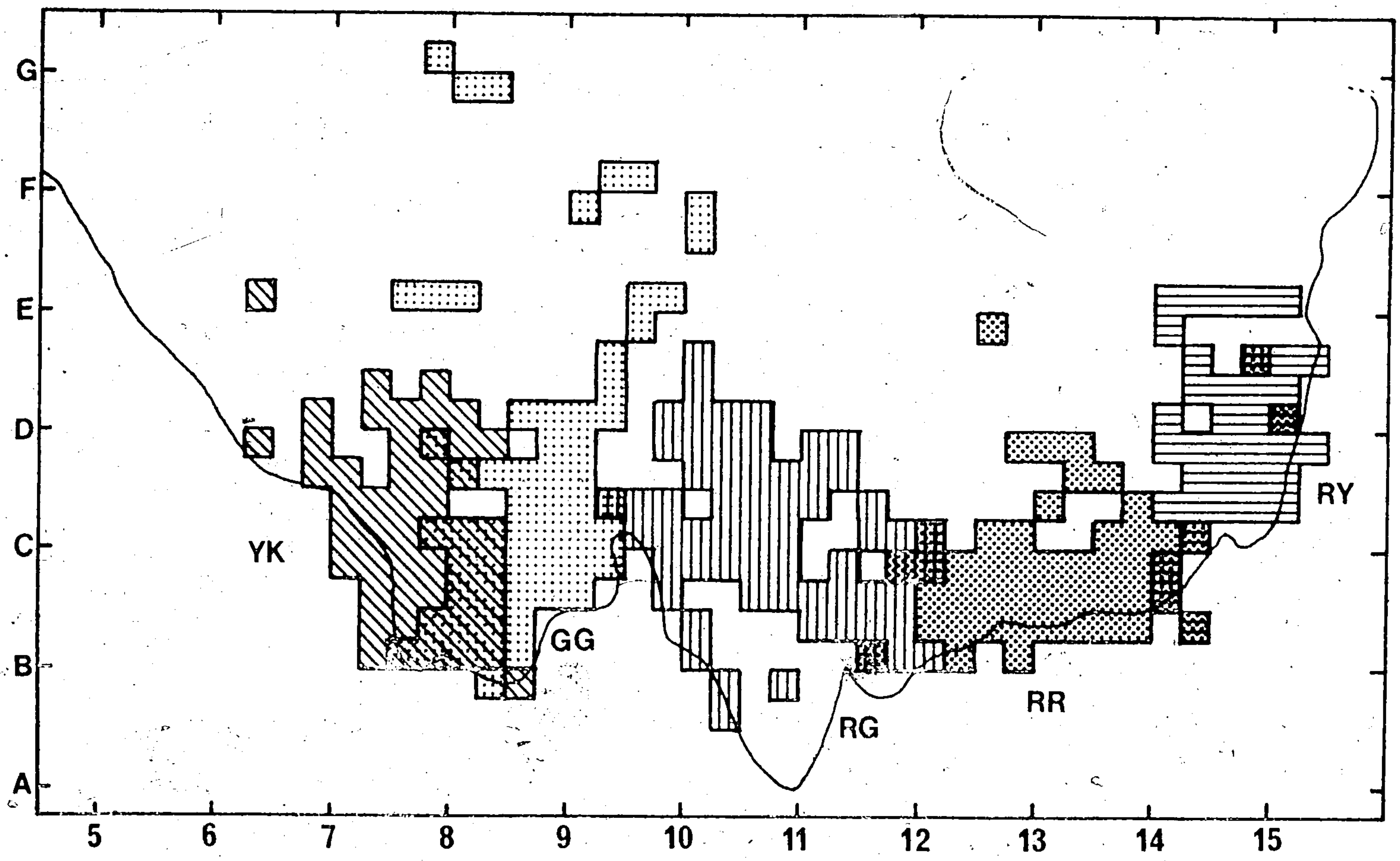

Fig. 15. Relationship among the home ranges of five adjacent males during late summer 1970. All animals were paired with females. Number of observations: YK = 266, GG = 226, RG = 184, RR = 208, RY = 138.

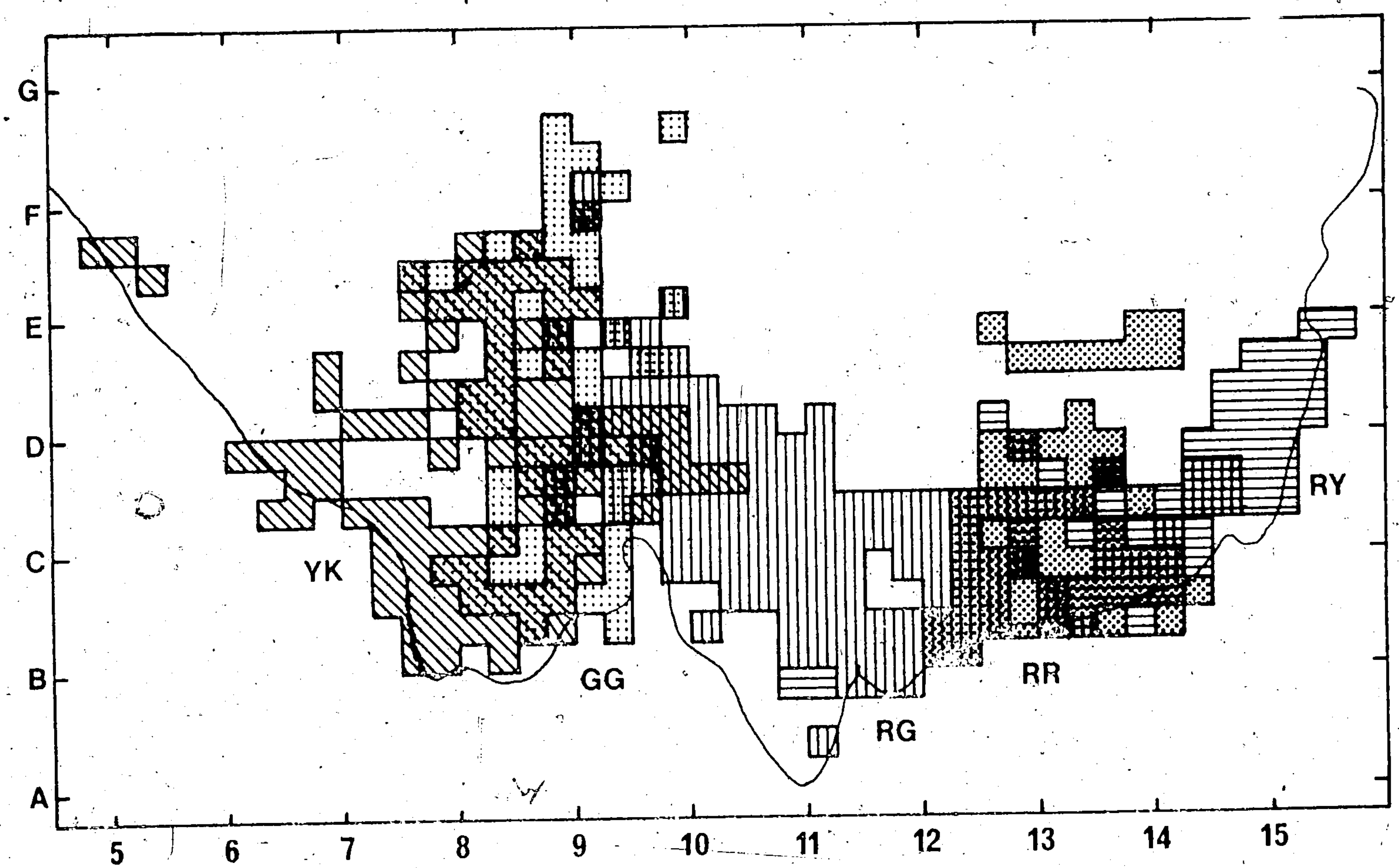

Fig. 16. Relationship among the home ranges of five adjacent males during early summer 1970. Number of observations: YK = 222, GG = 146, RG = 255, RR = 219, RY = 167.